Structure, strengthening and weakening of alkali activated metakaolin during ageing

Der Naturwissenschaftlichen Fakultät der
Gottfried Wilhelm Leibniz Universität Hannover

Zur Erlangung des Grades
Doktorin der Naturwissenschaften
Dr. rer. nat.

Genehmigte Dissertation von

Dipl.-Phys. Elżbieta Marta Mielcarek
Geboren am 01.02.1981 in Sulechów, Polen

2010

Referent: Prof. Dr. Claus Henning Rüscher

Institut für Mineralogie, Gottfried Wilhelm Leibniz Universität Hannover

Korreferent: Prof. Dr. Josef-Christian Buhl

Institut für Mineralogie, Gottfried Wilhelm Leibniz Universität Hannover

Tag der Promotion: 17.03.2010

ACKNOWLEDGEMENTS

First and foremost I want to thank my adviser Professor Dr. Claus H. Rüscher. It has been an honor to be his PhD. student. His wide knowledge and his logical way of thinking have been of great value for me.

I am thankful to Professor Dr. Josef-Christian Buhl, Institute of Mineralogy, Leibniz University of Hannover, because he introduced me to crystallography and for his priceless suggestions.

I am deeply grateful to Dr. Wolfgang Lutz, Trical Zeolites GmbH, Labor Berlin, for his detailed and constructive comments and encouraging me during my stay in Berlin.

My deepest thanks and gratitude to Dr. A. Ritzmann, Trical Zeolites GmbH, Labor Berlin, who introduced me to mechanical measurement of alkali activated cement.

I am deeply indebted to Professor Dr. Waltraud M. Kriven, who gave me the opportunity to work with her group in the Department of Materials Science at the Illinois University at Urbana-Champaign in USA. I warmly thank for a friendly and happy atmosphere in her group. In particular, I would like to thank Ryan Haggerty for his technical assistance in strength measurement. I wish to express my gratitude to Dr. Wacek Świech from Center for Microanalysis of Materials Frederick Seitz Materials Research Laboratory for his help with TEM measurement.

I owe my most sincere gratitude to PhD. Dr. Thorsten M. Gesing, Crystallography, University of Bremen for introducing me to X-ray diffraction and for his kind help during my stay in Hannover.

I would like to express my thank to whole Institute of Biophysics in Hannover for opportunity of using Raman equipment and creating friendly environment.

I wish to extend my warmest thanks to Fongjan Jirasit from Institute for Buildings materials in Hannover and Jakrapan Wongpa from Department of Civil Engineering, Faculty of Engineering, Kings Mongkut's University of Technology in Bangkok for constructive discussion and useful suggestions.

I am deeply indebted to Otto Diedrich from Institute of Mineralogy in Hanover for his precise polishing of geopolymers and glasses.

I wish to express my gratitude to Annette Quetscher from Institute of Mineralogy in Hannover for her assistance in glass preparation.

I gratefully thank Wanja Dziony from Institute of Mineralogy in Hannover for his help in micro probe measurement of glasses.

With no particular order I thank all of my colleagues: Tapas Debnath, Andrea Hartmann, Tanja Höfs, Lars Robben, Lars Schomborg for many constructive discussions and friendly help.

I am very grateful to thank my loving, supportive, patient family and boyfriend, whose faithful support during the final stages of this PhD. is so appreciated. Thank you!

I would like to thank everybody, who was important to the successful realization of the thesis, as well as expressing my apology, that I could not mention them personally one by one.

Finally, I would like to thank the Ministry of Science and Culture, Land Niedersachsen for providing me „Georg-Christoph-Lichtenberg Stipendium“.

ABSTRACT

Aluminosilicate gels were synthesized in systematic series of various compositions by alkali activation of metakaolin. A composition with Si/Al ratio of about 2 served as a model system to study geopolymerization mechanism in an optimal reacted gel (Cem.1) cured at room temperature. The ageing process of Cem.1 shows a favourable fast increase in mechanical strength up to 100 h followed by an unfavourable loss of almost the complete strength initially gained. The details of the structural changes were investigated by Molybdate measurement, Raman and Infrared spectroscopy. For the further interpretation, Raman and Infrared spectra of series of silicate and aluminosilicate glasses were used. The advantages and disadvantages of X-Ray, TEM, SEM/EDX and NMR method are considered and discussed. Using the combination of these methods reveal new fundamental insight in the structural change during geopolymerization, more than those presently achieved using X-Ray, TEM or NMR techniques as usually used for structure determination. The following new results are presented:

The relation between DOSPM (Density of States peak Maximum) of asymmetrical stretching and Al molar ratio (x=1/(1+Si/Al)) was estimated on the basis of micro-probe measurement and infrared investigations of aluminosilicate glasses. This relation comes remarkable close to that obtained by for faujasite type zeolites covering a wide range of Si/Al ratios. A close equivalence was found in DOSPM between $Q^4(4Al)$, $Q^4(3Al)$, $Q^4(2Al)$ and Q^0, Q^1, Q^2 for the aluminosilicates and silicates, respectively. Using the linear relations for glasses implies for the final DOSPM at 1016 cm^{-1} an Si/Al=1.9, which closely corresponds to a fully reacted body for Cem.1.

The results implied, that basically the formation of two structural units, with different time dependencies, dominate the structural properties: (I) A fast formation of longer (polymeric) silicate chains is caused by the consumption of hydroxide in the solution of metakaolin up to about 25 h of ageing. (II) A aluminosilicate network condense slowly enclosing the silicate units, as given by the DOSPM shift from 1025 cm^{-1} to 1016 cm^{-1}. The ageing process is accompanied with the destruction of the polysilicate chains, due to the increasing amount of hydroxide produced during network condensation. The structural changes above 100 h of ageing were indicated by variation in molybdate activity and covered by stable DOSPM at 1016 cm^{-1}. Kinetically controlled leaching experiment and systematic changes in the field of Si-OH stretching and H_2O bending mode confirmed the aluminosilicate network's change at further stage of geopolymerization. Thus the initial increase in mechanical strength between 25 h and 100 h is related to slow a network formation via enclosing and cross-linking of polycondensed silicate chains. Increasing the metakaolin to water glass ratio in series of Cem.3-7 increased the amount of unreacted metakaolin. This portion could be subtracted and the Si/Al ratio of the cement phase was estimated to be similar to Cem.1.

The Raman spectra of glasses confirm the similar behaviour of all bands in relation to silica content. The characteristic Raman band in lower frequency range has been related to T-O-T vibrations of aluminosilicate network. The explanation of peak's presence at 1064 cm^{-1} has been related to $Si\text{-}O^-$ non-bridging oxygen bonds in decomposed silica chains interacting with alkali ions in aluminosilicate cross-linked network.

Thermogravimetric TG and DTA were carried out in two runs and were discussed with respect to changes in the degree of condensation and water reabsorption of geopolymer.

Keywords: Geopolymer, alkali activated metakaolin, water glass

ZUSAMMENFASSUNG

Alumosilikat-Gel-Serien unterschiedlicher Zusammensetzungen wurden durch Alkali-Aktivierung von Metakaolin synthetisiert. Die Zusammensetzung mit einem Si/Al Verhältnis von etwa 2 diente als Modell zur Untersuchung von Geopolymerizationsprozessen in einem optimal reagierten, bei Raumtemperatur gealterten Gel. Während des Alterungsprozesses der hier Cem.1 genannten Gele zeigte sich eine rasche Zunahme der mechanischen Festigkeit innerhalb der ersten 100 Stunden, wohingegen im weiteren Verlauf die vorher erlangte Festigkeit teils wieder abnahm. Im Detail wurden die Änderungen in der Struktur mit der Molybdat-Methode, Raman- und Infrarot-Spektroskopie untersucht. Zur weiteren Interpretation wurden die Raman- und Infrarot-Spektren von silikatischen und alumosilikatischen Gläsern herangezogen. Vor- und Nachteile von Röntgen-Diffraktometrie, TEM, SEM/EDX und NMR Techniken wurden bedacht und diskutiert. Die Kombination dieser Techniken liefert neue, fundamentale Erkenntnisse über die strukturellen Veränderungen während der Geopolymerisation, die mit den gegenwärtig üblichen Methoden zur Strukturaufklärung wie Röntgen, TEM oder NMR alleine nicht erreicht werden können. Hier werden folgende neue Ergebnisse präsentiert:

Die Beziehung zwischen DOSPM (Density of States Peak Maximum) von asymmetrischen Streck-Schwingungen und dem molaren Al Verhältnis (x=1/(1+Si/Al)) wurde durch Elektronenstrahl-Mikrosonden-Analyse und Infrarot-Spektroskopie an Alumosilikat-Gläsern bestimmt. Diese Beziehung kommt bemerkenswert dicht an diejenige für Faujasit-Typ Zeolite heran, die einen weiten Bereich des Al/Si Verhältnisses abdecken. Es wurde eine gute Übereinstimmung für DOSPM zwischen $Q^4(4Al)$, $Q^4(3Al)$, $Q^4(2Al)$ und Q^0, Q^1, Q^3 für die Alumosilikate bzw. Silikate gefunden. Die lineare Abhängigkeit für Gläser impliziert für das letzte DOSPM bei 1016 cm^{-1} ein Si/Al Verhältnis von 1.9, was in guter Übereinstimmung mit dem durch die Wasserglas – Metakaolin Mischung gegebenen Verhältnis steht.

Die Ergebnisse ließen die Schlussfolgerung zu, dass die mechanischen Eigenschaften durch die Bildung zweier struktureller Einheiten - mit unterschiedlicher Zeitabhängigkeit - bestimmt werden: (I) Eine schnelle Bildung längerer Silikatketten (polymer) durch den Verbrauch von Hydroxid in der Metakaolin-Lösung bis zu 25 h nach Einsetzen des Alterungsprozesses. (II) Die Kondensation eines Alumosilikat-Netzwerkes. Dies wird deutlich durch die Verschiebung des DOSPM von 1025 cm^{-1} zu 1016 cm^{-1}. Der Alterungsprozess wird von der Zerstörung der Polysilikat-Ketten begleitet, verursacht durch den Anstieg der Hydroxid-Konzentration während der Kondensation des Netzwerkes. Die strukturellen Änderungen oberhalb von 100 h Alterung, die durch die Änderung der Molybdat-Aktivität angezeigt wurden finden bei gleichbleibendem DOSPM bei 1016 cm^{-1} statt. Kinetisch kontrollierte leaching-Experimente sowie systematische Feldänderungen der Si-OH Streck- und H_2O Biegeschwingungsmoden bestätigten die Veränderungen im alumosilikatischen Netzwerk während der fortschreitenden Geopolymerisierung. Der ursprüngliche Anstieg der Festigkeit zwischen 25 und 100 Stunden der Alterung ist demnach auf eine langsame Vernetzung- und das Einschließen von polykondensierten Silikatketten zurückzuführen. Eine Erhöhung des Metakaolin / Wasserglas Verhältnisses in Serie Cem.3-7 hatte ebenso einen höheren Anteil unreagierten Metakaolins zur Folge. Nach Eliminierung des unreagierten Metakaolin-Anteils wurde das Si/Al Verhältnis zu einem Wert bestimmt, der dem von Cem.1 ähnlich ist.

Die Raman Spektren von Gläsern bestätigen ähnliches Verhalten für alle Banden, die im Zusammenhang mit SiO_2 Gehalt stehen. Die charakteristische Bande im niedrigen Frequenzbereich wurde T-O-T Vibrationen des Alumosilikat-Netzwerkes zugeschrieben. Die Erklärung eines Peaks

bei 1064 cm^{-1} war komplexer und wurde letztendlich mit „non-bridging-oxygen“ $Si\text{-}O^-$ Bindungen von Kieselsäureketten in Zusammenhang gebracht, welche mit Alkali-Ionen im ineinandergreifenden Alumosilikat-Netzwerk interagieren.

Thermogravimetrische TG und DTA wurden in zwei Schritten durchgeführt und bezüglich der Kondensationsgradänderungen und Reabsorption von Wasser diskutiert.

Schlagwörter: Geopolymer, Alkali-aktiverter Metakaolin, Wasserglas

Table of Contents

1. INTRODUCTION

Aluminosilicate binders, called geopolymers are amorphous inorganic polymers typically formed by reaction of aluminosilicate powders (e.g. metakaolin, fly ash, industrial wastes, calcined clays, melt-quenched aluminosilicate, natural minerals) with highly concentrated alkali metal hydroxide or silicate solutions (*Glukhovsky (1957); Skvara (1997); Van Jaarsveld et al., (1997); Pacheco-Torgal et al., (2008))*. Nowadays, geopolymers are widely considered as a substitute of Ordinary Portland Cement (OPC). Alkali activated cement is strongly recommended because of fast hardening, high compressive strength, satisfying acid and fire resistance, waste encapsulation capability and up to 90 % less CO_2 emission, than commonly used cement. If we take into account, that the production of geopolymers absorbs 2-3 times less energy than Portland cements produces 4-8 times less carbon dioxide, the replacement of commonly used cement may crucially decrease the environmental pollution. In practice, the application of geopolymeric concrete is limited because of higher production cost than in case of usually used concrete, mainly due to the price of sodium and potassium hydroxide, which are consumed in large amounts in the synthesis of inorganic binders. Nevertheless, aluminosilicate binders are employed in some specific cases, if either high refractoriness or very fast hardening is required (*Davidovits (1991), De Silva et al. (2007)*).

Geopolymers are a part of a large family of synthetic alkali aluminosilicate materials. As written by *Breck (1974)* the pioneers of aluminosilicate investigation, are J. T. Way, R. Gans, and G. Wiegner, who focused their studies, at the beginning of XX century, on the structure and academic application of this new material. Systematic investigations on formation, in respect to application as adsorbents, catalysts, ion-exchanger, with reference to zeolite synthesis, were followed by *Breck (1974)* and *Barrer (1982)*. Alkali activated cements have been developed in the former Soviet Union, since the 1950s by V. D. Glukhovsky (*Glukhovsky (1957))*. Originally these materials were called “soil cements“. Glukhovsky, who was working with alkali-activated slags containing large amounts of calcium hypothesized, that the superior durability of ancient concretes resulted from the coexistence of cements containing calcium silicate hydrate (C-S-H) with some form of alkaline aluminosilicate hydrates (*Duxon et al., (1982); Kriven et al., (2003b); Roy (1999))*. Davidovits pointed out the importance of calcium-free systems. In 1976, he defined the structure of alkali activated binders and introduced the term “geopolymere” (*Davidovits (1991); Duxson et al., (2005c))*. Due to the compositional similarities to glass, ceramic and zeolite, geopolymeric binders are also called low-temperature aluminosilicate glasses (*Rahier et al., (1997))*, hydro-ceramics (*Bell*

et al., (2009); Skvara (2007)) and amorphous analogue of zeolites (*Antonić, et al., (1994); MacKenzie (2003))*. Recent research tide geopolymers (particularly those synthesized from 'pure' raw materials, such as metakaolinite) closely to the chemistry of aluminosilicate gels *[27-30]* and zeolites (*Provis et al., (1982))*, ceramics (*Bell et al., (2009)*; *Kriven et al., (2003b, 2005))* and glasses (*Rahier et al., (1997))*. According to Davidovits' theory, geopolymere may be considered as a random 3-dimensional network of silicate and alumina tetrahedra linked with oxygen atoms. Alkali metal cations as Na^+, K^+, Li^+, and Cs^+ provide charge balance in the structure. Geopolymers are an example of the wider class of alkali activated binders and nowadays, in the literature, this term is often used to describe alkali activated silicate and aluminosilicate sources (*Skvara (2007))*.

Davidovits *(1991)* has proposed the following empirical formula for alkali activated binders:

$$M_n[(SiO_2)_z \cdot AlO_2]_n \cdot wH_2O$$

where M is an alkali metal cation, "n" is a degree of polycondensation and "z" is the amount of silicate units, described with integer from 1 up to 32. The polymeric structure results from the condensation and cross-linking of polysilicate chains or sheets with the so called sialate link *–Si-O-Al-O*. A strict formalism was described as:

-polysialate M_n*-(-SiO-AlO-)$_n$, (PS)*,

-polysialate siloxo M_n*-(Si-O-Al-O-Si-O-)$_n$, (PSS)*,

-poly sialate-disiloxo M_n*-(Si-O-Al-O-Si-O-Si-O-)$_n$, (PSDS)* etc.

This nomenclature was determined on the basis of the observation, that X-Ray amorphous geopolymers contain exclusively tetrahedral coordinated silicon and aluminum, as observed in NMR spectroscopy. Davidovits' model excludes Al-O-Al linkages, based on interpretation of the Loewenstein's rule for aluminum avoidance (*Davidovits (1991))*. However, there is no theoretical basis for strict application of aluminum avoidance, but rather a thermodynamic preference giving a strong tendency towards Al-O-Al bonds avoidance. The polysialate nomenclature has been only adopted in practical sense for describing the superficial Si/Al ratio of geopolymers in research publication, where PS, PSS, PSDS describe the system with Si/Al ratios of 1, 2 and 3, respectively (*Kriven et al., (2003b))*.

A short time after Davidovits's notation, another description of the alkali aluminosilicate systems was specified by Engelhardt (*Engelhardt et al., (*1982*))*, which is commonly used to characterise aluminosilicate systems including glasses, gels, zeolites and minerals. The notation Q^n(mAl), where

$0 \leq m \leq n \leq 4$, "n" is the coordination number of the silicon centre and "m" is the number of Al neighbours, is applied to describe the connectivity of a silicon tetrahedron bridged through oxygen to aluminum and to other silicon centres. In contrary to Davidovits's nomenclature, this notation allows to describe aluminosilicate materials irrespective of the ordering degree (*Kriven et al., (2003b))*.

The concept of geopolymerization was described by Davidovits *[21-23]*:

$$n(Si_2O_5, Al_2O_2) + 2n(SiO_2) + 4n\,H_2O + NaOH\ or\ KOH \Rightarrow Na^+, K^+ + n(OH)_3 - Si - O - \underset{\underset{(OH)_2}{|}}{Al} - O - Si - (OH)_3$$

$$n(OH)_3 - Si - O - \underset{\underset{(OH)_2}{|}}{Al} - O - Si - (OH)_3 + NaOH\ or\ (KOH) \Rightarrow (Na^+, K^+) - (- \underset{\underset{O}{|}}{Si} - O - \underset{\underset{O}{|}}{Al} - O - \underset{\underset{O}{|}}{Si} - O -)n + 4n\,H_2O$$

Generally the in-total exothermic reaction involve three separate, but inter-related stages, i.e. dissolution/hydrolysis, transportation/orientation and polycondensation/gelation (*Davidovits (1997); Xu et al., (2000, 2002))*. The first step consists in a breakdown of the covalent bonds Si-O-Si and Al-O-Si, which happens when the pH of the alkaline solution raises. The dissolution of Si-O-Si bindings results in the formation of hydroxylated complex like silicic acids $Si(OH)_4$ and $Si\text{-}O^-$ anions. The alkalis balance the charge and form $Si\text{-}O^-\text{-}Na^+$ bonds. The hydroxyl groups have an impact on the Al-O-Si bonds in the same way, forming the complexes: $Al(OH)_4^{1-}$, $Al(OH)_5^{2-}$ and $Al(OH)_6^{3-}$. The next step of reaction involves the chemical bonding of geopolymers precursors (oligomers) by simultaneous removal of water molecules, known as polymerization. Condensation can occur between aluminate and silicate species or silicate species themselves, depending on the concentration of Si in the system. For the condensed ions of silicates the formulation with monomers (an isolated $[SiO_4]$), dimers ($[Si_2O_6]$), oligomers and polymers is also used. Here oligomers could describe silicate chains (ie. Q^2 groups) with length between dimers and polymers, across over to polymers may be given for chain length above 30 units. This relation is basically used by *Thilo et al., (1965)*, who determined such species using the so called Molybdate method, a special technique for the determination of the degree of condensation in silicate and aluminosilicate system. With mixtures of low Si/Al ratios, condensation predominantly occurs between aluminate and silicate species, resulting in mainly poly(sialate) polymer structures. If Si/Al=1, there are

principally only monomers formed. Likewise, when the Si/Al ratio increases (>1), the silicate species tend to condense among themselves to form oligomeric silicates. In turn, these oligomeric silicates condense with $Al(OH)_4^{4-}$, forming a rigid 3D network of polymer structures (poly(sialate-siloxo) and poly(sialate-disiloxo)) (*De Silva et al., (2007); Yunsheng et al., (2008)*. The negatively charged and tetrahedral coordinated Al^{3+} atoms inside the network are charge balanced with alkali metal cation from the activating solution (*De Silva et al., (2008)*). The setting time of the alkali activated cements is mainly controlled with the Al content and rises as the ratio Si/Al increases in the initial mixture. The influence of initial SiO_2/Al_2O_3 ratio on the strength and micro-structure of geopolymers have been reported by several authors (*Rowles et al., (2003); Fletcher et al., (2005); De Silva et al., (2007)*. In a review work, *Steveson et al., (2005)* concluded, that better strength properties are reported for the sample of molar ratios: Na_2O/Al_2O_3=1, SiO_2/Al_2O_3=(3.5-3.8) and H_2O/Al_2O_3=12.

Nowadays, the effect of accessory elements is also under investigation (*Perera et al., (2007a)*. In particular, the presence of Ca^{2+} seems to control the physical properties of the final geopolymer (*MacKenzie (2003); Yip et al., (2005)*. It has been stated, that calcium has a positive effect on the compressive strength of geopolymeric binders. The compositions with higher CaO content indicate the decrease in the porosity and the formation of amorphous Ca-Al-Si gel strengthens the final product (*Xu et al., (2002); Rüscher et al., (2010b)*. *Kim et al., (2006)* have drawn the attention to the organic containing geopolymer and studied the kerogen-derived binder. These authors pointed, that the small content of organics is the key parameter, that decides on the strength and durability of a large volume inorganic material.

Fig. 1.1 presents the theoretical structural model for K poly(sialate -siloxo) geopolymer proposed by *Davidovits (1991)*. As seen, the general model of geopolymerization suggests the structure including tetrahedral Al and Si units randomly distributed along the polymeric chains, which are also cross-linked to form cavities of sufficient size in order to accommodate the hydrated charge-balancing alkali metal ions [*21-23*]. On the basis of the results obtained with means of thermal analysis, mercury porosimetry, data obtained with measurement of BET isothermal curves and MAS NMR spectroscopy, this theoretical model was modified by *Rowles et al., (2003)*, who proposed the planar model for the structure of incompletely reacted and unstable geopolymer. This modified model emphasised the importance of hydration in cement application. The alkali cations are present in the structure in a solved form and they are bonded more weakly than in the crystalline

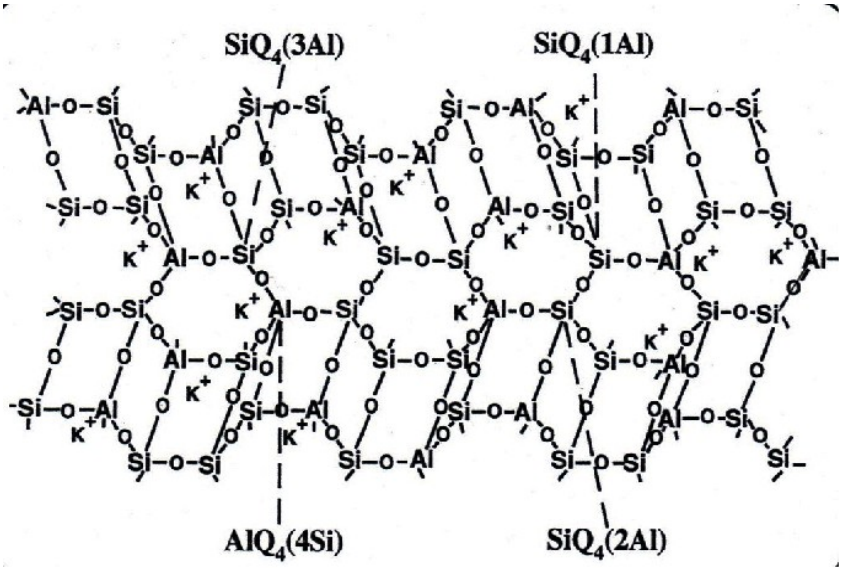

Fig. 1.1. Theoretical structural model for K-poly(sialate-siloxo) geopolymer after *Davidosvits (1991)*.

zeolites' structure. The structure of geopolymer materials is similar to aluminosilicate glasses. Both materials exhibit the same three-dimensional arrangement. However, there is no water present in the glass structure and it is practically without pores. The modified structural model of geopolymer gives consideration to porous body with pores size ranging from nanometers to micrometers (*Skvara (2007)*).

In many respects, the greatest strength of geopolymer technology is also its greatest weakness. It has been found, that some geopolymers may indicate good early strength development, but they become much weaker as time passes (*MacKenzie (2003)*). This effect is still not completely understood and up to now, the conventional mineralogical analysis has not provided satisfactory explanation of hardening mechanism. Nevertheless, without a detailed structural model, which should clarify the changes of aluminosilicate structure over curing time, it is impossible to understand the mechanical and thermal properties of alkali activated cement. The fundamental understanding through the systematic study of hardening process and structural changes in alkali activated binders is the core of this thesis. This work is largely devoted to the one simple homogeneous mixture of fully reacted alkali activated metakaolin (Cem.1), which served as a model of geopolymerization reaction. In order to find out the right composition with the best chemical and mechanical properties, as distinct to other works, which study many compositions with different Si/Al ratios and cations in alkaline solution (*Duxon et al., (2006); Granizo et al., (2007); Rowles et al., (2003)*), the main goal of this thesis is the deep study of one completely reacted mixture to answer to the following questions:

What does exactly happen when geopolymers form?
Why does the strength of alkali activated cements decrease?
What determines the properties of an aluminosilicate gel during ageing?

It is worked out here that only the Cem.1 of special composition with an Si/Al ratio of 2 can be seen as an optimal model system for such a study, although or just because of its decrease of an mechanical strength with longer ageing. In particularly for this geopolymer (Cem.1) the structural rearrangements could be analysed using combination of Molybdate, Infrared and Raman spectroscopy. The study of aluminosilicate glasses is given for the purpose of comparison of Raman and IR spectra.

2. EXPERIMENTAL

2.1. Characterization of raw materials

2.1.1. Metakaolin

Metakaolin is next to slag and fly ash a commonly used starting material for laboratory synthesis of alkali activated cements, although occupies the top position in regards to the consumption of energy, environmental impacts and cost (*Skvara (2003)*). Metakaolin is generated by thermal treatment of kaolinite clay. The dehydroxylation of kaolinite occurs at 550-800 °C and transforms into metakaolin disordered metastable phase. The process is endothermic due to the large amount of energy required to remove the chemically bonded hydroxyl ions. In order to produce a pozzolan, nearly complete dehydroxilization has to be reached without overheating, ie. it must be thoroughly roasted but not burnt. Overheating can cause sintering to form mullite (*Palomo et al., (1992))*. The solid-states NMR studies indicate, that metakaolin contains labile Al in octahedral, tetrahedral and possibly pentatomic coordination. After potassium silicate solution is added to metakaolin, the Al achieves the state of tetraheral coordination. According to *MacKenzie (2003)*, further change of Al coordination remains unchanged even if heated to 1200 °C. The metakaolin amorphous phase may contain some crystalline fraction like muscovite, faujasite and quartz. These residues of kaolin could influence the reactivity of metakaolin. Another factor governing the reactivity of solid is the size of particles. Metakaolin particles are nearly 10 times smaller than cement particles, what results in a denser, more impervious concrete. The increased size of metakaolin particles leads to higher porosity of geopolymer and substantial growth of structural defects, what results in low strength development and decrease of ultimate geopolymers' strength (*Davidovits (2008)*).

2.1.2. Water glass

Water glass is as liquid available or may be freshly prepared from the powder K_2SiO_4 or Na_2SiO_6 using KOH or NaOH solution. Chemically, it is either sodium silicate, potassium silicate or a mixture of both. Water glass is easily soluble in water, but the glassy solid dissolves slowly, even in boiling water. Potassium silicate is stable in neutral and alkaline solutions. In acidic solutions, the silicate ion reacts with hydrogen ions to form silica acids, which form silica gel - hard, glassy substance, while heated and roasted. Water glass has good adhesive properties and it is fire resistant. Alkaline water glass is used mostly for detergents and soap additives. Moreover, alkaline silicate

solution is applied as a cement for glass, pottery, and stoneware; for fireproofing paper, wood, cement, and other substances; for fixing pigments in paintings and cloth printing; for preserving eggs (it fills the pores in the eggshell, preventing entrance of air). In all the applications water glass is used to either create some sort of seal or to increase the binding properties of various products.

2.1.3. Glass

Glasses are highly disordered amorphous systems. The standard definition of a glass is a solid formed by rapid melt quenching. If the cooling is sufficiently rapid, then crystallization is prevented and instead of the disordered atomic liquid's configuration, it is frozen into the solid state at the glass transition temperature T_g. Other substances are added to simplify the processing. For example, the soda makes the glass water soluble and shifts the melting point to lower temperatures. The oxides, such as CaO, MgO, Al_2O_3 are added in order to provide better chemical durability. In this study, the attention was focused on three kinds of glasses: SiO_2 glass, sodium aluminosilicate glasses and potassium silicate glasses. Pure SiO_2 glass has a melting point of over 1700 ^oC and it is made with melting high purity silica into glass. Fused silica is type of glass, that primarily contains silica in amorphous form and is used to make various refractory shapes, such as crucibles, trays, shrouds and rollers for many high temperature processes and glass manufacture. Due to very low metallic impurity content, pure glass SiO_2 is transparent deeper into the UV light. Soda-lime glass does not allow the light to pass at a wavelength lower than 400 nm (UV light). When Na_2O is incorporated in the SiO_2 structure, the Si-O-Si network breaks and forms, non-bridging oxygen (NBO). Thus, in sodium silicate glasses the sodium atoms act as the network modifiers. However, in sodium aluminosilicate glasses with the composition of the Al/Na<1, the sodium atoms also act as charge compensator of the alumina tetrahedra AlO_4^- The non-bridging oxygen in sodium aluminosilicate glasses almost completely disappears at the composition of Al/Na= 1 (*Hanna (1964)*. Potassium silicate glass (K_2SiO_3) is a colorless melt synthesized from potassium carbonate and pure silica sand. As distinct from sodium silicate glass, the potassium silicate glass of equal molar silica to alkali ratio dissolves more rapidly and generally indicates higher refractive index, dispersive powers and electrical resistance (*Iler (1979)*.

2.2. Sample preparation

2.2.1. Preparation of metakaolin based geopolymers

The alkali activated cement Cem.1 (Table 3) characterized by following formula 1.2 K_2O * Al_2O_3 * 4.2 SiO_2 * 14 H_2O was synthesised from metakaolin Metastar 501 (Table 1) and potassium water glass Silirit M 60 (Cognis Deutschland GmbH) (Table 2). Because of homogeneous, almost fully reacted composition, Cem.1 was used for detailed analysis by Molybdate method, FTIR and Raman spectroscopy, thermal analysis, as well for testing mechanical properties.

To prepare one series of Cem.1 for FTIR and Raman experiments, 15 g of water glass and 9 g of metakaolin powder was used. These raw materials were mixed together in glassware manually forming homogeneous slurry. Due to the preparation of small amount of cements, use of automatic mixer was not necessary. After 3 min. of mixing, the geopolymeric yellow slurry (see Fig. 2.1) was transferred into 9 cylindrical alkali resistant moulds (2 cm in diameter and height 1.2 cm) and closed with plexi-cover. Alkali activated cement was kept closed to minimize the contamination with atmospheric carbonation and evaporation of water. The samples were cured at ambient temperature. Cem.1 always transformed from liquid alkali activated cement to rigid form after about 13 h. The solid geopolymer body was characterized with white and plain surface (Fig. 2.2).

Fig. 2.1. The image of geopolymeric slurry prepared by mixing of metakaolin Metastar 501 and potassium water glass . The composition of the mixture is given in Table 3.

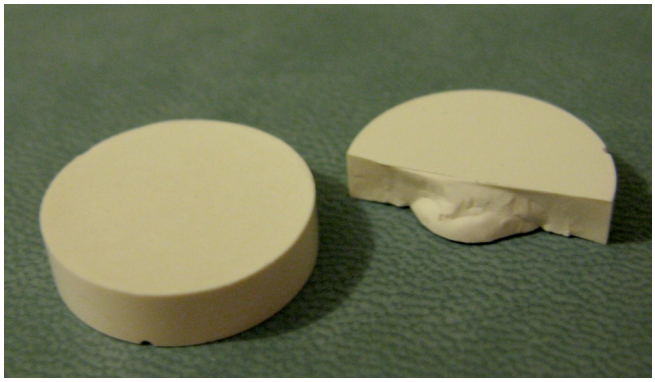

Fig. 2.2. The image of rigid alkali activated metakaolin with molar ratio Si/Al=2.09 cured at room temperature during 20 days.

Table 1:The chemical composition of metakaolin Metastar 501 (England) used for geopolymeric cements (Cem.1, Cem.2, Cem.3, Cem.4, Cem.5, Cem.6, Cem.7, Cem.8) preparation.

Metakaolin Metastra 501	**SiO_2**	**Al_2O_3**	**K_2O**	**H_2O**
Mass [%]	61.5	37.8	-	0.7

Table 2: The chemical composition of potassium water glass Silirit M60 (Cognis Deutschland GmbH) used for geopolymeric cements (Cem.1, Cem.2, Cem.3, Cem.4, Cem.5, Cem.6, Cem.7) preparation.

Potassium water glass	**SiO_2**	**Al_2O_3**	**K_2O**	**H_2O**
Mass [%]	19.3	-	24.5	56.2

Table 3: The chemical composition of potassium geopolymer Cem.1 prepared by mixing of potassium water glass and metakaolin Metastar 501.

Cem.1	**Composition**			
Water glass+Metakaolin 62,5+37,5 [%]	**SiO_2**	**Al_2O_3**	**K_2O**	**H_2O**
Mass [g]	843.0	340.2	367.5	849.3
Molar	4.2	1	1.2	14.2

The composition for the samples used for mechanical strength test is described in the Table 1. Prepared mixture was placed in cylindrical forms 3 cm/1.5 cm and kept closed during hardening process. The tensile and compressive force were measured for geopolymers cured at different temperatures: 25 °C, 50 °C, 90 °C, 130 °C. All data representing strength development are averages obtained from many experiments.

To study ageing effect of geopolymers with excess of water glass and possibly residues of unreacted metakaolin, other 6 compositions of different Si/Al ratio have been prepared. The samples were prepared from metakaolin Metastar 501 and potassium water glass Silirit M60. All alkali activated cements were sealed in plexi boxes and cured at ambient temperature. The variation of Si/Al ratios for Cem.2, Cem.3, Cem.4, Cem.5, Cem.6, Cem.7 resulted from different amount of water glass and metakaolin in each composition (Table 4).

Table 4: The composition of Cem.2, Cem.3, Cem.4, Cem.5, Cem.6, Cem.7 of alkali activated metakaolin (MK-metakaolin Metastar 501, WG-potassium water Silirit M60 *glass).*

Cement	**WG [%]**	**MK [%]**	**SiO_2 [mol]**	**Al_2O_3 [mol]**	**K_2O [mol]**	**Molar ratio Si/Al**
Cem.2	70	30	0.53	0.11	0.19	2.38
Cem.3	55	45	0.64	0.17	0.15	1.9
Cem.4	48	52	0.68	0.19	0.13	1.78
Cem.5	40	60	0.74	0.22	0.11	1.67
Cem.6	30	70	0.81	0.26	0.08	1.56
Cem.7	25	75	0.85	0.28	0.07	1.52

Cem.8 for Raman investigation was characterized with following formula 2.46 Na_2O * Al_2O_3 * 4.4 SiO_2 * 13 H_2O, prepared by mixing sodium water glass with metakaolin Metastar 501 (England). Sodium silicate solution with molar ratios Na_2O * 0.66 SiO_2 * x H_2O was prepared by dissolving fumed silica (Merck 594375) and sodium hydroxide pellets (Merck 106467) in deionized water. The solution was stirred overnight to dissolve completely the fumed silica. The sodium geopolymers were cured in sealed plexi-boxes at ambient temperature. The chemical composition of Cem.8 is given in Table 5. The significant excess of sodium (Na/Al= 2.46) was required for Raman investigations of inorganic binders' ageing process.

Table 5: The chemical composition of sodium geopolymer Cem.8 prepared by mixing of sodium silicate solution and metakaolin Metastar 501.

Cem.8	**Composition**			
Water glass+Metakaolin 65+35 [%]	**SiO_2**	**Al_2O_3**	**Na_2O**	**H_2O**
Mass[%]	34.05	13.23	19.828	30.425
Molar	4.4	1	2.46	13

2.2.2. Preparation of sodium aluminosilicate glasses

Sodium aluminosilicate glasses were prepared using SiO_2 (Merck 594375), Al_2O_3 (Fluka 06157) and Na_2CO_3 (Fluka 88975). The glasses were molten below 1700 ^oC and quenched at room temperature. The pure SiO_2 glass was molten at the highest temperature reaching about 1700 ^oC. The chemical composition of polished glasses: Glass.1, Glass.2, Glass.3, Glass.4 (Fig. 2.3) was verified with help of microprobe analysis (CAMECA SX-100) and given in Table 6. These data were applied in order to calculate the molar ratios Si/Al for each glass and served for further analysis.

Table 6: The chemical composition of glasses (by weight %): Glass.1, Glass.2, Glass.3, Glass.4 . from microprobe measurement (CAMECA SX-100)*, molar ratio Si/Al estimated from microprobe measurement.*

Glass	**SiO_2**	**Al_2O_3**	**Na_2O**	**Molar ratio Si/Al estimated from microprobe measurement**
Glass.1	98.8	0.01	0.02	>1000
Glass.2	90.5	5.8	2.5	12.1
Glass.3	76.3	15.5	7.9	4
Glass.4	68.8	19.9	12.3	2.8

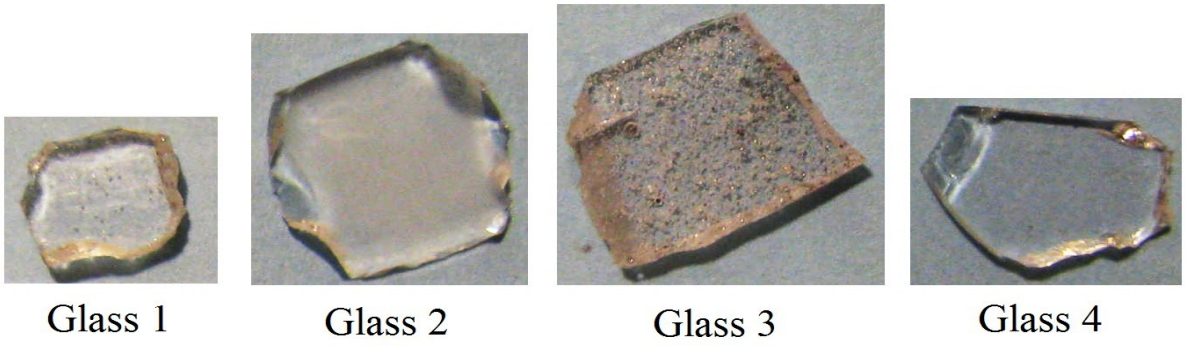

Fig. 2.3. The image of polished SiO_2 glass (Glass.1) and sodium aluminosilicate glasses (Glass.2, Glass.3, Glass.4).

2.2.3. Preparation of potassium silicate glasses

Two different samples of potassium silicate glasses were prepared for FTIR and Raman investigation. The first sample (Glass.5) was synthesized by mixing 8.5163 g of SiO_2 (Merck 594375) and 2.17 g of K_2CO_3 (Merck 104926), the second one (Glass.6) by 7.184 g of SiO_2 and 4.1316 g of K_2CO_3. Both glasses were produced by melting in platinum crucible at 1600 °C. Before heating the compositions were filed in a glass bottle and mixed by shaking the bottle. After taking out the crucible from the oven, the melts were poured out on the brass plate and cooled at room temperature. For a couple of days samples were held in exicator. Before measurement the glasses were polished and analysed with CAMECA SX electron microprobe equipment (CAMECA SX-100) (Table 7). The molar ratios for both glasses: 0.27 K_2O * 1.39 SiO_2 (Glass.5) and 0.37 K_2O * 1.08 SiO_2 (Glass.6) were estimated by means of microprobe analysis. Fig. 2.4 shows pictures of two unpolished samples of potassium silicate glasses.

Table 7: The chemical composition of potassium silicate glasses (by weight %) and molar ratio K/Si for Glass.5, Glass.6 was estimated from microprobe measurement (CAMECA SX-100).

Glass	SiO_2	K_2O	H_2O	Molar ratio K/Si estimated from microprobe measurement
Glass.5	83.5	14.08	1.7	0.39
Glass.6	65.3	20.07	14.63	0.6

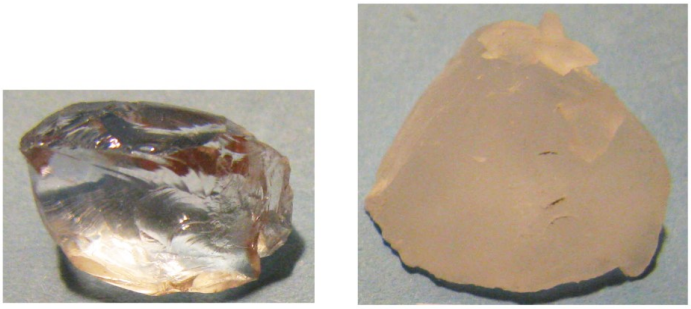

Fig. 2.4. The image of potassium silicate glasses: Glass.5, Glass.6.

2.3. Sample characterization methods

2.3.1. Infrared absorption spectroscopy (IR)

FTIR study was used as an effective tool for characterization the structure and ageing process of amorphous aluminosilicate. IR absorption spectra were taken on a Bruker FTIR iFS66v spectrometer. For the IR investigations 1 mg of sample was diluted into 200 mg of potassium bromide (KBr) and pressed under pressure of 10 tons for 3 minutes into pellet of 13 mm diameter. The IR spectra have been recorded in the infrared range between 370 cm^{-1} and 4000 cm^{-1} at a resolution 2 cm^{-1} for all tests.

2.3.2. Powder X-Ray diffraction (XRD)

X-ray method was used in order to estimate the type of crystalline phases in metakaolin and to study the structural changes after thermal treatment of alkali activated cements. X-ray patterns were recorded with the use of a diffractometer Bruker AXS D4 equipped with CuKα radiation source, over a 2θ range of 1-79.99 ° with a step size of 0.03 °. Before measurement the solid materials were powdered and placed in sample holder.

2.3.3. Raman spectroscopy

Two Raman spectrometers were used. The CRM 200 equipment (WITec GmbH, Ulm, Germany) consist of a confocal Raman microscope with maximal power of 20 mW. In comparison to other CRMs, this instrument is characterized with an efficient throughput of the Raman light. As an

optimal compromise between resolution and throughput a fiber with 50 μm diameter was used. The Raman scattering was excited by frequency-doubled Nd:YAG laser with an excitation wavelength at 532 nm. The laser light was focused onto the sample with a standard objective 20x (numerical aperture (N.A.=0.4). The light was spatially dispersed with a spectrometer (SP-308, Action) with a 6001 lines/mm grating (spectral resolution 12 cm^{-1} spectral accuracy: 2cm^{-1}). The spectra were reordered with a CCD camera (DU401-BR-DD, Andor), which was thermo-electrically cooled down to -70 °C. The second Raman spectrometer was attached to an FTIR spectrometer (Bruker FTIR iFS66v). Here Nd:YAG laser at wavenumber 1064 nm was used. For both the first and second Raman investigations the samples did not required any special preparation process before measurement.

2.3.4. Molybdate method

The Molybdate measurements were helpful in characterizing aluminosilicate gels, as they provided information about chains length of silicate units in silicates and aluminosilicates (*Thilo et al., (1065); Osswald et al., (2006)*. Under defined experimental conditions, easily soluble silicate undergoes the reaction with acids to silica-molybdate complex. The rate of this reaction gives the information about the structure of silicate anions. Following steps may be distinguished in this technique:

1) fast decomposition of -Si-O-Al- bonding at about 2 °C in 0.1 molar hydrochloric acid,
2) decomposition of dimeric, trimmeric, and oligomeric $(–Si-O-Si-)_n$ bonds to monomers at 25 °C in the presence of molybdic acid.

The reaction of silica acid with molybdic acid results in the formation of silica molybdate complex and it is given by the following reaction:

$$H_4SiO_4 + 12\,H_2MoO_4 \rightarrow H_4[Si(Mo_3O_{10})_4] + 12\,H_2O$$

The rate of yellowish silica molybdate acid complex formation is controlled with the use of photometric analysis (at a wavelength of 400 nm). The decomposition of dimeric, trimeric, and oligomeric $(–Si-O-Si-)_n$ bonds requires a longer time then monomers, what is reflected by the slower formation of the silico-molybdic acid complex. Fig. 2.5 shows the typical molybdate plots of characteristic silica anions. Here polymeric chain lengths are defined as 100 % molybdate inactive, which can be reached when the condensates are composed of more than 30 Si-O units.

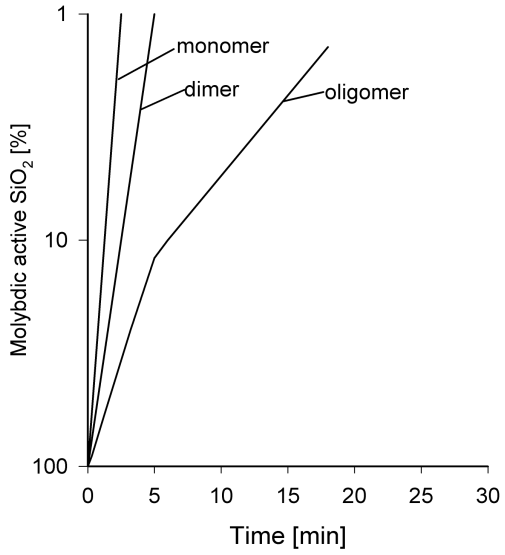

Fig. 2.5. Molybdate reaction curve of silica anions after *Herr et al., (2004)*.

2.3.5. Compressive and flexural force measurement

The mechanical properties of metakaolin based cement (Cem.1) were investigated in accordance with the procedures of European Standard BS EN 196-1:1995. The flexural and compressive force of the 3/1.5 cm cylindrical aluminosilicate pieces have been measured with the means of universal testing machine MEGA 2-3000-100 D, with a device specifically designed for measurement of small testing pieces.

2.3.6. Thermogravimetric measurements

The thermal analysis of aluminosilicates was carried out with SETARAM Setsys Evolution 1650 equipment. Before measurement, the samples were grounded to powder and about 30 mg of powder was put in ceramic crucible. Before heating, the air from chamber was evacuated. Stable He flow (20 ml/min) was kept during measurement. In the first experiment, Cem.1 was heated up to 1000 °C with rate of 2 °C/min and cooled with rate of 10 °C/min. In the second measurement, the alkali activated metakaolin was heated up to 600 °C with rate of 2 °C/min. Before the thermal treatment started, the loss of water was registered at 24 ^{o}C for 1 hour. After heating up to 600 ^{o}C the sample was get out from the sample holder and kept 1 day in the atmosphere of high humidity. Afterwards, the previously heated alkali activated cement was thermally treated again in 600 ^{o}C. The experiment was carried out for geopolymers characterized with different ageing time.

2.3.7. Method of acid leaching

To prepare acids leached sample 40 mg of fine ground geopolymer (Cem.1) and 0.1 ml of 1 % hydrochloric acid was used. The geopolymer powder was placed in small glass box and then carefully mixed with acid added with pipette. Afterwards, the wet sample was lightly shacked and closed. The acid treated cement was left for 2 hours at 4 ^{o}C. The experiment was carried out on geopolymeric cements characterized with different curing time. Five acid leached samples were prepared from each kind of inorganic binder. After the same time of acid leaching process each of the treated powder was used to prepare KBr pellet and tested with FTIR spectroscopy.

2.3.8. Microprobe analysis

The glasses were polished and coated with carbon layer for microprobe measurement. The chemical analysis of those samples was carried out with electron microprobe CAMECA SX-100, equipped with five wavelength-dispersive spectrometer and energy dispersive X-ray analyser. The samples were investigated, with the use of 10 nA beam current and 10 μm beam diameter. The integration time for silica and aluminium was 10 s. All data were obtained with the use of 15 kV acceleration potential.

2.3.9. SEM/EDX measurement

Scanning electron microscopy (SEM) and energy dispersive X-ray (EDX) micro-analysis were performed on JOEL JSM 6060 and JOEL 7000F analytical SEM equipment with an accelerating voltage of 20 kV. Additionally, EDX informations were collected with means of the first mentioned equipment. Before measurement, the samples were crushed and coated with gold using gold/palladium sputter coater in order to form a conducting surface layer.

2.3.10. TEM measurement

Transmission Electron Microscopy analysis (TEM) was carried out with means of JEOL 2100 Cryo TEM equipment. The alkali activated cement was grounded and then diluted with acetone. The solution was accurately mixed by shaking the bottle for 3 min. Small amount of solution was transferred onto TEM grid holders with the use of a pipette. After acetone evaporation, the TEM grid holders were carbon coated and examined with the TEM at an operating voltage 200 kV.

3. RESULTS

3.1. X-Ray, SEM and TEM experiments

The XRD powder diffraction pattern of metakaolin Metastar 501 and alkali activated metakaolin (Cem.1) are shown in the Fig. 3.1. The typical X-ray diffractograms of both the metakaolin and geopolymer indicate a characteristic broad hump centered between 24-27° 2θ and 27-29° 2θ, respectively. Sharps peaks show the presence of crystalline impurities, which have been assigned with means of Rietveld software to: muscovite ($KAl_2(AlSi_3O_{10})(F,OH)_2$), quartz ($SiO_2$), anatas ($TiO_2$) and mullite ($3Al_2O_32SiO_2$ or $2Al_2O_3SiO_2$). It is seen that geopolymerization results in a hump shift. This shift is consistent with the literature information (*MacKenzie (2003); Barbosa et al., (2000))*. The study of aging process at further stage of geopolymerization with X-ray diffraction pattern doesn't indicate any obvious changes. The impurity phase remain mostly unreacted (*Davidovits (2008))*.

The X-Ray diffraction pattern of six different compositions of alkali activated cement is given in Figure 3.2. Each cement indicates broad peak characterized with different intensity and peak's width. The broadening is determined with the composition and increases with the rise of metakaolin amount at the cost of water glass. The normalized half-width of broad hump related to alkali activated cements presented in the Fig. 3.2 is shown in Table 8. The half-width grows

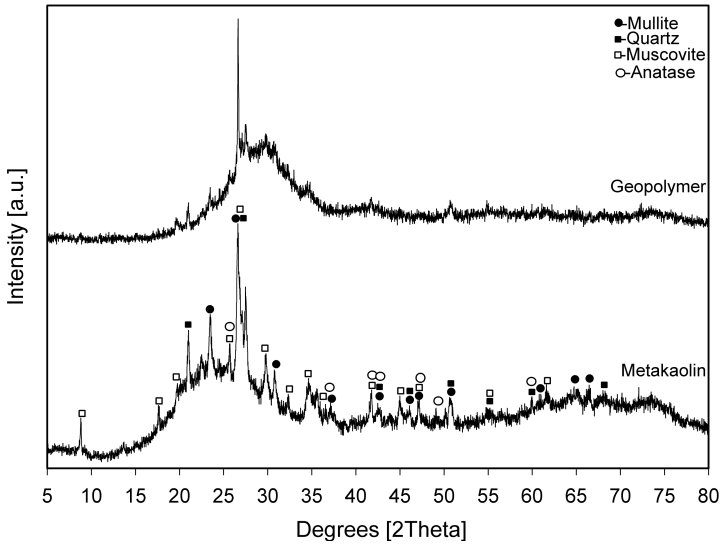

Fig. 3.1. X-Ray difftactogram of metakaolin Metastar 501 and alkali activated metakaolin with molar ratio Si/Al=2.09 aged 200 h at 25 °C. X-ray patterns were recorded with powder diffraction method using a diffractometer Bruker AXS D4 equipped with CuKα radiation source in Institute of Mineralogy Hannover. The determination of crystal fraction of metakaolin based geopolymer was realized with Rietveld-Refinement software.

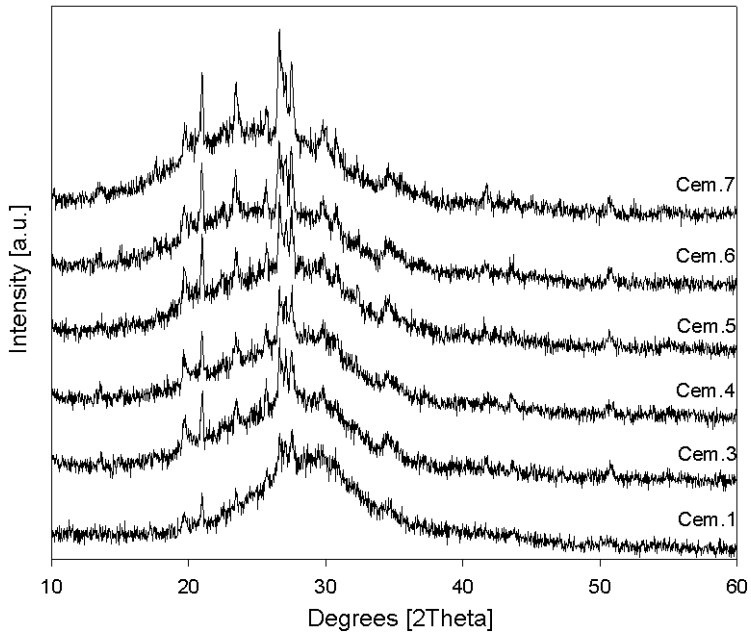

Fig. 3.2. X-ray diffraction pattern of Cem.1, Cem.3-7 aged about 200 h at 25 °C.

systematically with the increase of metakaolin amount. The broadest peak is observed for Cem.7, which contains the highest portion of metakaolin and the lowest amount of alkaline solution.

Table 8: The normalized half-width of Cem.7-3 and Cem.1 broad hump seen in the diffraction patterns given in Fig. 3.1.

Cement	Normalized half-width
Cem.7	1
Cem.6	0.9
Cem.5	0.86
Cem.4	0.78
Cem.3	0.69
Cem.1	0.54

The narrowest hump is noted for Cem.1, which has been prepared from the lowest mass of aluminosilicate solid and the largest amount of water glass. While decreasing the mass of water glass the intensity of the right peak shoulder diminishes in favor of the left one. The effect of the change in water glass to metakaolin will be investigated in more detail also by means of IR and Raman spectroscopy.

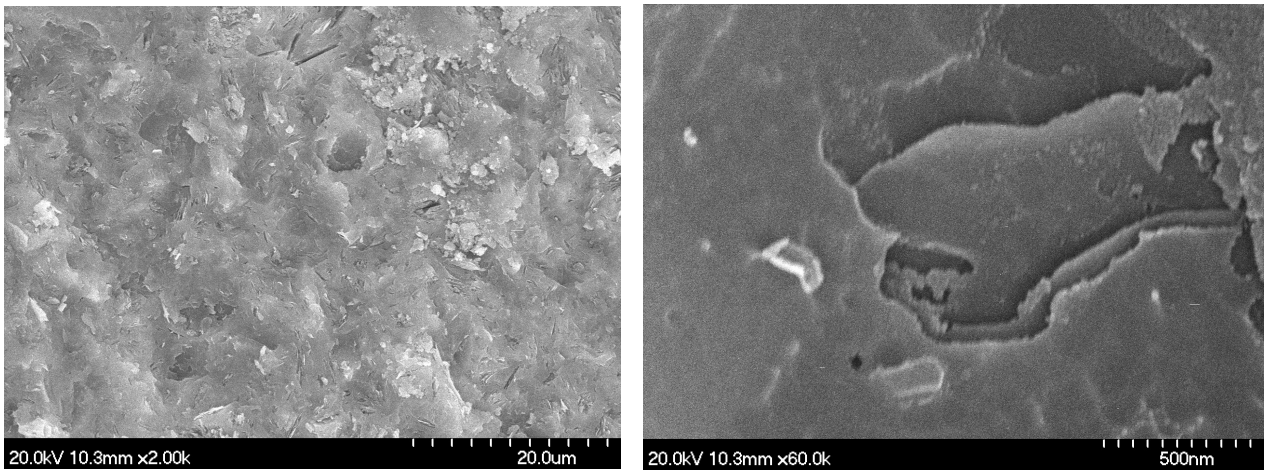

Fig. 3.3.SEM micrographs of alkali activated metakaolin (Metastar 501) with ratio Si/Al=2.09 synthesized from metakaolin and potassium silicate solution at higher and lower magnification. These images were obtained in Frederic Seitz Materials Research Laboratory (University of Illinois at Urbana- Champaign) with JOEL 7000F Analytical SEM equipment.

SEM investigations were carried out on alkali activated cement (Cem.1) cured 200 h at room temperature. As it has been showed in Fig. 3.3, the surface is characterized with fine and dense micro-structure with very low concentration of non-reacted material and porosity. The SEM studies of ageing process of Cem.1 did not show any characteristic variation in the structure of the same tested specimen. An averaged Si/Al=1.9 ratio of metakaolin based geopolymer (Table 9) was estimated by means of EDX analysis, which is in good agreement with theoretical molar ratio Si/Al=2.09 calculated from the initial composition.

Table 9: The averaged mass and molar content of Si, Al, K estimated from elemental EDX analysis of Cem.1.

Content	Si	Al	K
Mass [%]	22.5	11.08	18.86
Molar	0.80	0.42	0.4

The example of TEM micrographs of metakaolin based geopolymer (Cem.1) is seen in Fig. 3.4. Magnification of the right picture is 5 times higher than left picture at 10 nm and 2 nm. The selected areas represent fully reacted amorphous material and characteristic nanosized micro-structure. Until

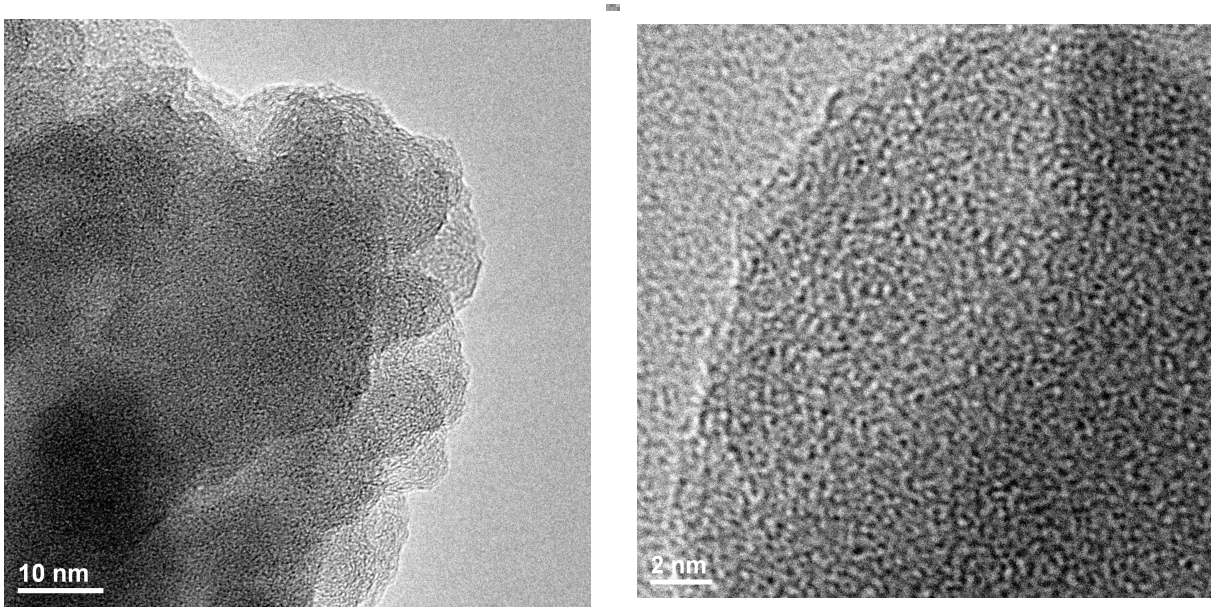

Fig. 3.4. TEM bright field micrographs of geopolymer with ratio Si/Al=2.09 synthesized from metakaolin Metastar 501 and potassium silicate solution. This image was carried out in Frederic Seitz Materials Research Laboratory (University of Illinois at Urbana- Champaign) by JOEL 2100 Cryo TEM equipment.

now, it is not clear, how the dark and bright spots should be interpreted. The systematic TEM investigations of aging process didn't indicate any changes in the structure. Besides, due to the loss of water at the beginning of each measurement, the shrinkage of analyzed specimens was observed.

3.2. Infrared spectroscopy of glasses and geopolymers

3.2.1. Infrared spectroscopy of glasses

FTIR spectroscopy of silica and sodium aluminosilicate glasses

Figure 3.5 shows the absorption spectra of four glasses compositions Glass.1-4 in the spectral range of 400-2000 cm^{-1}. The spectra were obtained with pressed pellet method. The molar ratios of all samples were calculated from the mass ratios estimated with help of micro-probe measurement (Table 6).

According to *Handke et al., (1992)* the infrared spectra of glasses generally consist of following characteristic vibrations: rocking (400-470 cm^{-1}), bending (700-800 cm^{-1}), stretching (1000-1200 cm^{-1}). The positions of bands at 480 cm^{-1}, 800 cm^{-1}, 1105 cm^{-1} in the spectrum of SiO_2 glass (Glass.1) are in good agreement with the literature. According to *Hanna et al., (1964)*, these vibrations correspond to the silicon-oxygen bending mode, stretching mode associated with oxygen atoms, stretching mode associated with silicon atoms, respectively. Glass.4 and Glass.3 indicate the deformation mode at 464 cm^{-1}, while in the spectra of Glass.2 and Glass.1 these vibrations are seen at 469 cm^{-1} and 470 cm^{-1}, respectively. In the further frequency region, the distribution of peak

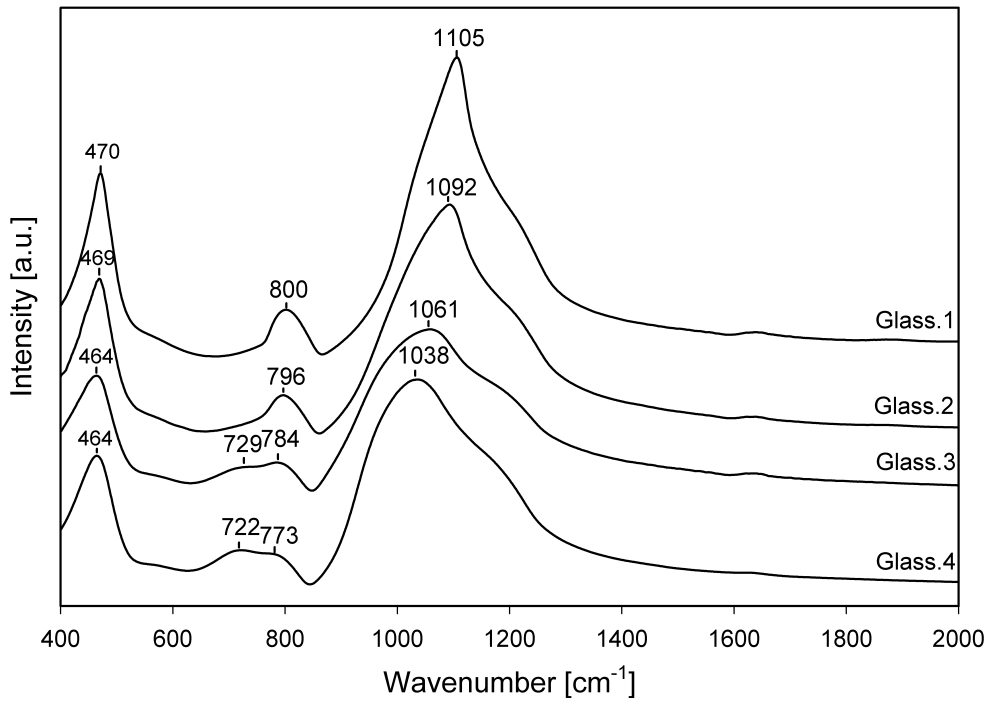

Fig. 3.5. FTIR spectra of Glass.1, Glass.2, Glass.3, Glass.4.

intensities are more diversified. The range 700-800 cm^{-1} is characterized with two maximums. The increase of silica content leads to the shift of the second maximum, resulting in peaks at: 773 cm^{-1}, 784 cm^{-1}, 796 cm^{-1}, 800 cm^{-1} for Glass.4, Glass.3, Glass.2 and Glass.1, respectively. Gradually decrease of Al leads to lower intensity of the first maximum and finally to its complete disappearance. According to some literature, the regime 650-860 cm^{-1} is attributed to the number of $Si\text{-}O^{-}$ non-bridging oxygen bonds, while the peak shift to higher frequencies is related to higher polymerization of three dimensional aluminosilicate framework (*Hanna et al., (1964))*. The absorption band at 722 cm^{-1}, which was found in sodium aluminosilicate glass does not exist in the spectra of silicate glasses, which is explained by the absence of Al-O bonds (*Handke et al., (1992))*.

The most intensive band in the range of 1000-1200 cm^{-1} could represent a superposition of some bands situated close to each other. The maximum of asymmetrical stretching is observed at 1036 cm^{-1}, 1058 cm^{-1}, 1092 cm^{-1} and 1105 cm^{-1} for Glass.4, Glass.3, Glass.2 and Glass.1, respectively. Introduction of aluminum into the silicate network shifts 1105 cm^{-1} peak towards lower wavenumbers. Moreover, the increase of Al content results in lower intensity and peak broadening. Hence, the highest band width is indicated by Glass.4 and the smaller one is exhibited by Glass.1.

FTIR spectroscopy of potassium silicate glasses

Fig. 3.6 shows the infrared spectra of two potassium silicate glasses in the range of 400–2000 cm^{-1}. According to Table 7, the glasses are characterized with different molar ratios K/Si: 0.38 (Glass.5), 0.68 (Glass.6). The absorption spectra of potassium silicate glasses are very similar to the infrared spectra of aluminosilicate glasses. However, the peaks appear at somewhat different frequencies. According to the literature, three major bands are related to the following characteristic vibrations: silicon-oxygen bending mode (400-470 cm^{-1}), stretching mode associated with oxygen atoms (700-800 cm^{-1}), stretching mode associated with silicon atoms (950-1200 cm^{-1}). Glass.5 exhibits distinct lines at 465 cm^{-1}, 785 cm^{-1} and 1081 cm^{-1}. In the spectrum of Glass.6 these characteristic bands are displaced to lower frequencies: 461 cm^{-1}, 766 cm^{-1}, 1021 cm^{-1}. Moreover, both glasses additionally show the maximum at 1630 cm^{-1}, what is related to the water bending mode vibrations. The high intensity for Glass.6 compared to Glass.5 indicate a high content of water. Evaluation of microprobe data could imply a water content of 1.7 % and 14 % of total mass for Glass.5 and Glass.6, respectively (Table 7). Introducing of potassium ions into the silicate structure shifts the maximum of all peaks towards lower wave numbers. The most radical changes are seen in the high frequency

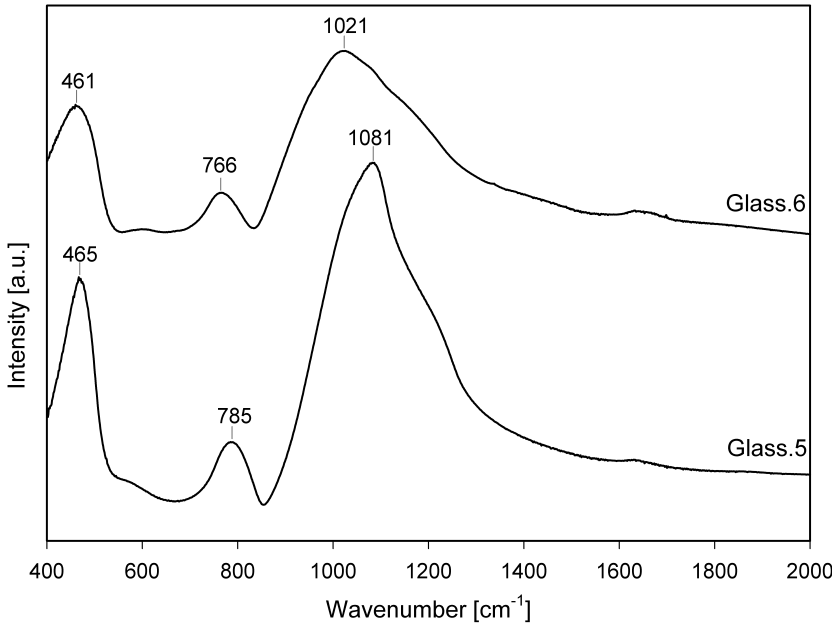

Fig 3.6. FTIR spectra of potassium silicate glasses: Glass.5, Glass.6.

region, where the increase of alkali oxide content has led to the peak displacement from 1081 cm^{-1} to 1021 cm^{-1}. This effect is explained with the decrease of the force constant due to the higher concentration of the non-bridging oxygen atoms of the $Si\text{-}O^-$ interaction with Na^+ ions (*Handke et al., (1992))*. The spectrum of potassium silicate glass with higher content of alkali ions is characterized with higher width and lower intensity of T-O-T band.

3.2.2. Infrared spectroscopy of metakaolin-based Cem.1

Infrared vibrations of metakaolin-based geopolymer

IR characteristic bands of geopolymer and relevant vibrations are listed in Table 10. Interpretation of these vibrations is based on assignments given in the literature for inorganic binder, irrespectively of initial composition. Fig. 3.7 shows the IR spectra in the range of 400-1200 cm^{-1} of metakaolin Metastar 501 and geopolymer aged 100 h at room temperature. The absorption pattern of raw aluminosilicate exhibits peaks at: 460 cm^{-1}, 588 cm^{-1}, 644 cm^{-1}, 803 cm^{-1} and 1070 cm^{-1}. The band at 460 cm^{-1} is assigned to Si-O in-plane bending vibration, while the band at 644 cm^{-1} is related to Si-O symmetrically stretching vibration (*Yunsheng et al., (2008))*. A peak at 588 cm^{-1} is also seen in the spectrum of alkali activated geopolymer, which should, however, be an indication of a newly formed structure element in a geopolymer. The 803 cm^{-1} band is caused by six-coordinated Al–O

stretching vibration, which disappears in IR spectrum of alkali activated Cem.1. This means, that in dissolution process six-coordinated Al transforms into another coordination.

Geopolymerization shows obvious changes in IR spectrum of raw solid material, which results from the formation of new products with different micro-structure. The bands at 440 cm^{-1}, 588 cm^{-1}, 702 cm^{-1}, 880 cm^{-1}, 1016 cm^{-1}, 1371 cm^{-1}, 1435 cm^{-1}, 1640 cm^{-1} represent typical infrared pattern of metakaolin based geopolymer with molar ratio Si/Al=2.09. The strongest vibrations are seen in the regions of 420-500 cm^{-1} and 950-1250 cm^{-1} related to bending mode of Si-O-Si, O-Si-O vibrations and asymmetric stretching of Si-O-Si and Si-O-Al, respectively. 702 cm^{-1} band appears as the consequence of dissolution process, which is assigned to Si-O-Si and Al-O-Si symmetric stretching. The band at 880 cm^{-1} corresponds to Si-O stretching in Si-OH group. The major peak at 950-1250 cm^{-1} has been assigned to the asymmetric stretching of Si-O-Si and Si-O-Al. During geopolymerization, the prominent band at 1070 cm^{-1} in IR spectrum of metakaolin shifts to 1016 cm^{-1}. The character of the shift depends on the initial composition of alkali activated binder and was attributed to the partial replacement of SiO_4 tetrahedron by AlO_4 tetrahedron, resulting in change in the local chemical environment of Si-O bond. The peak in range 1400-1480 cm^{-1} which are absent in metakaolin, are due to potassium carbonate species. All geopolymers show a peak at 1640 cm^{-1} and a broad absorption peak in the range of 2800-3800 cm^{-1} related to the H-OH bending and O-H stretching vibrations of the water included molecules.

Table 10: The identification of IR bonds and relevant wavelength for geopolymers from literature.

Wavelength [cm^{-1}]	**Group**	**References**
420-500	bending Si-O-Si and O-Si-O	[5, 49, 60, 83,]
500-690	symmetric stretching Al-O-Si	[49]
690-830	Si-O-Si and Al-O-Si symmetric stretching	[5, 49, 83, 68,]
830-950	Si-O stretching in Si-OH groups	[11, 29, 49]
950-1250	asymmetric stretching Si-O-Si Si-O-Al	[29, 30, 43, 49, 57, 66]
1400-1480	O-C-O	[43,60]
1630-1660	bending mode of molecular water H-O-H	[6, 43, 60]
2800-3800	O-H stretching	[43, 60, 66]

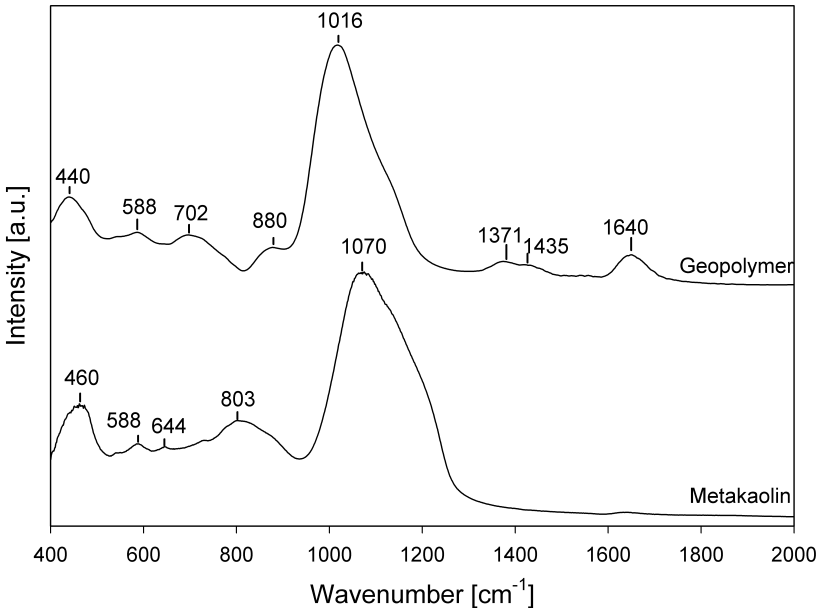

Fig. 3.7. The FTIR spectra of metakaolin Metastar 501 and alkali activated metakaolin (Cem.1) after 100 h of curing at room temperature.

FTIR study of ageing process of Cem.1

The detailed study of ageing process of metakaolin based geopolymer (Cem.1) was carried out with help of FTIR spectroscopy. Fig. 3.8 represents series of the IR spectra of alkali activated cement recorded after different curing time. The analysis was performed for geopolymers characterized with the same compositions, curing conditions and preparation time, several times showing the same results. The spectra of potassium water glass and metakaolin have been given to show the relation between IR spectra of raw materials and corresponding geopolymer.

After one hour of ageing bending mode shifts from 455 cm^{-1} to 440 cm^{-1} and remains at the same position during further ageing. The next characteristic vibration at 588 cm^{-1} is visible both in the IR spectra of metakaolin Metastar 501, but becomes more pronounced during ageing of Cem.1. The intensity of symmetrical stretching at 702 cm^{-1} increases during first 2 days of ageing and remains unchanged during further ageing. The peak 880 cm^{-1} related to the Si-O stretching in Si-OH groups, shows visible changes in intensity over ageing. The detailed analysis of this infrared vibration in relation to ageing time will be given below.

Strong changes both at earlier and later stage of geopolymerization are observed in the range of asymmetrical stretching. The position of the maximum of this peak will be called DOSPM (density

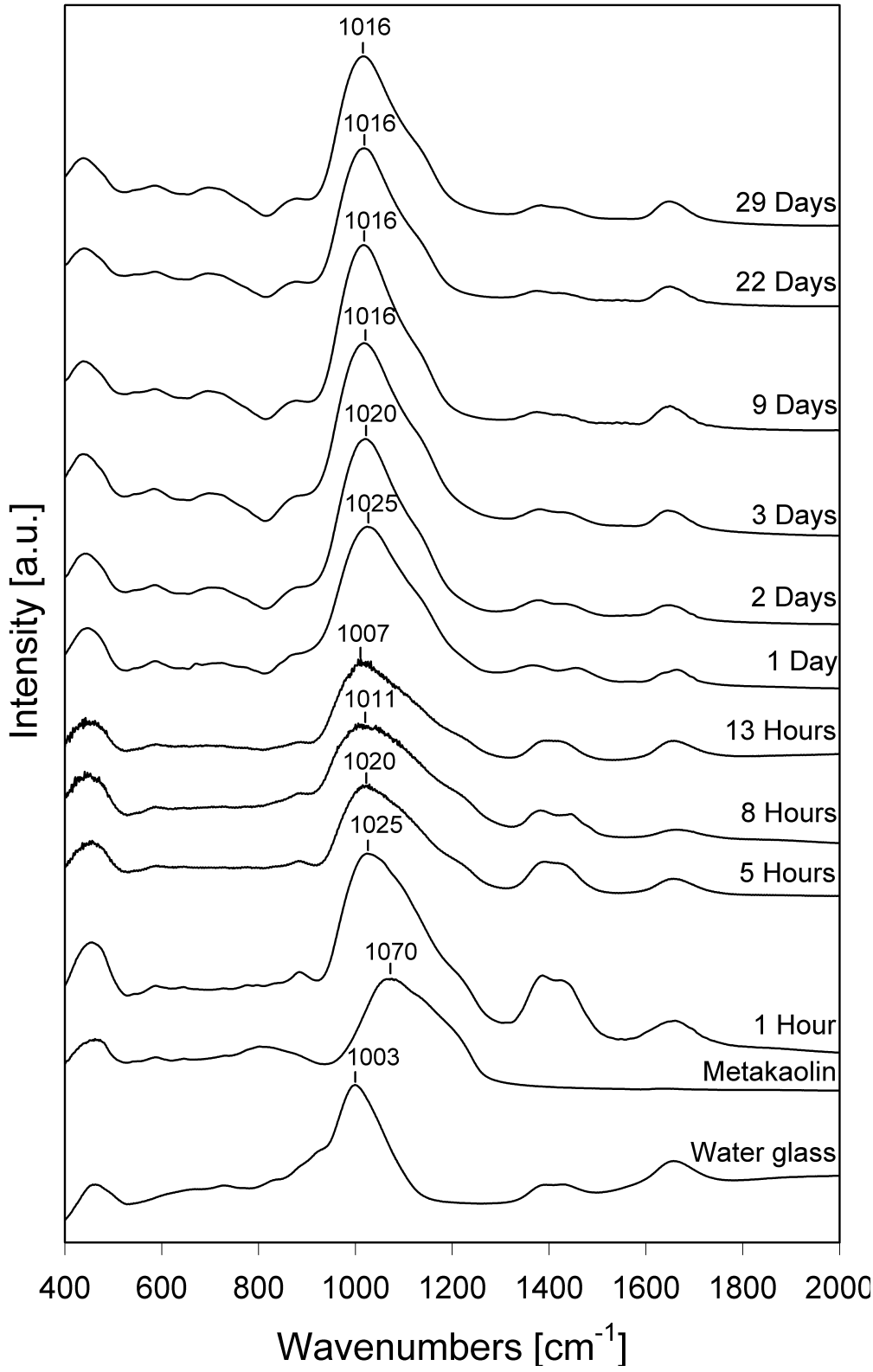

Fig. 3.8. The FTIR study of alkali activated metakaolin (Cem.1) during 29 days of ageing at room temperature; infrared absorption spectra of potassium water glass and metakaolin Metastar 501.

of states peak maximum). After stirring the metakaolin diluted with alkaline solution and taking a spectrum after 1 h and 5 h the DOSPM shows the maximum at about 1025 cm^{-1} and 1010 cm^{-1}, respectively. This trend continues up to 1007 cm^{-1} at 13 h of ageing. For ageing above 13 h the DOSPM shifts back towards higher wavenumbers and after 24 h of ageing reaches the position at 1025 cm^{-1}. Above 24 h a systematic displacement in the DOSPM again turns back to 1020 cm^{-1} after 48 h, and further to 1016 cm^{-1} after 72 h. Above about 3 days of ageing DOSPM remains at the same position but covers further structural changes as shown below. The variation of the DOSPM during ageing is shown in Fig. 3.9. The peaks at 1371 cm^{-1} and 1435 cm^{-1} are related to the presence of carbonate species. The highest concentration of O-C-O stretching is seen at the beginning of curing.

The preparation of KBr pellets with 1 mg of this sample was difficult due to the fluid and thick consistency of alkali activated cement during first 24 h of ageing. The sharpening of asymmetrical stretching band during further ageing is related with the hardening process. Thus at earlier stage of geopolymerization the region of 950-1200 cm^{-1} is characterised with broad peak and broad maximum. The trend of DOSPM development during first day of ageing was verified by several measurements showing similar results to those shown for Cem.1.

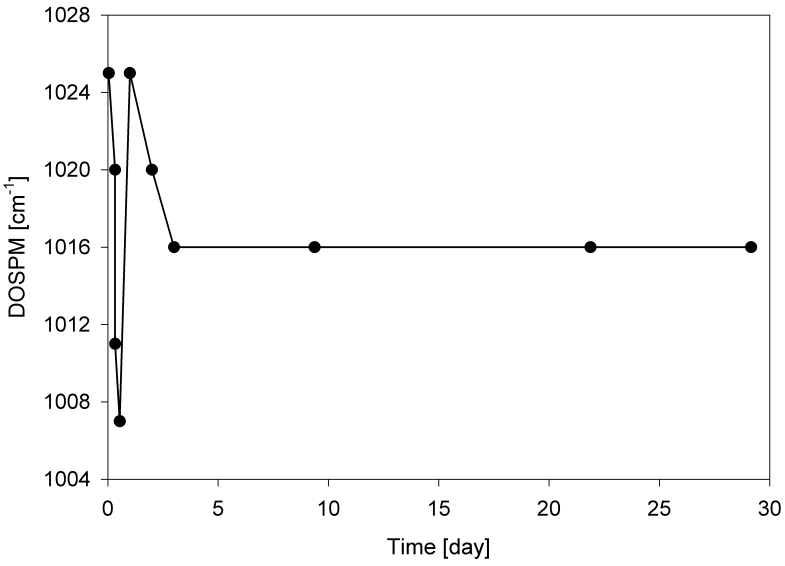

Fig. 3.9. The dependence between DOSPM of asymmetrical stretching and ageing time of Cem.1 estimated from FTIR study of ageing process given in the Fig. 3.8.

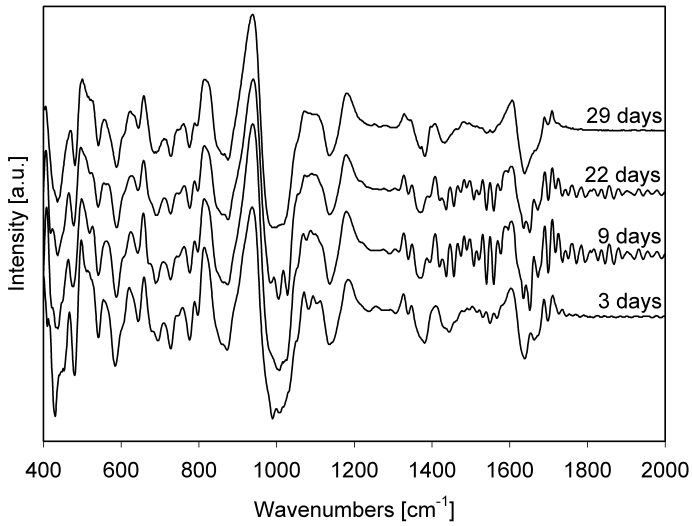

Fig. 3.10. The second derivative of FTIR spectra of Cem.1presented in the Fig. 3.8 after 3 days, 9 days, 22 days and 29 days of curing at room temperature.

Although the DOSPM above about 100 h of ageing remains unchanged (Fig. 3.9), there are structural changes. In order to show this, the IR spectra recorded after 3 days, 9 days, 22 days and 29 days of ageing were transferred to the second derivative (Fig. 3.10). It is seen that**,** the distribution of intensity around the DOSPM is different. These results thus suggest the presence of structural development in further stages of geopolymerization.

Infrared vibrations of water glass and high condensed alkaline solution

The potassium silicate solution is sensitive for pH changes and polycondensation of silicate units occurs upon the reaction with acid (*Iler (1979)*. This effect was studied by FTIR spectroscopy.

The infrared spectra of potassium water glass and silicate solution reacted with hydrochloric acid shows strong changes relative to unreacted water glass (Fig. 3.11). The infrared spectrum of water glass is characterized by the vibrations: 460 cm^{-1}, 730 cm^{-1}, 835 cm^{-1} in the range of lower frequency. The lowest frequency mode is ascribed to O-Si-O bending mode. A band at 835 cm^{-1} corresponds to the vibrations of silanols groups. The most dominant band appears at 1003 cm^{-1}, which is related to asymmetric Si-O stretching of monomeric and dimeric groups. The position of that band obviously depends on the concentration of alkali ions and the degree of silicate condensation. The value of the Si-O stretching frequency has been observed in many silicate solutions close to 1000 cm^{-1} and is assigned to isolated tetrahedra (*Beard (1972)*). In the further

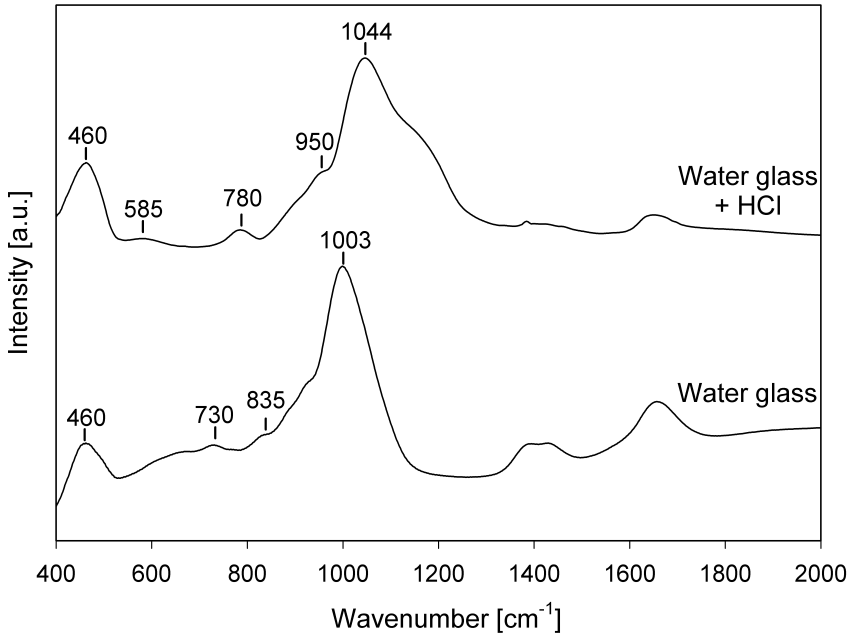

Fig. 3.11. The FTIR study of potassium water glass solution and potassium water glass reacted with hydrochloric acid pressed in KBr pellets.

frequency range O-C-O (1380 cm^{-1}, 1430 cm^{-1}) and water bending vibrations (1655 cm^{-1}) are visible. As it has been noted, only the peak at 460 cm^{-1} is insensitive for pH change and it remains at the same position after acid treatment. However, the rest characteristic bands shifts to other positions: 585 cm^{-1}, 950 cm^{-1}, 1044 cm^{-1}. Condensation of silica leads to broadening of Si-O bands and the appearance of shoulders. The 950 cm^{-1} peak is related to the stretching vibrations of the silanol groups. According to the literature, the shift of characteristic peak in the range of asymmetrical stretching from 1003 cm^{-1} to 1044 cm^{-1} corresponds to the condensation and the increase of molecular weight of the relevant silicate species (*Osswald et al., (2006)*.

DOSPM of asymmetrical stretching of Cem.1

The ageing behaviour of Cem.1 were investigated in 6 more series as given in the Fig. 3.12. The averaged values of DOSPM are shown in the Fig. 3.13. The attention has been focused on DOSPM development between 1st and 29th day of curing. According to that, DOSPM development of Cem.1 might be divided into two stages: I) below 100 h characterized with the DOSPM shift towards lower frequencies, II) above 100 h with stable DOSPM. Similar tendency of DOSPM displacement has been seen for all tested sets of Cem.1. However, the initial and final peak position have not been the same for every geopolymer tested after 24 h and 100 h of ageing, respectively. The position of

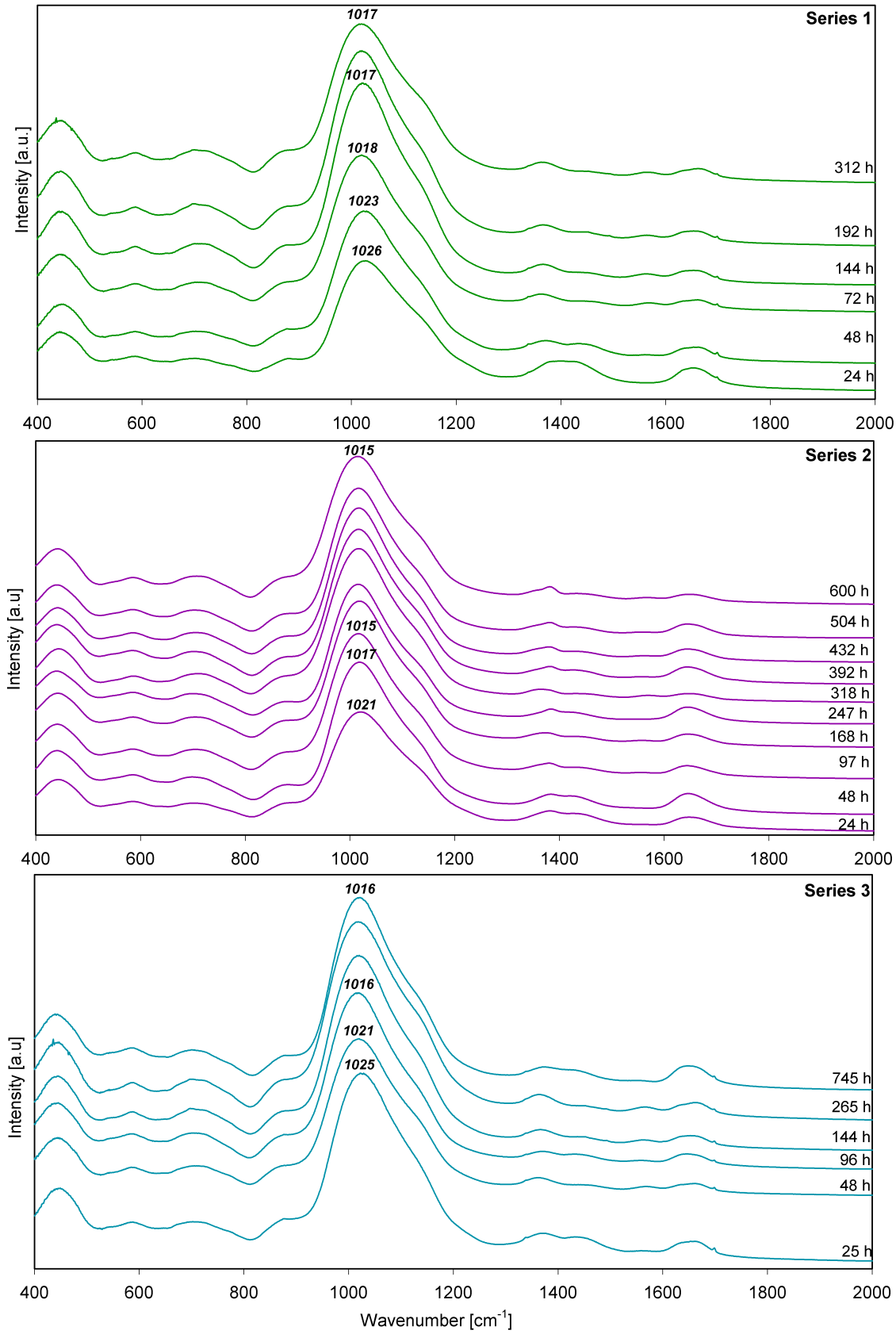
Series 1
1017
1017
1018
1023
1026
312 h
192 h
144 h
72 h
48 h
24 h
Intensity [a.u.]
Series 2
1015
1015
1017
1021
600 h
504 h
432 h
392 h
318 h
247 h
168 h
97 h
48 h
24 h
Intensity [a.u]
Series 3
1016
1016
1021
1025
745 h
265 h
144 h
96 h
48 h
25 h
Intensity [a.u]
400
600
800
1000
1200
1400
1600
1800
2000
Wavenumber [cm-1]

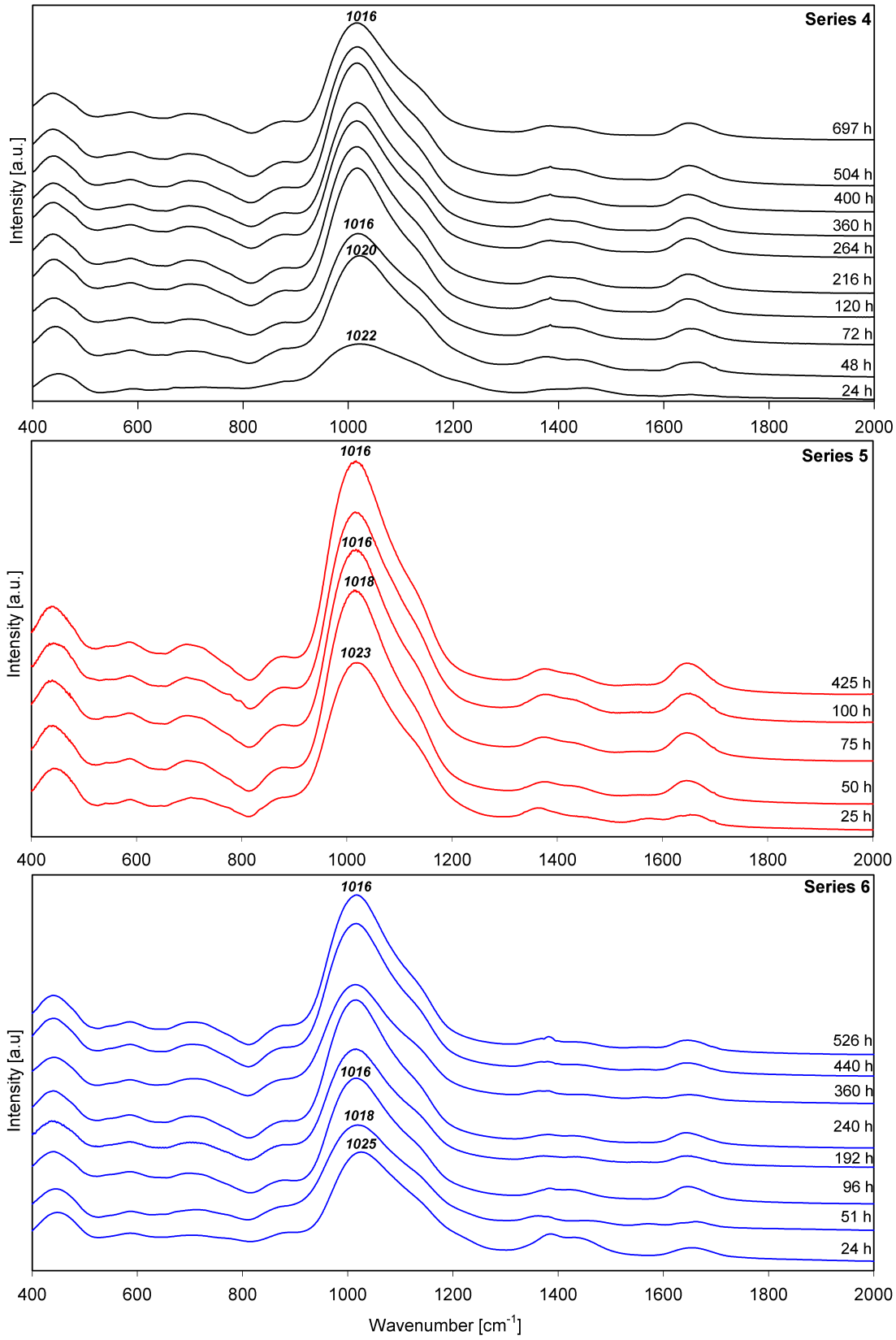

Fig.3.12. The infrared study of ageing process of Cem.1.

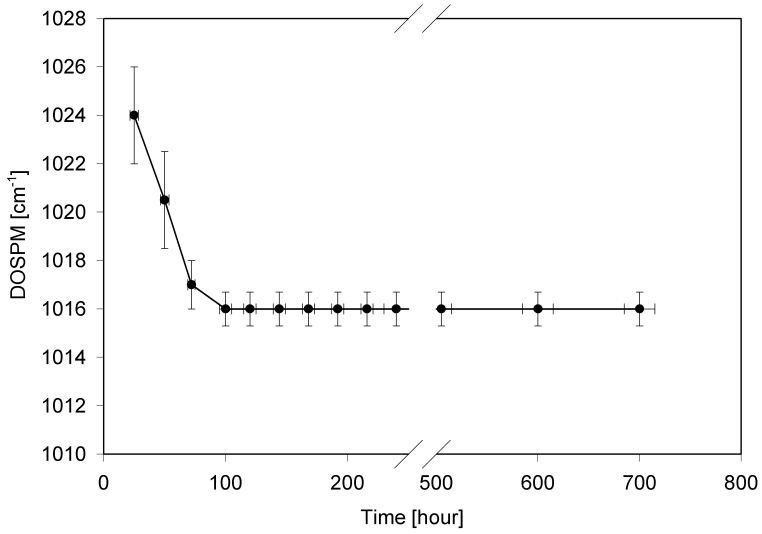

Fig.3.13. The averaged development of DOSPM of asymmetrical stretching over curing time of Cem.1. The average dependence between DOSPM and ageing time was estimated from infrared measurement given in the Fig. 3.12.

DOSPM for Cem.1 after 1 day, 2 days and 4 days of ageing oscillates in the range of 1022-1026 cm^{-1}, 1018-1022 cm^{-1}, 1017-1015 cm^{-1}, respectively. Some series of Cem.1 reach the final DOSPM after about 3 days, whereas another geopolymer require 4 days. Cem.1 with DOSPM at 1025 cm^{-1} or at higher wavenumbers after 24 h of curing reaches the final DOSPM at 1016-1017 cm^{-1} after 3-4 days of ageing (series 1, 3, 6). However, Cem.1 with a DOSPM at 1025 cm^{-1} or at lower wavenumbers after 24 h of curing gains the final position in the range of 1016-1017cm^{-1} (series 2, 4, 5).

Study of Si-OH and H-O-H vibrations in Cem.1

A variation in peak intensity has been observed in the infrared regime assigned to Si-OH vibration (830-910 cm^{-1}) and bending mode of H_2O (1630-1660 cm^{-1}) (Fig. 3.12). In order to find out the relation between the intensity in both regions and ageing time, a method for precise estimation of peak intensity has been worked out. With help of OPUS software from BRUKER the intensity at 880 cm^{-1} and 1640 cm^{-1} has been measured from 6 series (Fig. 3.12) together with spectra spectra recorded from separated FTIR measurement. The basis line for intensity estimation at 880 cm^{-1} has been set up parallel to the axis of wavenumber axis, drawn through the point of the lowest intensity at 810 cm^{-1}. The basis line for the intensity determined at 1640 cm^{-1} has been set up parallel to to the intensity axis, drawn through the point of minimal intensity in the range of 2000-2500 cm^{-1}.

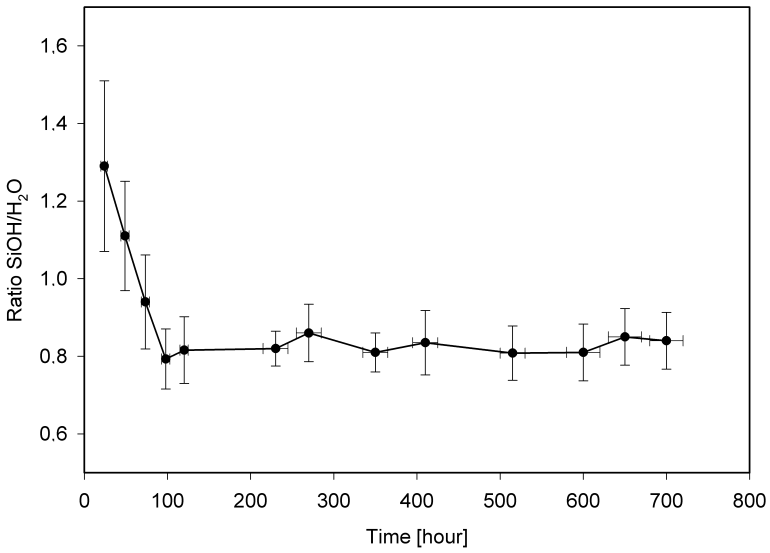

Fig.3.14. The averaged variation of SiOH/H_2O ratio over ageing time of Cem.1.

The values has been calculated from intensities read out at different frequencies in the range of Si-OH vibrations to exclude the influence of DOSPM shift on the value of SiOH/H_2O ratio. The changes of SiOH/H_2O ratio over ageing time were similar irrespective of frequency at which the intensity was read out, therefore intensities obtained at 880 cm^{-1} and 1640 cm^{-1} were used. The dependency between the arithmetical mean of ratio SiOH/H_2O and ageing time of Cem.1 is given in Fig. 3.14. The maximal ratio SiOH/H_2O=1.29 is reached after 24 h of ageing. During further ageing, the intensity of SiOH band decreases gradually and after about 100 h it achieves the minimum of SiOH/H_2O ratio followed by a rather slight increase during further curing. Similar tendency in SiOH/H_2O changes over ageing has been observed for all tested sets of Cem.1. The variation of intensity of SiOH and H_2O bands indicates some relation to DOSPM development. Moreover, the minimum of intensity at 100 h of 880 cm^{-1} band correlates with the dynamics of DOSPM shift from 1025 cm^{-1} to 1016 cm^{-1}.

Another indication from acid leaching experiments

To prepare acid leached sample, the drop of HCl acid has been placed on the surface of the sample. After several minutes, the reacted layer has been separated from the non-reacted part and mixed with 200 mg of potassium bromide. Fig. 3.15 shows, that the characteristics infrared bands of Cem.1 appear at 440 cm^{-1}, 588 cm^{-1}, 702 cm^{-1}, 880 cm^{-1}, 1016 cm^{-1}, 1371 cm^{-1}, 1435 cm^{-1}, 1640 cm^{-1} before reaction. After reaction with high concentrated hydrochloric acid the position of all peaks is

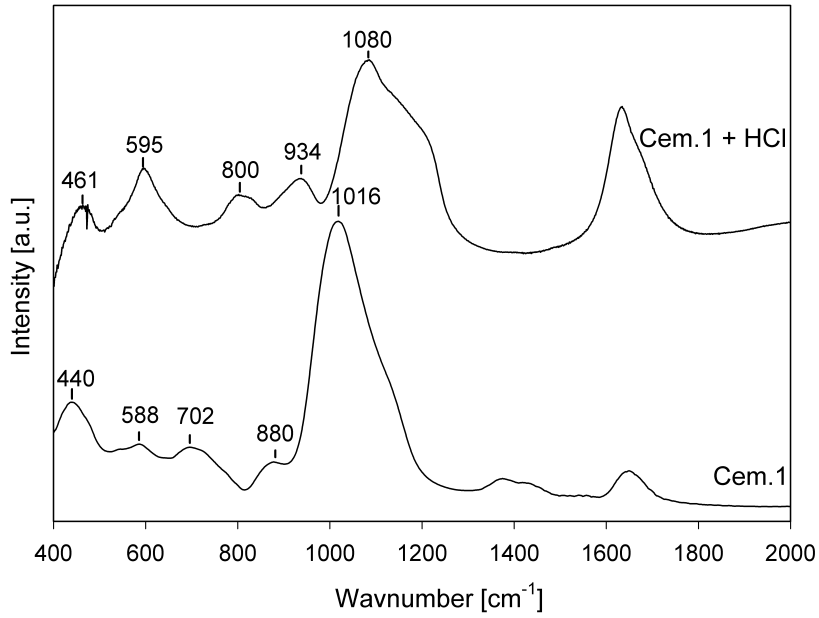

Fig 3.15. The FTIR spectra of alkali activated metakaolin (Cem.1) before and after treatment with high concentrated hydrochloric acid.

changed and occurs at: 461 cm^{-1}, 595 cm^{-1}, 800 cm^{-1}, 934 cm^{-1}, 1080 cm^{-1}. The peak shift is associated with extraction of both K and Al. The peak at 461 cm^{-1} is related to bending mode Si-O-Si and O-Si-O. The peak at 800 cm^{-1} is assigned to the symmetric stretching Si-O-Si. The most significant change is seen in the range of asymmetrical stretching, where DOSPM shifted from 1016 cm^{-1} to 1080 cm^{-1}. Independent on curing time of tested Cem.1, geopolymer treated with hydrochloric acid indicates DOSPM of asymmetrical stretching at 1080 cm^{-1}. Generally Al-O-Si bonds becomes separated by the acid leaching and a silica condensation causing the DOSPM shift toward higher wavenumber (*Bakharev et al., (2005a)*. After acid attack, high frequency peak becomes broaden and indicates lower intensity. At 1200 cm^{-1} a characteristic shoulder becomes more pronounced and the carbonate disappears. The bending of H-O-H is observed at 1632 cm^{-1} after reaction with acid.

In the next experiment Cem.1 has been leached with weak concentrated acid. As distinct from previously described investigation, before acid treatment, the geopolymer was powdered and after mixing with HCl was held at 4 ^{o}C. The FTIR spectra of geopolymers before and after acid attack are shown in Fig. 3.16 for Cem.1 aged at: 96 h, 168 h, 318 h, 504 h, 600 h. DOSPM of asymmetrical stretching for this cements has been measured at 1016 cm^{-1}. In the limit at long time of acid leaching, the DOSPM always tends to the position at 1080 cm^{-1}, irrespectively of ageing time.

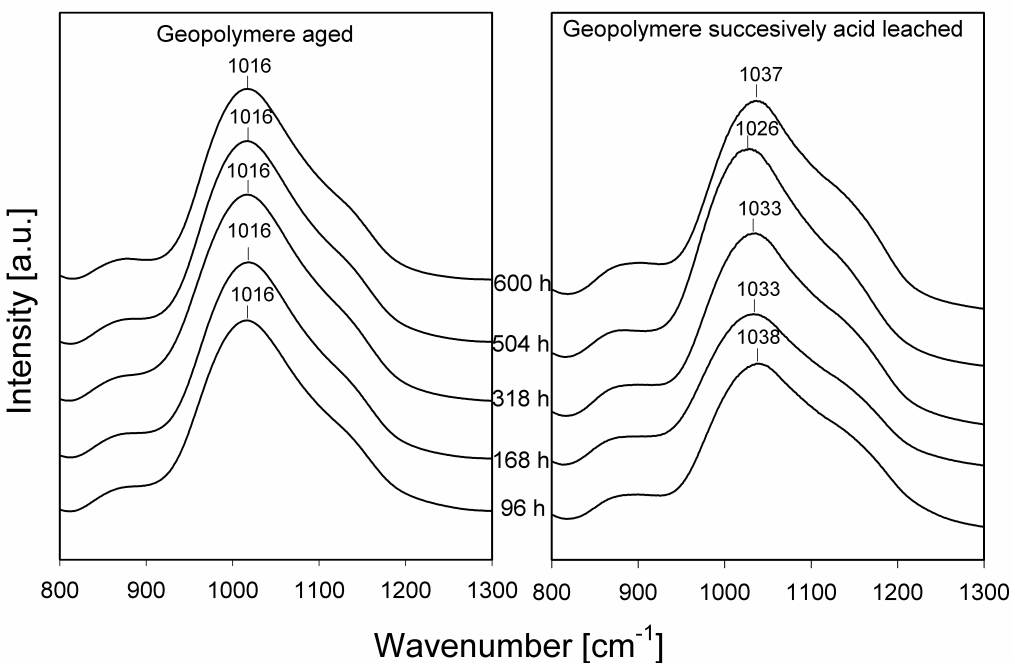

Fig. 3.16. The DOSPM of asymmetrical stretching of alkali activated metakaolin (Cem.1) characterized by different curing time before and after treatment with low concentrated hydrochloric acid.

However, after 2 hours of diluted acid leaching experiment the DOSPM positions have been observed: 1038 cm^{-1}, 1033 cm^{-1}, 1033 cm^{-1}, 1026 cm^{-1}, 1037 cm^{-1} in the IR spectra of geopolymers aged during: 96 h, 168 h, 318 h, 504 h, 600 h, respectively. The lowest shift towards higher wavenumbers is noted for Cem.1 aged 504 h. During longer and shorter ageing the shift becomes more pronounced. This also shows that the structure of the Cem.1 changes during ageing above 96 h, although the DOSPM is observed an-shifted at 1016 cm^{-1}.

3.2.3. Comparison study of metakaolin-based Cem.1-7 in infrared absorption

Seven different compositions of geopolymer have been prepared to study the dependence between molar ratio Si/Al of alkali activated metakaolin and DOSPM of asymmetrical stretching. Molar ratio Si/Al resulted from mixing of different portion of metakaolin and the alkali potassium silicate solution. Comparison of the spectra obtained for Cem.7, Cem.6, Cem.5, Cem.4, Cem.3, Cem.2, Cem.1 aged at 1 day and 20 days is seen in Fig. 3.17 as given in Table 4. With the increase of the nominal Si/Al ratio the position of bending mode shifts from 440 cm^{-1} (Cem.1) to 458 cm^{-1} (Cem.7). Cem.2 is an exception of that rule, as it indicates bending mode at higher wavenumbers than the rest of tested geopolymers. The peak at 588 cm^{-1} remains at the same position irrespectively of ratio Si/Al. The relative intensity of that peak grows with the rise of metakaolin amount. Cem.7 exhibits peaks at 644 cm^{-1} and 830 cm^{-1}. These spectral lines are close to 644 cm^{-1} and 803 cm^{-1} vibrations, which are observed in the absorption spectrum of metakaolin. The increase of silica shifts these bands to higher frequencies. Finally, the intensity at 803 cm^{-1} disappears and new band at 880 cm^{-1} appears, which is assigned to Si-O stretching in Si-OH groups. The intensity of 880 cm^{-1} peak increases with the decrease of Al in the initial composition of geopolymers.

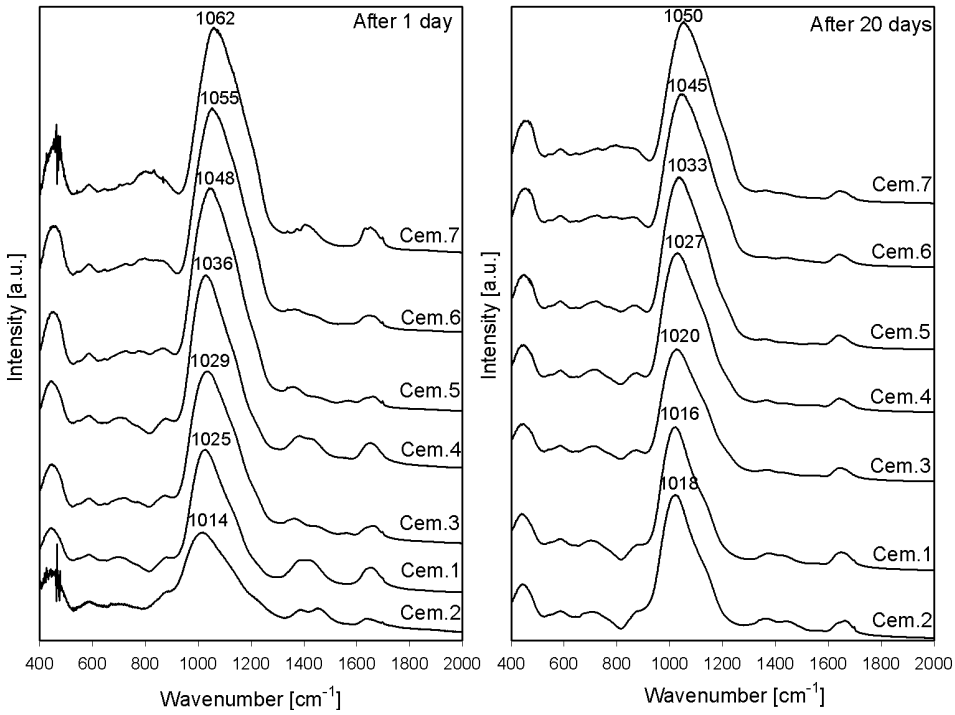

Fig. 3.17. The FTIR spectra of seven samples of alkali activated metakaolin (Cem.1-Cem.7) recorded after 1 day and 20 days of ageing at room temperature.

Comparing the infrared spectra recorded after 1 day and 20 days of ageing the most visible changes occur with the position of the DOSPM. With the exception of Cem.2, after 1 day of ageing all geopolymers show DOSPM shift to lower wavenumbers. The following changes in peak position have been observed: 1062-1050 cm^{-1}, 1055-1045 cm^{-1}, 1048-1033 cm^{-1}, 1036-1027 cm^{-1}, 1029-1020 cm^{-1}, 1025-1016 cm^{-1} for Cem.7, Cem.6, Cem.5, Cem.4, Cem.3, Cem.1, respectively. Cem.2 shows DOSPM shift from 1014 cm^{-1} to 1018 cm^{-1}.

The amount of unreacted metakaolin in Cem.3-7 during ageing

In the first stage of this spectral analysis, the initial and final DOSPM position of Cem.3-7 have been considered. To shift the DOSPM observed after 1 day of ageing (spectrum A) to the final position of DOSPM recorded for each cement after 20 days of curing (spectrum C), a proportional part of the metakaolin spectrum (spectrum B) has been subtracted. The portion of removed spectrum A depends on the distance between initial and final DOSPM position and for each composition it has been considered individually. The portion of subtracted metakaolin spectrum must be always the larger, the higher the distance between initial and final DOSPM position is. It thus has been related to the difference between non-reacted portion of metakaolin after the first and 20^{th} day of ageing. The absorption spectra obtained from that procedure were denoted as spectra C*. As it is seen in Figure 3.18 **,** the spectrum C* indicates similar peak distribution to spectrum C, so it can be said that C*=C.

It can be assumed, that DOSPM at 1016 cm^{-1} in the spectrum of Cem.1 (spectrum D) always indicate a fully reacted metakaolin. To estimate the amount of reacted metakaolin in geopolymer after 20 days of ageing, some part of spectrum A has been subtracted from spectrum C. The amount to be subtracted has been estimated with the shift to the position at 1016 cm^{-1}. The portion of subtracted metakaolin spectra thus just gives the unreacted contribution of metakaolin for Cem.3-7 after 20 days of ageing. The final spectra has been denoted as spectra D*. Spectrum D is similar to spectrum D*, D*≈D.

To obtain spectra E*, from each spectra A has been subtracted some part of spectrum B. The portion of removed spectrum B is the sum of subtracted part of spectrum B from spectrum A and spectrum C.

All the stages of subtraction process of metakaolin spectrum from the spectra of Cem.3-7 described

above are presented in Figure 3.18. Moreover, intermediate steps are also shown. The equations used in order to shift DOSPM of asymmetrical stretching are given in Table 11. The first formula shows, how much metakaolin should be subtracted from the spectra A to reach the final DOSPM position related to spectra C. The largest fraction of raw solid is removed from the spectra A of Cem.7, whereas the lowest one from the spectra of Cem.3. The second formula has been used to shift DOSPM in the spectra C to the position at 1016 cm^{-1}. It has been observed, that this numerical spectral processing is accompanied with peak sharpening. To shift the final DOSPM to 1016 cm^{-1}, the highest fraction of metakaolin spectra has been subtracted from infrared spectra of Cem.7. The lowest part of spectra B has been removed from the spectra of Cem.3. According to *Table 4,* Cem.7 has been prepared with the highest metakaolin to water glass ratio and the lowest mass of water glass, whereas Cem.3 has been mixed with the lowest one. The third formula given in Table 11 has been used in order to estimate the DOSPM position after removing the sum of metakaolin portion from the first and the second formula. The DOSPM of spectra E* of Cem.3-7 occurs in infrared regime 1007-1015 cm^{-1}.

Table 11:The formulas applied to shift the DOSPM of asymmetrical stretching of Cem.3-7 to lower frequencies, where: A-spectra recorded after 1 day of ageing, B-spectra of metakaolin Metastar 501, C-spectra recorded after 20 days of ageing, D-spectra of Cem.1 after 20 days of ageing

Cement	Formula I	Formula II	Formula III
Cem.7	A-0.35B	C-0.68B	A-(0.35+0.68)B
Cem.6	A-0.26B	C-0.55B	A-(0.26+0.55)B
Cem.5	A-0.17B	C-0.35B	A-(0.17+0.35)B
Cem.4	A-0.09B	C-0.17B	A-(0.09+0.17)B
Cem.3	A-0.07B	C-0.16B	A-(0.07+0.16)B

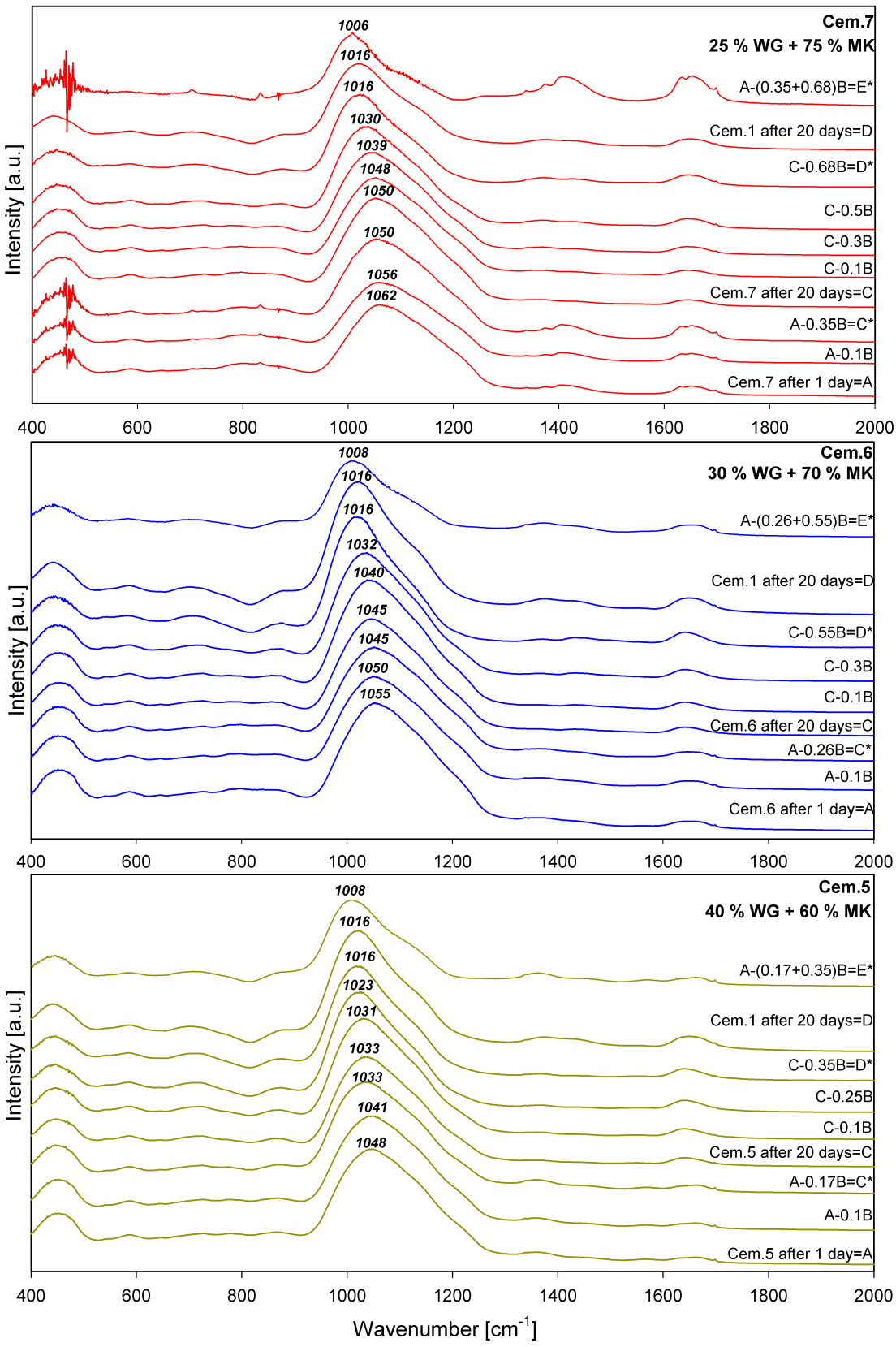
Cem.7
25 % WG + 75 % MK
1006
1016
1016
1030
1039
1048
1050
1050
1056
1062
A-(0.35+0.68)B=E*
Cem.1 after 20 days=D
C-0.68B=D*
C-0.5B
C-0.3B
C-0.1B
Cem.7 after 20 days=C
A-0.35B=C*
A-0.1B
Cem.7 after 1 day=A
Cem.6
30 % WG + 70 % MK
1008
1016
1016
1032
1040
1045
1045
1050
1055
A-(0.26+0.55)B=E*
Cem.1 after 20 days=D
C-0.55B=D*
C-0.3B
C-0.1B
Cem.6 after 20 days=C
A-0.26B=C*
A-0.1B
Cem.6 after 1 day=A
Cem.5
40 % WG + 60 % MK
1008
1016
1016
1023
1031
1033
1033
1041
1048
A-(0.17+0.35)B=E*
Cem.1 after 20 days=D
C-0.35B=D*
C-0.25B
C-0.1B
Cem.5 after 20 days=C
A-0.17B=C*
A-0.1B
Cem.5 after 1 day=A
Intensity [a.u.]
Intensity [a.u.]
Intensity [a.u.]
400
600
800
1000
1200
1400
1600
1800
2000
Wavenumber [cm-1]

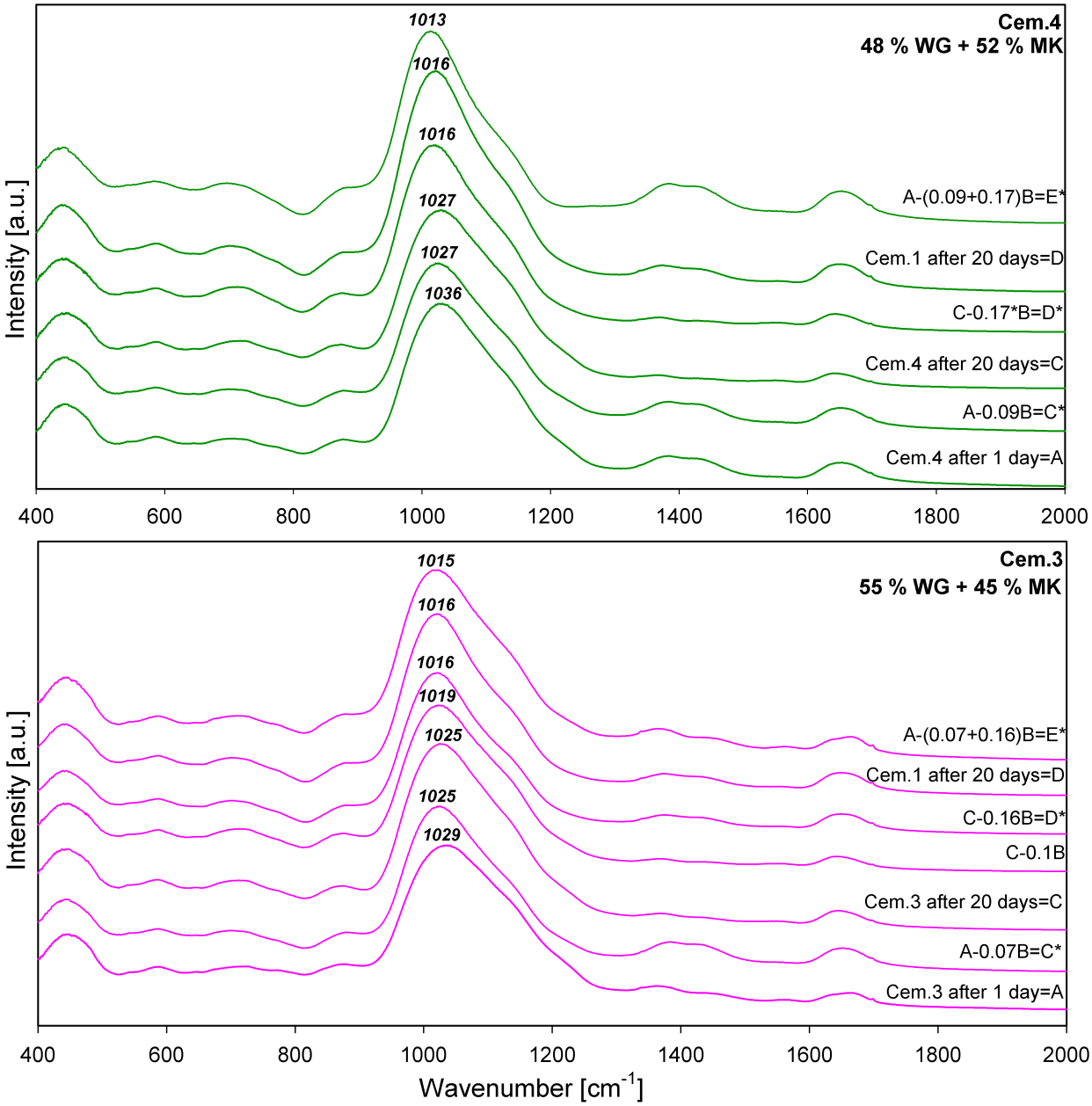

Fig.3.18. Numerical processing of IR spectra of Cem.3-7 aged during 20 days at room temperature.

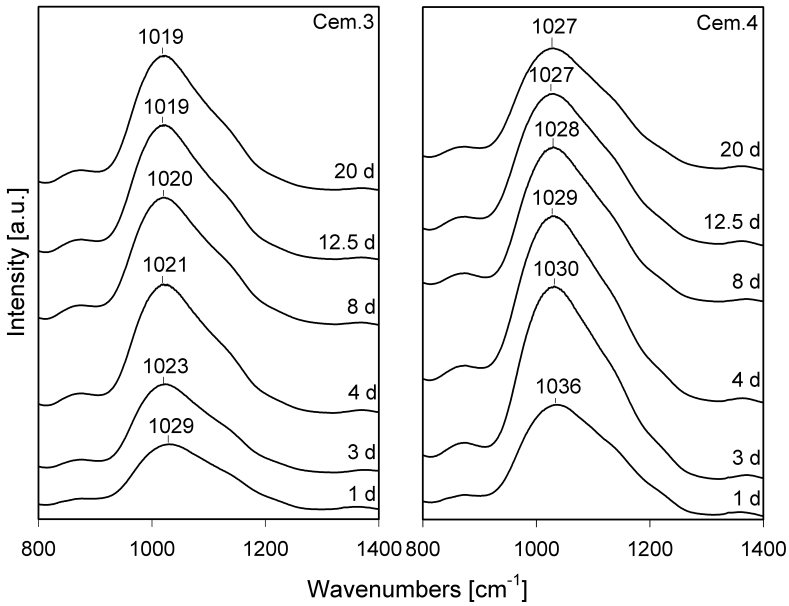

Fig 3.19. The detailed FTIR study of ageing process of Cem.3 and Cem.4 in range of asymmetrical stretching.

A detailed study of DOSPM of asymmetrical stretching of Cem.3 and Cem.4 up to 20 days is shown in Fig. 3.19. Cem.3 shows a DOSPM shift from 1029 cm^{-1} to 1019 cm^{-1}, whereas for Cem.4 a shift from 1036 cm^{-1} to 1027 cm^{-1} is observed. Both Cem.3 and Cem.4 reach the final DOSPM position between 8th day and 13th day of ageing.

3.3. Characterization of geopolymers by Raman spectroscopy

3.3.1. Raman spectroscopy of glasses

Raman spectroscopy of sodium aluminosilicate glasses

Fig. 3.20 shows the Raman spectra of following silica (Glass.1) and 3 aluminosilicate glasses: Glass.2, Glass.3, Glass.4. Compare Table 6 for compositions, the spectra are in excellent agreement with data given by *McMillan et al., (1972)*. The most intense and broad band is related to the vibrations of glass network (*Furukawa et al., (1981); McMillan et al., (1982, 1986)*. The maximum of that peak is indicated at following frequencies: 475 cm^{-1}, 462 cm^{-1}, 439 cm^{-1}, 433 cm^{-1} for Glass.4, Glass.3, Glass.2, Glass.1, respectively. Introduction of Al into glass network shifts the maximum from 433 cm^{-1} to higher frequencies due to a new set of force constants for the motion of T-O-T bridged oxygen. The displacement to higher wave numbers is accompanied with the peak broadening and the decrease of intensity of 485 cm^{-1} band. This process is related to the increases of Si-O-Al linkages concentration. The next characteristic peak at 585 cm^{-1} is observed in the spectra of Glass.1, Glass.2 and shifts towards lower wavenumbers, finally reaching the position at 605 cm^{-1} (Glass.1). This peak is assigned to Al-O-Al vibration. In the further frequency range of Glass.1 spectra 800 cm^{-1} band occurs. The increase of Al shifts this peak to the position at 790 cm^{-1}, what is visible in Raman spectrum of Glass.4.

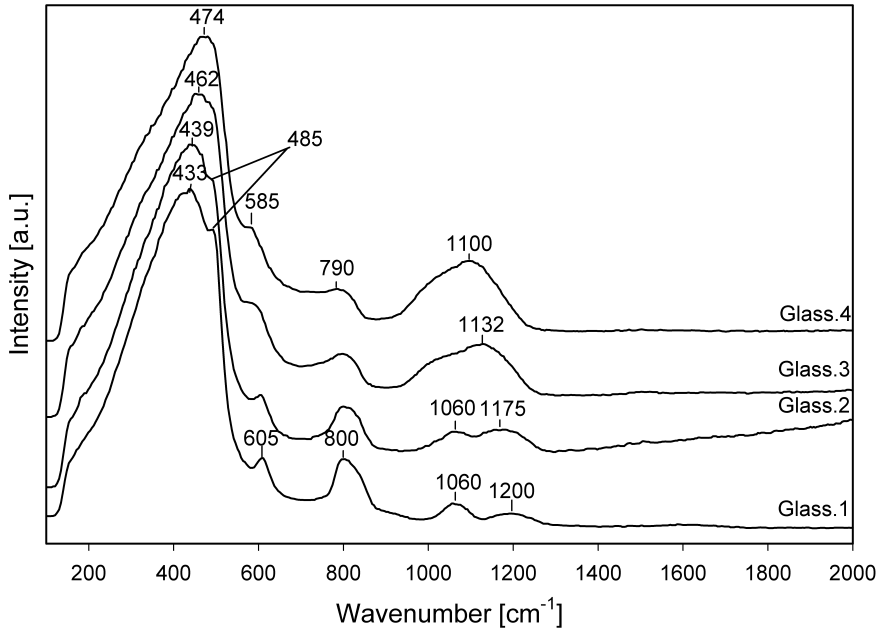

Fig. 3.20. The Raman study of Glass.1, Glass.2, Glass.3, Glass.4. The measurement was carried out by CRM 200 equipment.

The high frequency region corresponds to Si-O vibrations with aluminum acting only as perturbation on these. In the range 1000-1250 cm^{-1} the small broad band is characterized with two maximums. According to ratio Si/Al, both bands in the spectra of glasses systematically vary in the position and intensity. Glass.1 indicates peaks at 1060 cm^{-1} and 1200 cm^{-1}. These bands are assigned to the silicon-oxygen stretching vibrations in a fully-polymerized tetrahedral silicate framework. The decrease of silica increases the intensity and leads to the disappearance of the second maximum. Introduction of Al results in following infrared vibrations: 1060 cm^{-1} and 1175 cm^{-1} in Glass.2, 1132 cm^{-1} in Glass.3 and 1100 cm^{-1} in Glass.4.

Raman spectroscopy of potassium silicate glasses

Two kinds of potassium silicate glasses characterized with molar ratio K/Si=0.39 (Glass.5) and 0.69. (Glass.6) (compare *Table 7*) show Raman spectra as given in Fig. 3.21. The differences between the Raman spectra of these glasses result from different ratio between alkali and silica. The spectra of potassium silicate glasses indicates the characteristic vibrations in regions 400-500 cm^{-1}, 580-650 cm^{-1}, 700-880 cm^{-1} and 1000-1200 cm^{-1}. Low frequency region is related to the vibrations of glass network and in case of silicate glasses, corresponds to Si-O-Si bonds. The maximum of the low frequency range is seen at 433 cm^{-1} in the spectra of Glass.1, also given in Fig. 3.21. The

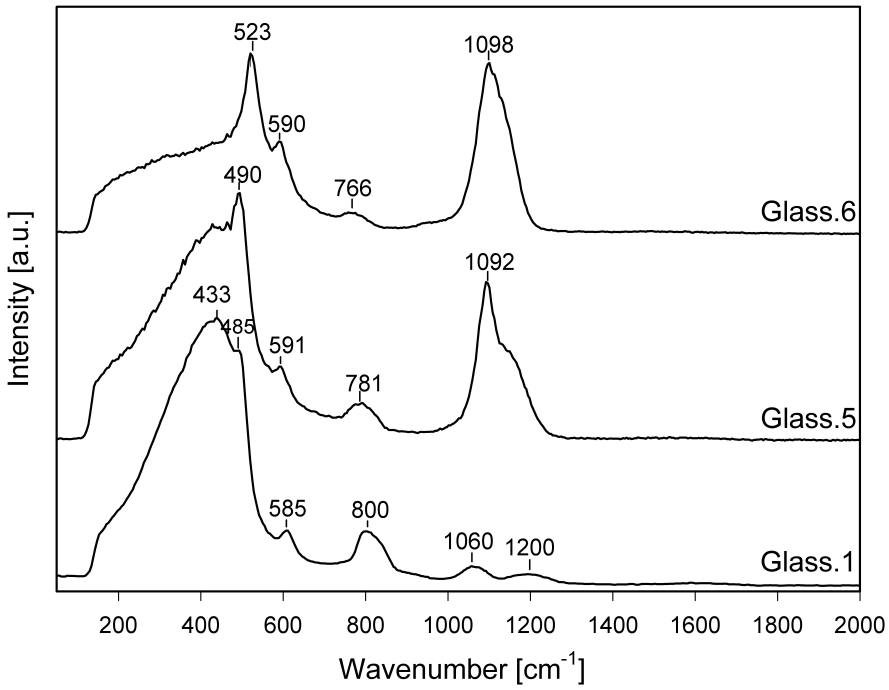

Fig. 3.21. The Raman study of SiO_2 glass (Glass.1), potassium silica glasses: 0.37(K_20) * 1.08(SiO_2) (Glass.5), and 0.27(K_2O) * 1.39(SiO_2) (Glass.6). The measurement was carried out with CRM 200 equipment.

increase of potassium leads to the gradual decrease of this band's height. Hence, Glass.6, which has the highest content of potassium, indicates the lowest intensity in region 400-500 cm^{-1}. The characteristic peak at 485 cm^{-1} in the spectrum of Glass.1, shifts with the rise of alkali ions to 490 cm^{-1} for Glass.5 and to 523 cm^{-1} for Glass.6. These changes result from the decrease of average Si-O-Si angle, often accompanied with the decrease in average polymerization of the silicate units (*McMillan et al., (1982))*. In the further frequency regime appear 605 cm^{-1} ,591 cm^{-1}, 590 cm^{-1} peaks in the spectra of Glass.1, Glass.5 and Glass.6, respectively. Moreover, these bands show the gradual growth of intensity with the rise of potassium. It is seen that the 880 cm^{-1} band of Cem.1 shifts towards lower frequencies with the increases of alkali amount: for Glass.5 and Glass.6 it is noted at 781 cm^{-1} and 766 cm^{-1}, respectively. The band group at 800 cm^{-1} involves motion of silicon against tetrahedral cage, although the degree of oxygen participation in this motion is controversial. In the higher frequency region, SiO_2 glass shows two maximums at 1060 cm^{-1} and at 1200 cm^{-1}. As it has been mentioned before, this region is assigned to Si-O stretching (*Furukawa et al., (1981))*. High frequency regime changes significantly after introduction of potassium ions into silicate network. The maximum of broad band occurring between 1000-1250 cm^{-1} shows the maximum at 1092 cm^{-1} and 1098 cm^{-1} for Glass.5 and Glass.6, respectively. The right shoulder of high frequency peak decreases with lower content of potassium ions, what confirms the complex nature of that peak. According to *McMillan et al., (1986)*, in the system of sodium silicate glasses 1100 cm^{-1} band is indicative of Q^3 species (SiO_4 units with one non-bridging oxygen).

3.3.2. Raman spectroscopy of geopolymers

Raman study of Cem.1-7

The Raman investigation of geopolymers has been carried out with CRM 200 and FT-Raman. The green laser line shows a higher separation of complex bands and presents more characteristic vibrations of alkali activated cement. Fig. 3.22 shows Raman spectrum of alkali activated metakaolin. The Raman spectra of metakaolin based binders are characterized with the high background intensity. The chemical composition of all tested samples is presented in ***Table 4.*** Unfortunately, due to very high fluorescence, the measurement of Raman spectrum of metakaolin was impossible. The decrease of metakaolin fraction in initial composition reduces this background. Hence, the highest intensity of background is seen in the Raman spectrum of Cem.7 and the lowest one in the spectrum of Cem.2. Raman spectra of geopolymers are dominated with strong bands in 400-500 cm^{-1} and 1100-1200 cm^{-1} region. In the spectra obtained with the help of green line laser

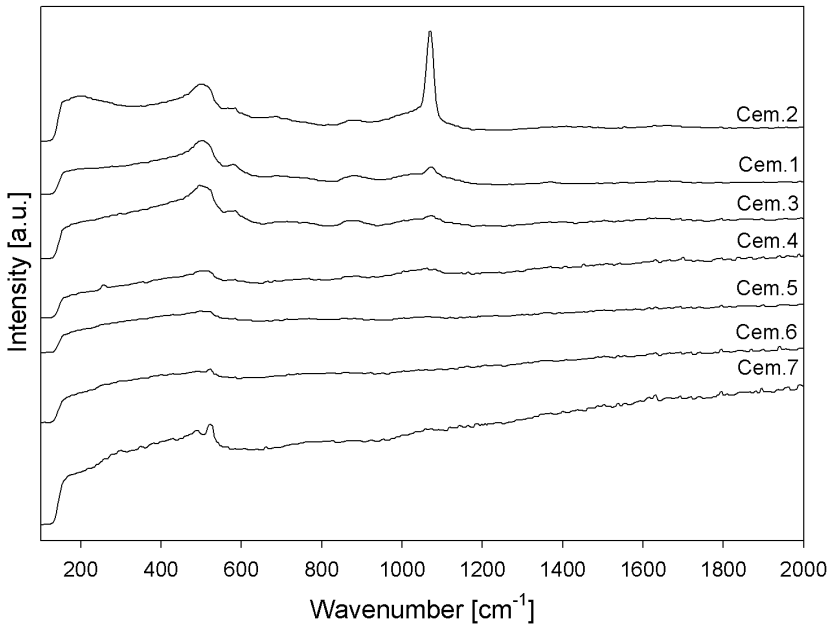

Fig. 3.22. The Raman study of alkali activated cements with residues of unreated metakaolin (Cem.3, Cem.4, Cem.5, Cem.6, Cem.7), excess of potassium water glass (Cem.2), and fully reacted composition (Cem.1). The measurement was carried out with CRM 200 equipment.

the vibrations at 580 cm^{-1} and 890 cm^{-1} are also observed. In lower frequency region, the rise of silica content leads to the peak sharpening and band shift from 520 cm^{-1} (Cem.7) to 490 cm^{-1} (Cem.1). The 520 cm^{-1} peak is almost invisible in the spectra of geopolymers prepared from small amount of water glass and high mass of metakaolin. Introduction of higher amount of silica into geopolymer structure leads to the increase of intensity at 890 cm^{-1}, what justifies the presence of that band due to silicate species. In the region of higher frequencies a peak at 1064 cm^{-1} occurs. The sample richest in silica shows the highest intensity of that peak, what emphasizes the role of silica in this spectral range. In aluminum rich geopolymers the disappearance of that band is observed. The position at 1064 cm^{-1} remains constant irrespectively of Si/Al ratio of the initial geopolymer composition.

Fig. 3.23 shows Raman spectra of K_2CO_3, Na_2CO_3, potassium (Cem.1) and sodium geopolymer (Cem.8). The spectra of alkali activated metakaolin have been recorded in nitrogen atmosphere to avoid CO_2 absorption from atmosphere. The characteristic bands in the high frequency region of K_2CO_3 and Na_2CO_3 occur at 1060 cm^{-1} and 1078 cm^{-1}, respectively. As it is seen, both geopolymers, irrespectively of the type of alkali ions, indicate the characteristic band at the same position. This peak doesn't overlap with vibrations indicated with potassium and sodium carbonate.

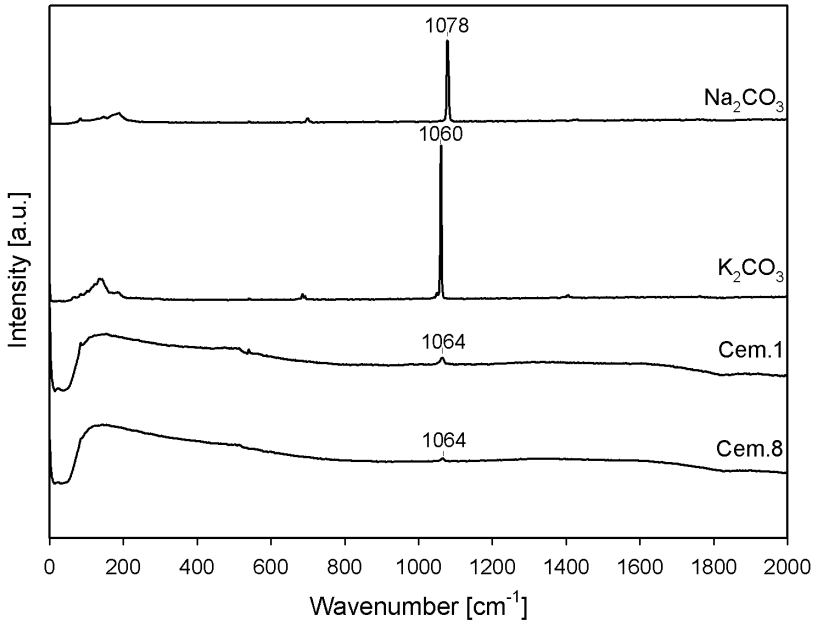

Fig. 3.23. The Raman spectra of Na_2CO_3, K_2CO_3, potassium geopolymer (Cem.1) and sodium geopolymer (Cem.8). The measurement was carried out with FT-Raman equipment.

Another indication from acid leaching experiments

To prepare acid treated geopolymer, the small drop of high concentrated H_2SO_4 acid has been put on the surface of Cem.1. Afterwards, the sample has been set between two clamps to avoid the changes in sample position during measurement. In order to avoid carbonation process, the investigation has been carried out in nitrogen atmosphere with the means of infrared laser. Fig. 3.24 shows Raman spectra before and upon reaction of Cem.1 with acid. Raman spectra of acid treated binder have been recorded after 30 s, 60 s, 120 s, 180 s of reaction. The low frequency range doesn't indicate any changes after reaction with H_2SO_4. In the further Raman region a new band at 987 cm^{-1}appears, which may be assigned to the formation of K_2SO_4. During longer reaction time, the left shoulder of that band slightly increases in relative intensity, what confirms complex behaviour of that peak. Moreover, 1064 cm^{-1} band indicates small increase in relative intensity and remains at the same position.

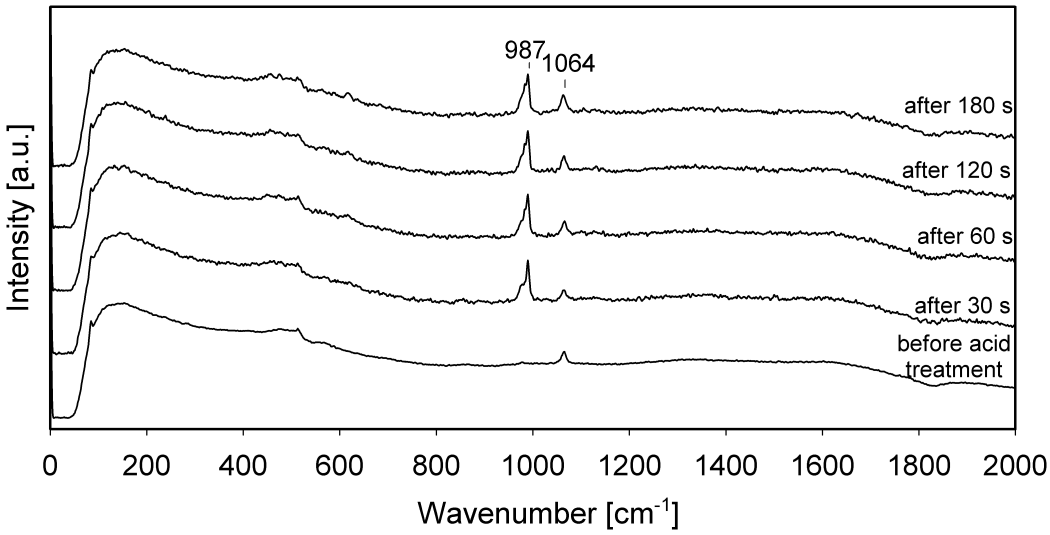

Fig. 3.24. The Raman spectra of alkali activated metakaolin (Cem.1) cured 216 h at room temperature before and after 30 s, 60 s, 120 s, and 180 s of H_2SO_4 acid treatment. The measurement was carried out with FT-Raman equipment.

Taking the advantage of liquid samples investigations of CRM 200 equipment, the Raman signal of silicate solution has been measured. Fig. 3.25 shows the Raman spectra of raw potassium water glass and silicate solution reacted with hydrochloric acid. The Raman spectrum of alkaline solution indicates five distinct lines at: 452 cm^{-1}, 592 cm^{-1}, 918 cm^{-1}, 1018 cm^{-1}, 1027 cm^{-1}. All this peaks are attributed to silicate ion. After reaction with HCl, the silicate species undergo condensation, what is reflected with the change of peak distributions. Due to the decrease of pH value following bands are indicated: 428 cm^{-1}, 565 cm^{-1}, 791 cm^{-1}, 852 cm^{-1}, 919 cm^{-1},1060 cm^{-1}. Most dominant bands in the spectrum of water glass reacted with acid are: 565 cm^{-1} and 1060 cm^{-1}.The characteristic shift from 1027 cm^{-1} to 1060 cm^{-1} corresponds to the concentration of alkali ions. According to the literature, the band above 1000 cm^{-1} disappears in the solution having large amount of potassium hydroxide (*Beard (1972)*).

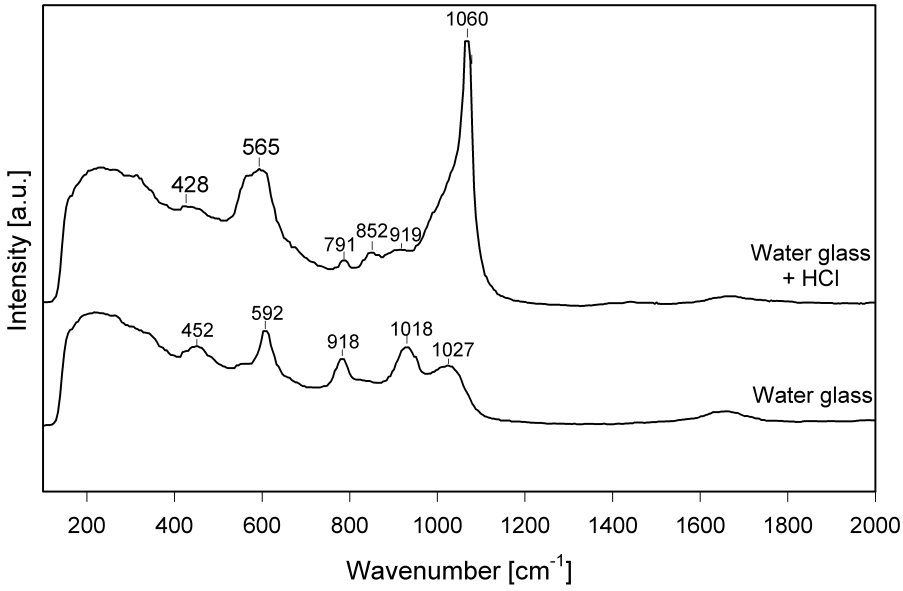

Fig. 3.25. The Raman spectra of potassium water glass and potassium water glass reacted with hydrochloric acid. The measurement was carried out with CRM 200 equipment.

Raman study of ageing process of Cem.1 and Cem.8

Fig.3.25 shows the Raman study of ageing process of sodium and potassium geopolymers. The samples have been aged in closed boxes at room temperature and opened shortly before Raman measurement under nitrogen atmosphere conditions using the FT-Raman. The geopolymers have been aged at room temperature for: 24-700 h and 22-600 h for Cem.1 and Cem.8, respectively. Both types of alkali activated cements are well reacted compositions with a slight excess of alkali ions (K(Na)/Al>1). According to the *Table 4* and *Table 5*, potassium geopolymer contains lower ratio between alkali and silica than sodium geopolymer. The spectra of potassium and sodium geopolymer are dominated with bands in two regions: 400-500 cm^{-1} and 1100-1200 cm^{-1}. The sharpening of broad band at lower frequencies is accompanied with the increase of intensity at 1064 cm^{-1}. This band is visible after 72 h of ageing in the spectrum of Cem.1. However, in the spectrum of Cem.8, it appears after about 96 h of curing. At early stage of ageing the 1064 cm^{-1} peak both in the spectra of Cem.1 and Cem.8, is not present. The potassium geopolymer indicates small changes of intensity in high frequency region over time. Sodium inorganic polymer indicates significant decrease of intensity of 1064 cm^{-1} peak above 360 h of ageing. The relative intensity of this peak in the spectrum of Cem.8 is lower than in the spectrum of Cem.1. The position of high frequency peak remains constant during ageing process of Cem.1 and Cem.8.

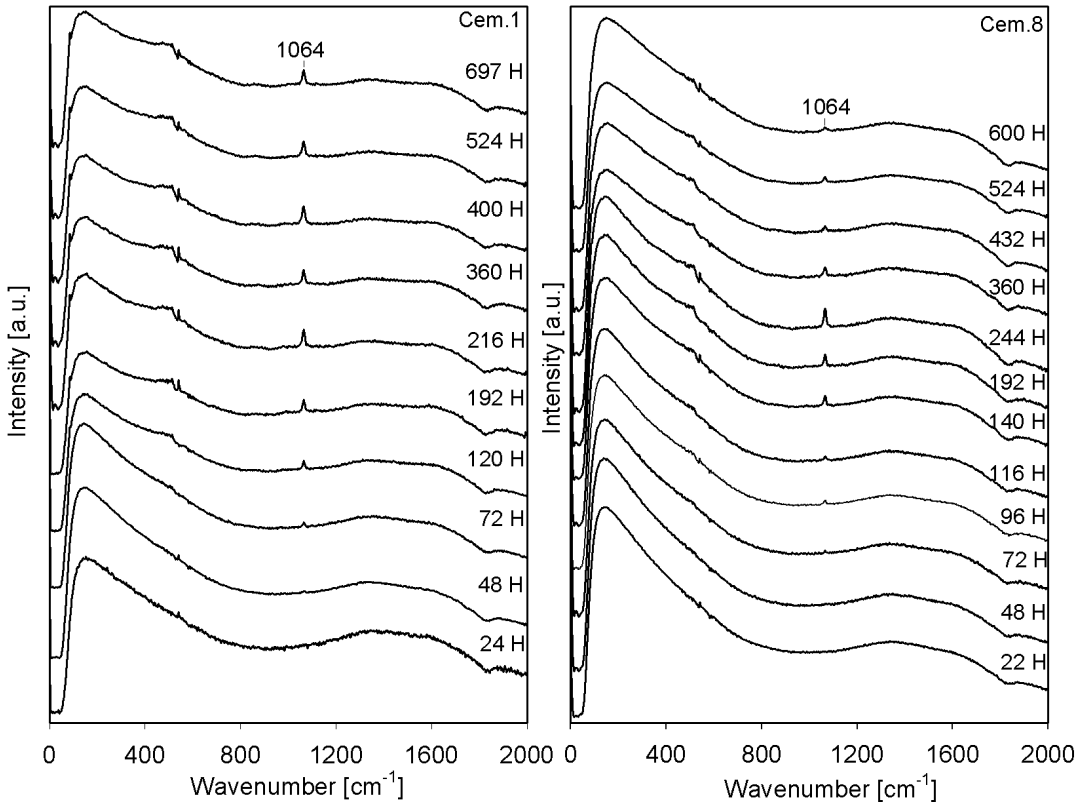

Fig. 3.26. The Raman study of ageing effect of potassium (Cem.1) and sodium geopolymer (Cem.8). The measurement was carried out with FT-Raman equipment.

Many efforts have been made to study the systematic variation in the relative intensity of band at 1064 cm^{-1} over curing time. It has been noted, that the relative intensity of 1064 cm^{-1} peak may be significantly changed through longer exposure to laser light. However, low frequency range grows systematically in intensity with the rise of exposure to laser light. These effects show, that the relation between intensity of 490 cm^{-1} and 1064 cm^{-1} peak may considerably vary during different exposure to laser light. This effect has been observed in the study carried out both with green laser line and infrared laser and is not present during whole curing time of the studied cement. Fig. 3.27 shows the dependence between the intensity at 1064 cm^{-1} and exposure time to laser radiation. As it has been mentioned before, the Raman band in the range of lower frequencies increases systematically in relative intensity during exposure to laser light. This property has helped to estimate the variation in relative intensity at 1064 cm^{-1}. In case of Cem.1, the dependence between peak height and exposure time of laser light is noted between 100^{th} and 500^{th} hour of ageing. Beyond this time interval, the increase of intensity due to longer laser radiation has not been noted. According to the Raman study of other compositions of alkali activated cement, 1064 cm^{-1} band

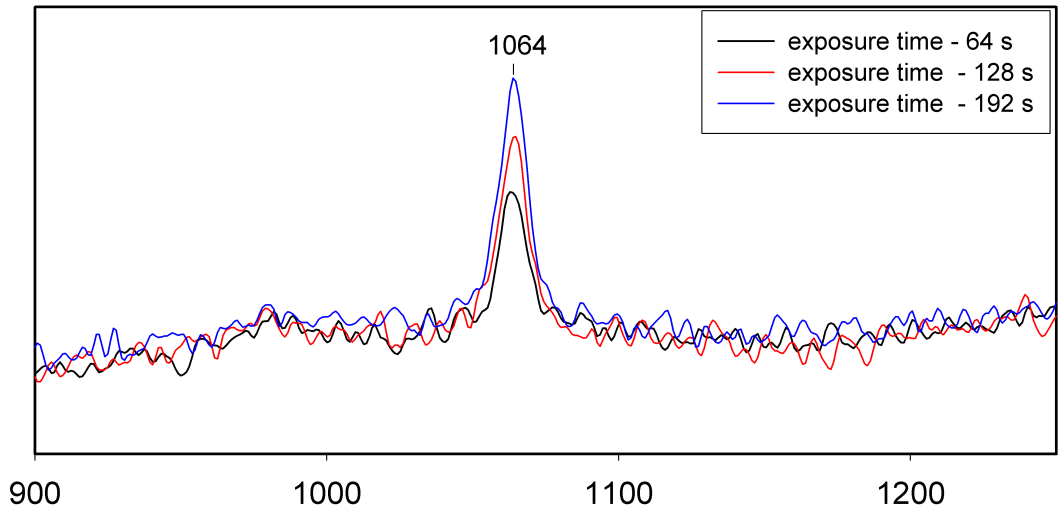

Fig. 3.27. The relation between the intensity of Raman band at 1064 cm^{-1} and exposure time to IR laser light in the spectra of Cem.1 cured during 192 h at room temperature. The relative intensity was estimated with help of Raman region 400-500 cm^{-1}, which is insensitive for longer laser radiation.

doesn't exist in the spectra of geopolymer with deficit of water glass (K(Na)/Al<1). In such composition even in case of longer exposure to laser light this peak is not observed.

3.4. Characterization of geopolymers by thermal analysis

3.4.1. Thermal analysis of metakaolin based geopolymer Cem.1

The thermal analysis of inorganic polymers consists of three experiments: heating up to 1000 °C, heating up to 600 °C and twofold heating up to 600 °C. All TG investigations have been measured with FTIR spectroscopy. The individual stages of heating up to 1000 °C have been additionally investigated with X-ray diffraction method. To avoid the loss of water, the samples have been cured in closed plastic tubes at room temperature. Shortly before the measurement the inorganic binders have been removed and powdered. Afterwards, about 30 g of powdered cement has been set in ceramics crucible and heated.

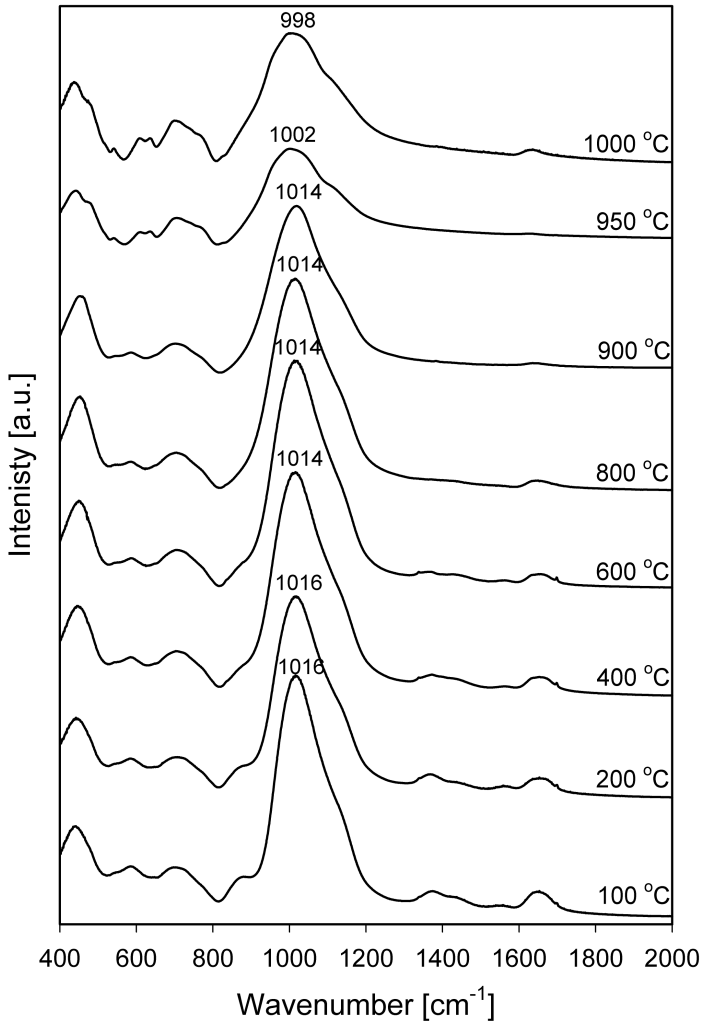

Fig. 3.28. The FTIR study of alkali activated metakaolin (Cem.1) aged during 200 h at room temperature heated up to 100 °C, 200 °C, 400 °C, 600 °C, 800 °C, 900 °C, 950 °C, 1000 °C.

As it has been previously presented in Fig. 3.7, the infrared spectrum of Cem.1 cured at room temperature is dominated with following peaks in the range of symmetrical stretching: 440 cm^{-1}, 588 cm^{-1}, 702 cm^{-1}, 877 cm^{-1}. These vibrations are weak sensitive to heating, hence no considerable changes is observed after thermal treatment below 950 ^{o}C (Fig. 3.28). The spectra of samples heated above 950 ^{o}C indicates bands: 436 cm^{-1}, 480 cm^{-1}, 538 cm^{-1}, 606 cm^{-1}, 634 cm^{-1}, 700 cm^{-1}, 770 cm^{-1}. During heating systematic decrease of intensity at about 877 cm^{-1} is observed, which is assigned to Si-OH groups. This band becomes smaller and finally only its shoulder remains. Due to the de-carbonation process, the significant fade of vibrations related to O-C-O stretching at 1371 cm^{-1} and 1435 cm^{-1} is noted. The decrease in intensity of water bending mode at 1630 cm^{-1} is seen. The strongest band in infrared spectra of Cem.1 is noted at 1016 cm^{-1}. This peak remains at the same position during heating up to 200 ^{o}C. The most significant shift in the range of asymmetrical

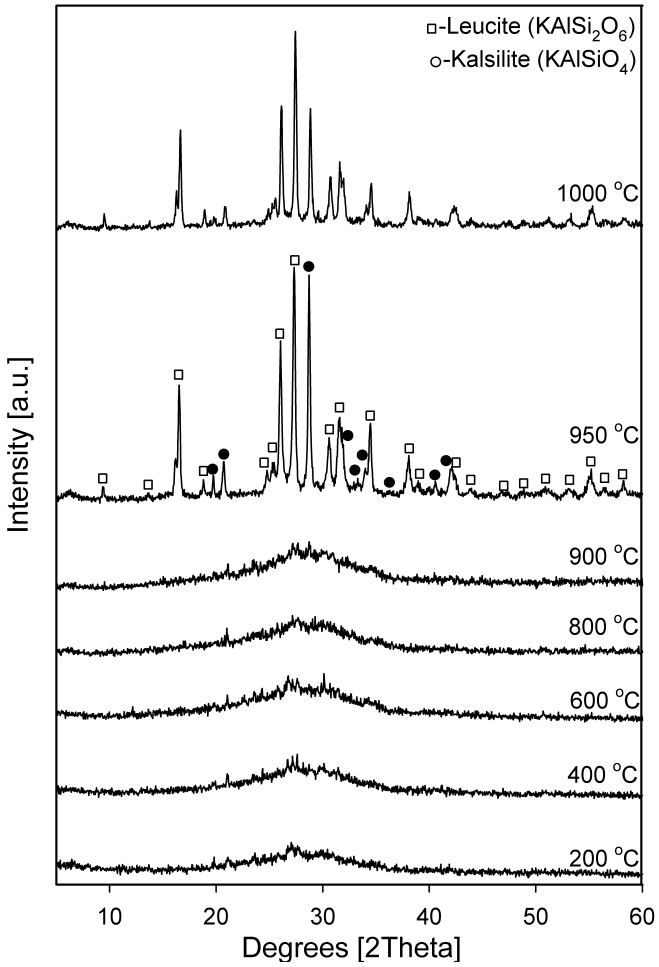

Fig. 3.29. X-Ray diffraction pattern of geopolymer (Cem.1) aged about 200 h at room temperature heated up to 100 °C, 200 °C, 400 °C, 600 °C, 800 °C, 900 °C, 950 °C, 1000 °C; the formation of leucite (PDF [38-1423]) and kalsilite (PDF [33-989]).

stretching takes place above 900 °C and is accompanied with the peak broadening.

The formation of aluminosilicate crystalline phases at elevated temperatures of hydroxy-sodalith ($Na_2OAl_2O_32SiO_22.5H_2O$) above 200 °C, carnegieit ($NaAlSiO_4$) above 800 °C and nephelin ($(K,Na)AlSiO_4$) above 900 °C as typical modifications of sodium silicate is not observed in the presence of potassium ion (*Lutz (1999)*). Moreover, no other formation of crystalline phases as zeolites is noted here, which is typical for aluminosilicates under hydrothermal conditions at temperatures between 80-100 °C. Similar to the FTIR data, the X-ray experiments of samples heated below 950 °C does not exhibit any meaningful changes in the diffraction pattern (Fig. 3.29). Above 950 °C the X-Ray pattern indicates many sharp peaks and partial disappearance of amorphous broad hump. This effect is typical for the crystallization process. With help of Rietveld software the type of formed crystallines could be assigned to leucite and kalsilite.

3.4.2. Thermal experiment of Cem.1 cured at different time

About 30 mg of geopolymer powder were given into the ceramic crucible and held 1 h at room temperature under He flowing atmosphere (20 ml/min) subsequently heating up to 600 °C and cooling with a rate of 2 °C/min. The loss of mass and the variation in heat flow were measured in parallel. In the first heating runs samples of Cem.1 cured for: 24 h, 48 h, 72 h, 120 h, 225 h, 432 h, 800 h were investigated. Geopolymers characterized with curing time between 24^{th}-432^{nd} hour reach a total loss of initial mass between 26 % and 29 % (Fig. 3.30). The 800 h and 72 h aged cements indicate the highest mass loss. During the first hour of experiment carried out at 20 °C, geopolymers indicate 2-7 % loss of initial weight. The maximal mass loss is noted for samples aged 24 h and 800 h.

After the first thermal treatment up to 600 °C, the samples have been held in humid environment during 24 hours and again heated up to 600 °C. This twofold heating experiment were carried out on samples aged for 48 h, 120h, 225 h, 432 h and 800 h. The loss of mass and heat flow of samples in the second heating up to 600 °C is shown in Fig. 3.31. There is a loss of weight in the range of 7-13 %, ie. about 20-50 % of the effect obtained in the initial heating. This shows a much less capability of rehydration compared to zeolites where 100 % is reached. The second thermal experiments indicate the highest reduce of mass for the 800 h aged sample, whereas the lowest weight loss is obtained for the sample cured 48 h at room temperature. The rest of tested cements indicate about

12 % of total mass loss. During the first hour of curing at 20 °C, the maximal loss of weight is observed for the 800 h aged sample. For all other samples it equals 2 % of total weight. This observations are similar to those obtained in the first run which may thus indicate a surface hydration.

The large endothermic peak appearing at low temperature can be related to the dehydration of the adsorbed water of the geopolymer. The position of that peak could be related to the rate of water release from aluminosilicate structure. In the first thermal treatment, the temperature of endothermic peak is between 75 °C and 90 °C. The exception of that rule is for the 800 h aged Cem.1, which indicates an endothermic peak at 60 °C. During the second heating the 800 h sample exhibits an endothermic peak at 55 °C. DTA thermograms of the samples aged during 48^{th} -432^{th} hour display the shift of that peak to higher temperatures 60-75 °C.

Besides the changes in the position of the endothermal peak, its width is also varying in relation to the curing time. According to *Xu et al., (2003)*, the width of endothermic peak increases with the extend of disorder of the cement phase. The DTA phases of Cem.1 heated in the first run indicates similar peak width for all tested geopolymers with the exception of the 800 h and 24 h samples. Twofold thermal treatment shows the broadest endothermal peak of 800 h and 48 h cured samples. The endothermic peaks seen in the first heating are generally narrower than bands given with twofold heating.

All samples were also measured by IR measurement after their thermal treatment. The variation in the range of the DOSPM after one and twofold heating up to 600 °C of Cem.1 cured during 225 h is shown in Fig. 3.32. Due to the heating the width of DOSPM becomes broader at lower and higher wavenumbers. After the second heating of Cem.1, the width of the DOSPM peak slightly increases towards higher wavenumbers. The peak position after the first thermal treatment is close to 1014 cm^{-1} and remains unchanged from the second heating. The rest tested samples indicated similar changes in the range of DOSPM during heating up to 600 °C.

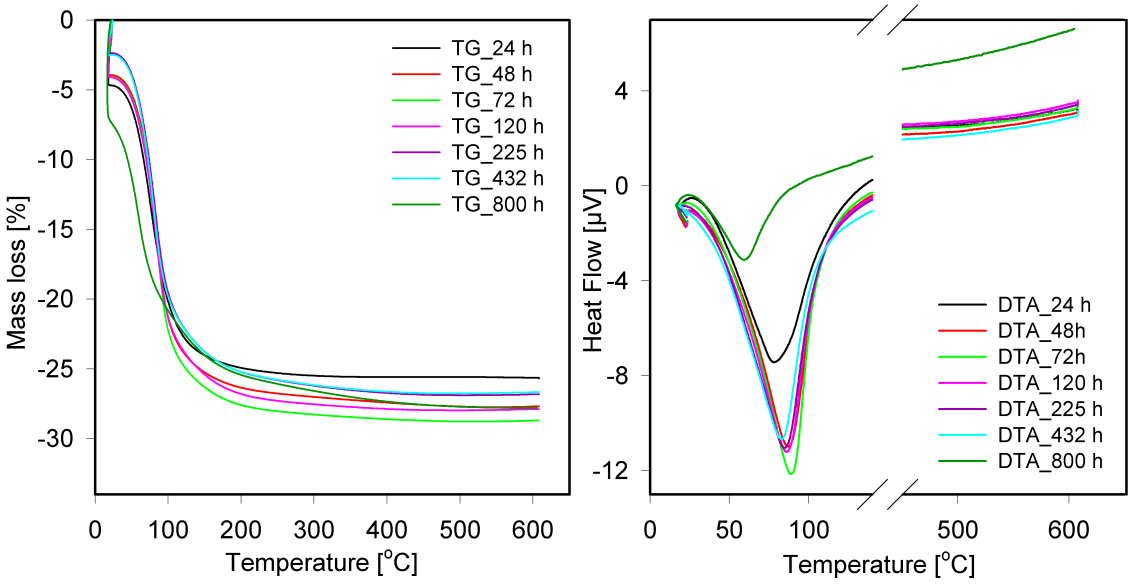

Fig. 3.30. TG and DTA of metakaolin based geopolymer (Cem.1) in the first heating up to 600 °C.

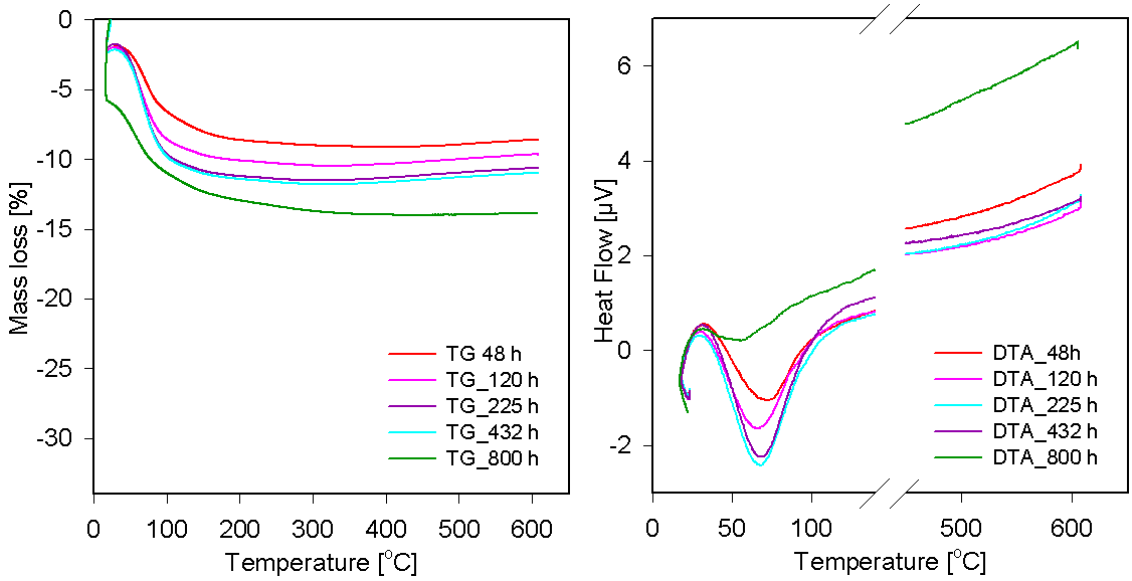

Fig. 3.31. TG and DTA of metakaolin based geopolymer (Cem.1) in the second heating up to 600 °C.

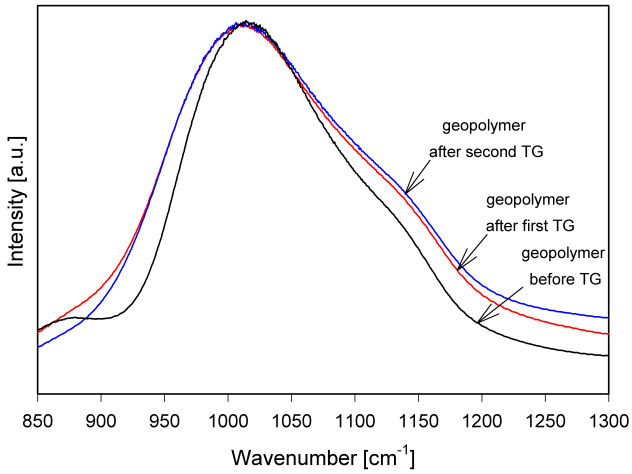

Fig. 3.32. The range of DOSPM of asymmetrical stretching of geopolymer (Cem.1) aged 225 h at room temperature before thermal treatment, after the first TG up to 600 ºC and after the second TG up to 600 ºC.

3.5. Characterization of geopolymers by Molybdate method

Structural changes in the degree of polymerization of silicate units were investigated for Cem.1 series aged between 13 h and 700 h using the Molybdate method approving earlier results (*Lutz (1999)*. It has been shown that oligomeric silicate molecules of water glass solution are Molybdate active, whereas longer SiO_2 units (condensates of more than about 30 silicate units) are Molybdate inactive (*Thilo et al., (1965)*. Polymeric silicate units from metakaolin are inactive. The results show strong changes of molybdic active fraction of SiO_2 during ageing time of Cem.1 (Fig. 3.33). The total amount of silicate species of molybdate active portion decreases during ageing between 13 h and 25 h from about 82 % to about 78% of total silicate species amount. During further ageing, the molybdate active species increases constantly up to 99% at 525 h of ageing. Above 525 h the molybdic active SiO_2 decreases again to about 61 % at 700 h of curing. The space over the curve indicates the amount of all molybdic inactive silicate units. The fraction of molybdate inactive silicate species corresponds to the difference between the molybdate active species and the total amount of silicate species. Thus the amount of molybdate inactive species behaves complementary to the molybdate active part. A separation of the molybdate active fraction into monomeric+dimeric and oligomeric fraction is given in Fig. 3.34. A significantly decrease of oligomeric units occurs from 13 h (59 %) to 25 h (57 %) of curing time. During further ageing up to 525 h, the oligomeric fraction increases to about 81 % and after reaching that point the changes in oligomeric portion are followed with the decrease to 50 % at 700 h of curing. The fraction of monomeric and dimeric units

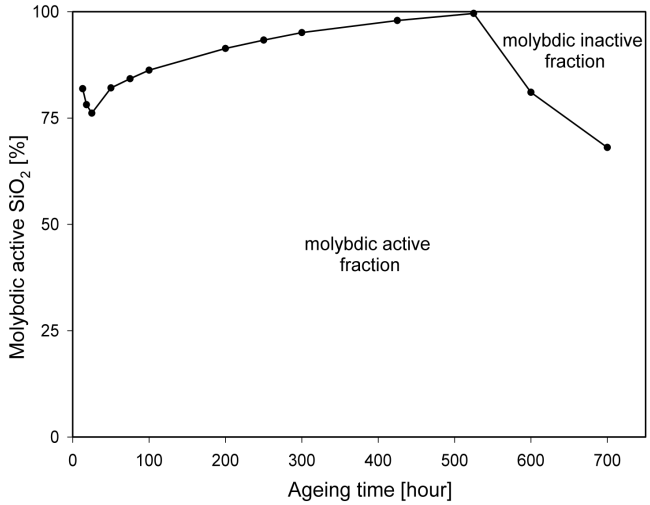

Fig. 3.33. The variation of total molybdate active fraction of alkali activated metakaolin (Cem.1) during ageing at room temperature.

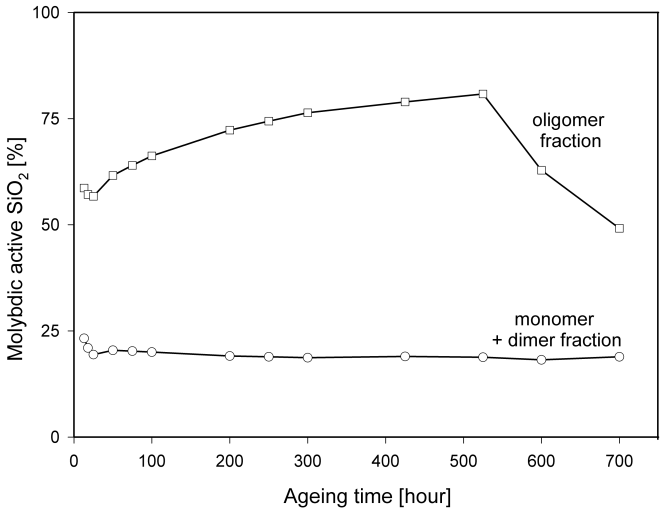

Fig. 3.34. The relation between the development of molybdate active species of alkali activated metakaolin (Cem.1) during ageing of Cem.1 (squares: oligomeric fraction; circles: monomer + dimmer fraction).

decreases during ageing between 13-25 h from about 25 % to 19% and remains stable during further curing. This indicates that during ageing between 25th and 700th hour the gain and loss of oligomeric units are directly related to the loss and gain of polymeric fraction. The decrease of molybdat active units for ageing above 520 h is related to the existing decreasing force of an aluminosilicate gel to separate into silica gel and an aluminosilicate approaching Si/Al≈1.

3.6. Characterization of geopolymers by strength measurement

The force measurement has been carried out for one composition of alkali activated metakaolin (Cem.1) cured at different temperatures: 25 °C, 50 °C, 90 °C and 130 °C approaching the results reported by *Lutz (1999)*. Fig. 3.35 and Fig 3.36 show, that the shape of curves is similar for both types of strength properties showing a strongly variation with temperature. The strengths of samples cured at 130 °C and 90 °C decrease monotonously with increasing time to a plateau arriving at 50 °C and 25 °C a maximum in strength at about 7 h and 100 h, respectively. The increase of temperature contributes to a faster rate of hardening process (*Bakharev et al., (1999)*). Alkali activated metakaolin cured at 50 °C indicates the highest value of compressive force, which gains the maximum after 7 hours of ageing. The lowest maximal compressive force is noted 20 minutes after preparation of Cem.1 cured at 130 °C. The same cement also shows the lowest final force after 325 h of curing. Similar course of hardening process of Cem.1 in respect to curing temperatures is indicated with flexural force measurement.

As it has been mentioned in the introduction, the improvement of strength of alkali activated cement is not the purpose of this study, so the value of compressive and flexural force are not going to be considered in further chapters. The author will mainly discuss the effect of strengthening and weakening of Cem.1 cured at 25 °C in the following.

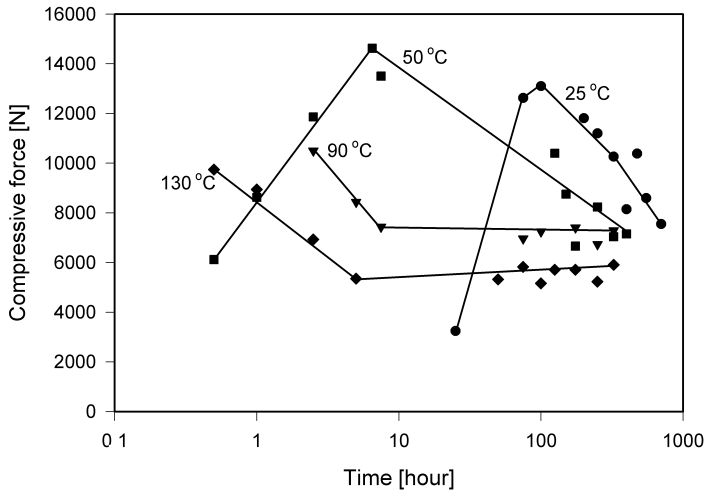

Fig. 3.35. Compressive force development during ageing time of alkali activated metakaolin (Cem.1) at 25 °C, 50 °C, 90 °C and 130 °C. after *Lutz (1999)*.

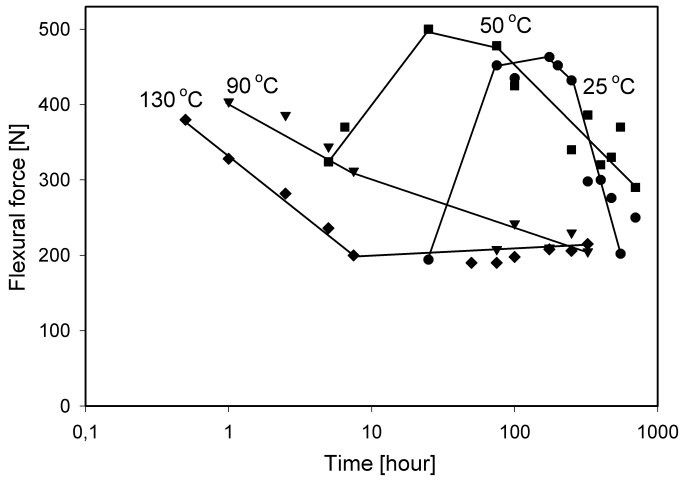

Fig. 3.36. The flexural force development of alkali activated metakaolin (Cem.1) at 25 °C, 50 °C, 90 °C and 130 °C after *Lutz (1999)*.

4. DISCUSSION

4.1. Commonly used techniques for study of gepolymerization: XRD, SEM/EDX, TEM, NMR

There are many studies, which try to understand the structure of geopolymers using X-Ray, SEM and TEM techniques. Such methods might be useful for certain aspect of investigation but may at the present stage not be useful to provide further insight in the structural rearrangements during ageing.

The commonly used method for structural investigations and phase analysis is X-Ray powder diffraction technique. As it is shown in the Fig. 3.1, the alkali activation of metakaolin reveal just a shift of the broad peak to higher angles centred around 27-29° 2θ as reported in the literature (*Kriven et al., (2003a); Yunsheng (2007)*. The position of that peak is related to the initial composition of geopolymer. It has been found, that the increase of water glass fraction at the cost of metakaolin in geopolymer composition leads to the sharpening of this peak. Less alkaline solution results in smaller amount of dissolved solid, which is related with lower intensity of the high angle shoulder and increase of the low angle shoulder intensity (Fig. 4.2). According to that, the diffraction pattern of Cem.3-7 indicates the coexistence of amorphous binder phase and undissolved amorphous metakaolin. Cem.1 indicates the narrowest peak due to the almost completely reacted solid and therefore the absence of metakaolin (Fig. 3.2, *Table 8*). The widest band is noted for Cem.7, prepared from the highest amount of metakaolin and the lowest portion of alkaline solution showing the highest fraction of non-reacted material. It can be seen that details about the geopolymerization itself (ageing) may not be obtained by such conventional X-Ray method. However, X-Ray diffraction methods allow to identify the crystalline fraction in the raw solid materials, which has been assigned to muscovite, faujasite and quartz. These amounts are small and doesn't react during geopolymerization, according to the presence in the final product (*Steveson et al., (2005)*.

SEM/EDX have been found helpful for the analysis of inorganic binders' curing process detecting morphological and compositional changes. For Cem.1 it has been found, that the surface doesn't indicate any visible changes depending on curing time. Cem.1 is characterized by very low amount of non-reacted metakaolin and highly homogeneous surface. With help of EDX measurement, the

verification of the average molar ratio of Cem.1, which is Si/Al=1.9, has been done. This value is in good agreement with the nominal molar ratio Si/Al=2.09 estimated from the chemical reactants (Table 9). This fact indicates the dissolution reaction of almost the whole portion of metakaolin, too. According to *Duxson et al (2005a)*, a ratio Si/Al obtained with EDX is lower than nominal one, if the amount of non-reacted metakaolin is very small.

TEM in so far does not show any meaningful changes in geopolymeric structure during ageing process. Due to the measurement under vacuum conditions and elevated temperature on the sample, the study was accompanied with the evaporation of molecular water and geopolymer body's shrinkage. The structural changes over ageing time are sensitive for external conditions, the water loss and high temperature treatment could obscure the rate of reactions in geopolymer body. These adverse conditions excluded the detailed study of structural changes during curing time in geopolymer structure of Cem.1. Studies including environmental microscopy techniques might be more helpful in plane.

Another technique known to be powerful for the structure analysis of local environments in crystalline and amorphous material is NMR spectroscopy. With help of NMR spectroscopy, it was possible to look deeper into the dynamic of dissolution process and verify the changes in the coordination of Al during the raw aluminosilicate's akali activation (*MacKenzie (2003)*). The structural changes during ageing time of compositions of Cem.1 were investigated by *Lutz (1999)*. The ^{27}Al MAS NMR signal of metakaolin Metastar 501 and alkali activated metakaolin cured at 25 °C after 25 h and 750 h of ageing time are shown in the Fig. 4.1. Metakaolin shows signal intensity at 27,3 ppm and 3-10 ppm, related to pentahedral and octahedral coordination's signal of Al, respectively. Additionally a significant concentration of Al is indicated with the signal intensity at 58.6 ppm. However, alkali activated metakaolin indicates only Al in fourfold coordination. *^{29}Si MAS NMR* data of metakaolin exhibits a wide peak between -80 ppm and -120 ppm. The featureless signal is similar to that of a silicate glasses containing Si in a range of sites with statistical predominance of $SiQ^4(3Al)$. For example, in this chemical shift regime, zeolite A reveal one peak related to $Q^4(4Al)$ groups, and zeolite Y shows five peaks assigned to $Q^4(0\text{-}4Al)$ groups (*Lutz et al., (2002)*. A perfectly ordered silica gel contains only Q^4 groups which is characterized with an individual band at -112 ppm, while worse ordered gels indicate peaks in the range characteristic for zeolite Y (*Lutz et al., (2001)*). Although, the spectra are very similar to each other, small changes in the distribution of signal intensities may be observed. The maximum noted at - 89 ppm for 25 h old

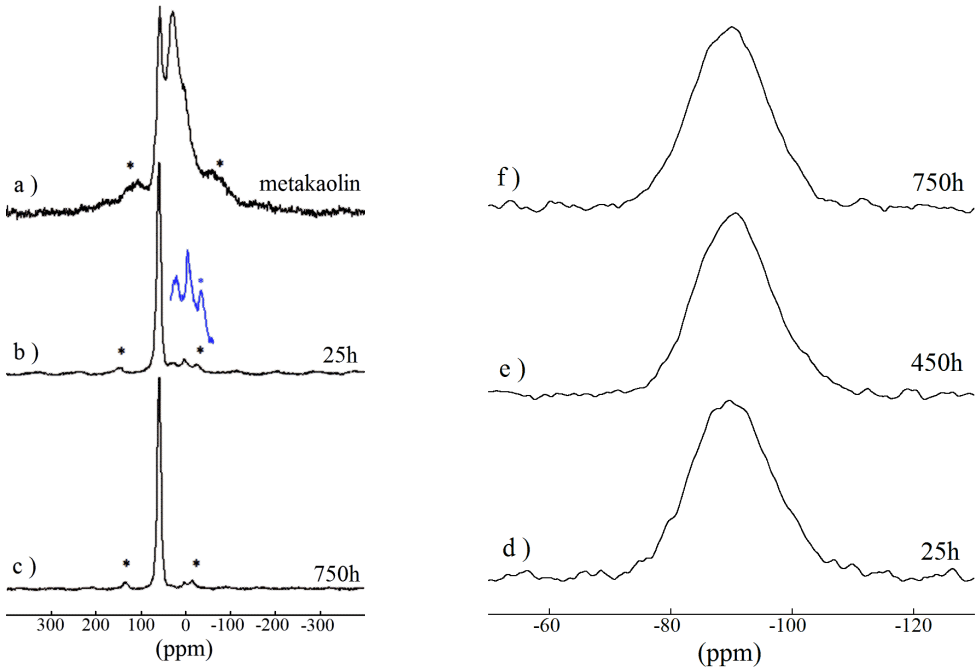

Fig. 4.1. ^{27}Al MAS NMR spectra (on the left) of metakaolin Metastar 501 (a), Cem.1 aged 25 h at 25 °C (b), Cem.1 aged 750 h at 25 °C (c). ^{29}Si MAS NMR spectra (on the right) of Cem.1 aged 25 h at 25 °C (d), Cem.1 aged 425 h at 25 °C (e), Cem.1 aged 750 h at 25 °C (f) after *Lutz (1999)*.

***-rotation side-bands**

sample, during further ageing shifts to -91 ppm. Unfortunately, in the further stage of geopolymerization, besides the changes in the coordination of Al in alkali activated cement, nothing meaningful may be concluded from NMR analysis after dissolution of raw solid. Hence, it has been decided to study ageing process of geopolymer with other techniques as discussed in the flowing chapters.

4.2. Ageing process of geopolymers

4.2.1. Infrared absorption of geopolymers (Cem.1), glasses and silicate solution.

Despite the different physicochemical nature of geopolymers and glasses their IR absorption properties closely resemble. Besides the similar distribution of peak intensity, also the variation of geopolymer composition acts on the peak position analogous to the linear dependence for aluminosilicate glasses. As described in the previous chapter, characteristic vibrations of aluminosilicate glasses appear in following regions: 400-470 cm^{-1}, 700-860 cm^{-1}, 1000-1200 cm^{-1} (Fig. 3.5) In the same regimes, the most intense vibration of metakaolin based geopolymer are observed. On the basis of infrared study of silicate materials and according to the literature, the characteristic infrared regimes were assigned to bending mode (400-500 cm^{-1}), symmetrical stretching (500-950 cm^{-1}) and asymmetrical stretching (950-1200 cm^{-1}) of the silicate units (Table. 10). Similarly to the nature of infrared glasses bands, the position of absorption bands, as well as the width and intensity of individual peaks depends on chemical composition of geopolymers. Introduction of alumina in silicate glass leads to the significant changes in infrared spectra. A main signature is the shift of all characteristic bands towards lower frequencies accompanied with the appearance of new band in the range of symmetrical stretching, which has been assigned to Al-O vibrations beside broadening of T-O-T bands. The peak shift is related to the formation of following groups: $Q^4(4Al)$, $Q^4(3Al)$, $Q^4(2Al)$, $Q^4(1Al)$, with an intensity destruction related on the extent of aluminium substitution. A similar effect is seen in the aluminosilicate geopolymer system, where the DOSPM could shifts towards higher wave numbers with the increase of Si/Al ratio, which could be due to the smaller force constant of Al-O bonds compared to Si-O (*Duxson et al., (2006)*. If the concentration of vibration species decreases per unit volume, the intensity of DOSPM becomes lower. Referring to the literature, all polymorphs of SiO_2 show three characteristic groups of frequencies about 1100 cm^{-1}, 800 cm^{-1} and 480 cm^{-1}, which are related to a stretching mode associated with oxygen atoms, a stretching mode associated with silicon atoms, and a silicon-oxygen bending mode, respectively (*Hanna et al., (1964)*. *Rüscher et al., (2010b)* observed characteristic band of silica-rich geopolymer made from rice husk-bark ash (RHBA), fly ash (FA) and sodium water glass (see Appendix, Table 13-14**,** and spectra shown in the Fig. 7.2) in a similar absorption range as observed here for Cem.1.

These authors showed, that the increase of Al in geopolymer structure shifts the final DOSPM peak

position ie. at long ageing time (Fig. 7.2) to lower frequencies. This conclusion is obtained observing the relation between DOSPM and composition in the aluminosilicate glasses' system as described in this work. (Fig. 4.2). The DOSPM region in infrared spectra of geopolymers is due to the vibrations with the predominant character of silicon-oxygen stretching. It is generally known, that silica glass consists of a three dimensional framework of SiO_4 tetrahedra, and that alkali oxides break the Si-O-Si bridging oxygen leading to the formation of NBOs (non-bridging oxygen). The absence of aluminium, which balances the charge in glass network, contributes to the formation of $Si\text{-}O^-$ units and depolymerization of silicate framework (*Kriven et al., (2004)*. It has been found out, that the potassium concentration's increase, at the cost of silica in the system of potassium silicate glasses, results in the displacement of DOSPM to lower frequencies. This process should be related with the partial decomposition of silicate network and the formation of $Si\text{-}O^-$ groups (*Clark et al., (1977)*. Due to higher concentration of NBOs in the structure and lower polymerization of silicate framework, the increase of potassium fraction in glass composition shifts the DOSPM towards lower frequencies (Fig.3.6).

The study of DOSPM can be extended to water glass and solution reacted with acid. For many decades, the alkaline silicate solutions have been described in terms of silicon concentration, pH and viscosity. The degree of aqueous silicate solutions oligomerisation is favoured with low alkalinity, high silicon concentration and low temperatures (*Iler (1979)*. The position of the T-O-T band contains the information about the condensation of SiO_2 units and alkali element concentrations (*Osswald et al., (2006)*. It has been shown here, that the T-O-T peak of pure water glass embedded in KBr appears at about 1003 cm^{-1}. This position is characteristic for infrared absorption range of monomeric and dimeric silicate species. Polycondensation of potassium water glass shifts the DOSPM from 1003 cm^{-1} to 1044 cm^{-1} (Fig. 3.11). The DOSPM of potassium water glass may indicate a majority of monomeric/dimeric Q^0/Q^1 silicate units, whereas the DOSPM of polycondensed water glass corresponds with a mixture of mainly chain-type Q^2 together with some higher condensed Q^3 units. It can be worked out, that the relation between the position of DOSPM of asymmetrical stretching and the degree of polymerization of silicate units in the system of silicate glasses and silicate solution resembles the dependence between DOSPM and Si/Al ratio of aluminosilicates (Fig. 4.2). Accordingly a close equivalence in DOSPM is observed between $Q^4(4Al)$, $Q^4(3Al)$, $Q^4(2Al)$ and Q^0, Q^1, Q^2 for the aluminosilicates and silicates, respectively.

In the past, a lot of authors reported the frequency shift of infrared stretching vibration with

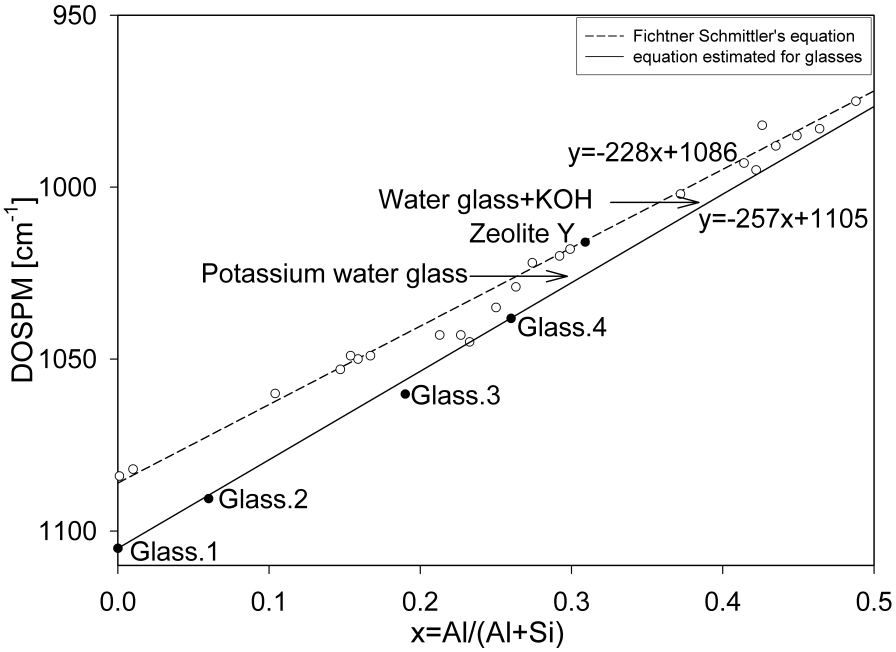

Fig.4.2. The relation between the DOSPM of asymmetrical stretching and x=Al/(Al+Si) for Glass.1, Glass.2, Glass.3, Glass.4 (solid line); the dependence between DOSPM of asymmetrical stretching and x=Al/(Al+Si) for faujasite zeolites after *Fichtner-Schmittler et al., (1990)* (dashed line).

substitution of tetrahedral Al for Si in aluminosilicate network. In zeolitic network, similarly to glasses and geopolymers, the stretching modes are sensitive to Si/Al ratio of framework composition and are shifting to lower wavenumbers with increasing Al content. A linear relation between the Density of States Peak Maximum (DOSPM) of the $[Si\text{-}O_4]\text{-}T_4$ units of asymmetrical vibrations and the Al molar fraction may be postulated (Fig. 4.2). This is compared to results given by *Fichtner-Schmittler et al., (1990)*, for the characterization of the Si/Al ratio of faujasite type zeolites. In order to estimate the relation between composition and DOSPM for glasses, the molar Si/Al ratio calculated from microprobe measurement (*Table 6*) has been used. The obtained relationship (y=-257+1105) coincides with that proposed by *Jirasit et al., (2006)* and used in systematic investigations (*Rüscher et al., (2010a))*. It is important to realize, that the residues of non-reacted solid influence the absorption spectra. Hence, only the most reacted composition of Cem.1 may be considered for the determination of the Si/Al ratio directly. The final position of DOSPM of Cem.1 has been found at 1016 cm^{-1}, what implies molar ratio Si/Al=1.9 using the relation for the glasses (Fig. 4.2). This value is in good agreement with the nominal composition (Si/Al=2.09) and that value estimated by EDX analysis (Si/Al=1.9).

Relation between DOSPM and Molybdate study

According to the Fig. 3.8, DOSPM shifts during 5h of curing from 1025 cm^{-1} to 1010 cm^{-1}. This trend continues up to 13 h of curing, reaching the DOSPM at 1007 cm^{-1}. This stage of ageing is related to the rapid dissolution of the metakaolin to potassium alumina and potassium silicate units, leading to pH value decrease. This leads to a polycondensation of silicic acid. According to Molybdate measurement, 20 % of polycondensed silicate units are formed during ageing between 13 h and 25 h. These units thus must originate from the water glass. This polycondensation of the water glass units can be seen with the rapid shift of the DOSPM from 1008 cm^{-1} to 1025 cm^{-1} in the same ageing time. The dependence between the condensation process of silica in silicate solution and its alkalinity is well known from chemistry and has been seen here in reaction with HCl. Further shifts of the DOSPM towards lower wave numbers, occur finally reaching the position at 1016 cm^{-1}. This shift is dominated with the slowly growing aluminosilicate and cross-linking network covering the polysilicate and oligomeric chains. This, however lead to a higher alkalinity which in turn enforces the decomposition. Cross-linking could include monomeric (Q^4(4Al)) and dimeric (Q^4(3Al)) units, which have been formed within the first 25 h and represent about 20 % of the total mass of molybdate active silicate. This amount remains constant as the cross-linking contact is given via sialate bonds as discusses by *Davidovits (2008)*.

The increase of molybdate activity indicates significantly the structural changes within first 525 h of ageing. The DOSPM on the other hand reaches a stable position at 1016 cm^{-1} after 100 h of curing, therefore covering all modifications running at further stages of ageing.

The second derivative of infrared absorption spectra shows some changes in the range of asymmetrical stretching above 100 h of ageing, which proves further development in the structure of Cem.1 (Fig. 3.10), even though this is not directly visible in DOSPM.

An additional proof that further structural changes occur after three days of ageing is given by kinetically controlled acid leaching experiments of Cem.1, with use of low concentrated acid (Fig. 3.16). It has been found, that the DOSPM of asymmetrical stretching of acid treated geopolymer depends on its ageing time. A minimum shift for the acid treated cement is noted for 504 h aged sample, while the maximum shift is observed towards lower and high ageing time. This results are in line with the results obtained with the molybdate method. As it has been mentioned before, the acid treatment within the molybdate method is followed with all silicate complexation, thus forming

monomers, what leads to the characteristic yellow colour. On the contrary, in the performed acid leaching experiment, the degree of polymerisation of silicate units increases and leads to the DOSPM shift towards higher wave numbers (*Rüscher et al., (2009))*. Finally, after long time of acid treatment the DOSPM always tends to 1080 cm^{-1} for all samples, irrespective of initial ageing time (Fig. 3.15). Hence, a minimal DOSPM shift for acid treated samples indicates the highest stability against acid, which can be attributed to the most suitable protection of Al-O-Si bonds within an aluminosilicate network. In comparison, the crystalline counterpart zeolite X with Si/Al=1 immediately decomposes during acid treatment, whereas zeolite Y with Si/Al =2.5 withstands much longer time, what is direct consequence of the increased amount of Si-O-Si bonds (*Rüscher et al., (2006))*.

Relation between Si-OH and H-O-H absorption intensities during ageing

The absorption regime related to Si-OH vibrations and water bending mode showed, that both effects are inversely correlated in intensity, ie. the increase of peak height in the first range versus the decrease of intensity in the second region and vice versa. This tendency is similar for all tested series (Fig. 3.14). The averaged value of $SiOH/H_2O$ ratio related on ageing time, shows a decrease from 24 h, to a minimum value after about 100 h. Above 100 h of ageing a slight increase occurs. The decrease in ratio between 24 h and 100 h correlates with the shift of DOSPM from 1025 cm^{-1} to 1016 cm^{-1}. The peak at 880 cm^{-1} weakens because silanols groups condense to form Si-O-T groups (*Duxson et al., (2006))* and H_2O is set free. This can be related to the effect of strong condensation according to the reaction: $OH^- + OH^- \rightarrow O^{2-} + H_2O$, where O^{2-}denotes a bridging oxygen. In other words, the variation of $SiOH/H_2O$ ratio indicates the aluminosilicate network's formation and could results from two simultaneously running processes: decomposition of silicate chains and geopolymeric network's condensation. It might be suggested, that the $SiOH/H_2O$ ratio below 24 h of ageing might increase from the beginning of ageing, because of initial dissolution process of alumina and silicate from metakaolin, which creates SiOH and consumes water (*Rahier et al., (1997); Xu et al., (2003))*. However, at the same time condensation of silica is enforced because KOH is used in the dissolution process. After about 100 h of ageing, the $SiOH/H_2O$ ratio slightly increases and remains almost stable during further curing, what indicates a less intense condensation of the three dimensional framework.

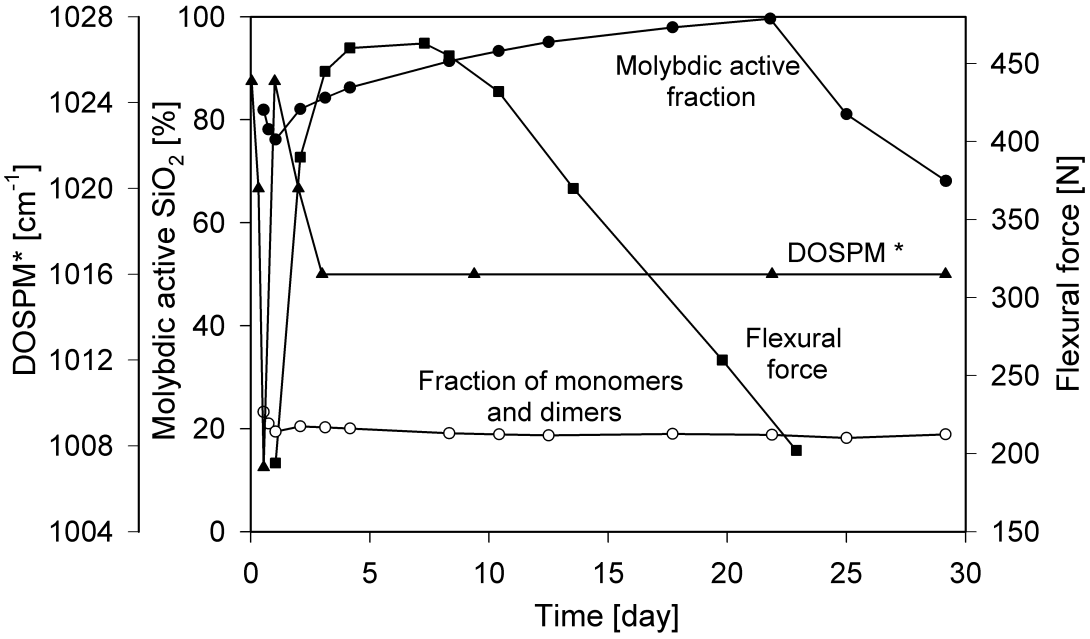

Fig. 4.3. The development of flexural force, Density of States Peak Maximum (DOSPM) of asymmetrical stretching and molybdate active fraction over ageing time of Cem.1.

Relation between DOSPM, Molybdate activity and strength development

As it has been mentioned before, this study goal is not to improve the absolute strength of geopolymer, but to find the explanation for to primary increase in strength followed by the significant weakening. The important question is, how the gain and loss of Cem.1 strength is related to the variation in molybdate activity and in DOSPM. According to flexural force measurement of Cem.1 cured at 25 °C**,** the maximum of alkali activated metakaolin strength can be found between 100-200 h of ageing, whereas the significant drop starts after about 200 h of ageing. The gradual increase of oligomeric fraction during ageing between 25 h and 525 h, covers both the increase and decrease of flexural force. The increase of molybdate active fraction corresponds to the formation of an aluminosilicate network. The maximum portion of molybdate active SiO_2 units is seen at 525 h of ageing (Fig. 4.3). Thus the maximum of flexural force and the highest degree of aluminosilicate network's condensation don't correlate in time, what suggests, that the reason of early strength has more complex nature than expected. It must be concluded, that the kinetics of more parallel running reactions controls the development of the mechanical properties.

The DOSPM development on ageing time is also given in Fig. 4.3. Realising that the total amount of metakaolin has reacted after about 13 h of ageing (minimum value in DOSPM), the increase in

DOSPM to 1025 cm^{-1} is explained with polycondensation of silicate units. This coincides with the change in molybdate activity observed with the minimum, ie. correspondingly in maximum polycondensation units at 25 h of ageing. The renewed crossover into the decrease in DOSPM is related to the further enclosing and cross-linking of polymeric chain type silicate units via the slowly forming aluminosilicate network. Here cross-linking may occur via sialate linkages of monomeric and dimeric units, which will not change the amount of these units. On the other hand the network formation inversely produces free KOH which immediately attacks the polymeric chains and will shorten them. This shortening finally will lead to a significant weakening in the mechanical strength or with the other word, the slowly forming network (cross-linking) can no longer compensate for the effect of chain destruction.

So far, the conventional mineralogical analysis hasn't provided satisfactory explanation for hardening and weakening mechanism of alkali activated cement. In general, better hardness of cement is achieved, if instead crystalline, amorphous solid is used (*Davidovits (1999)*). The reduction in ultimate compressive strength of geopolymer, characterized with lower molar Si/Al ratios is believed to be a result of non-reacted material influence, which is very soft and acts as a defect in the binder phase (*Kriven et al., (2003b)*). *Duxon et al., (2005a)* stated, that the reduction of ultimate compressive strength may result from the effects of non-reacted material. Cem.1 is almost fully reacted composition, so this explanation doesn't fit in with presented hardening process. Additionally the results obtained here imply the unreacted metakaolin improves the mechanical properties as the weakening occurs less much. In particular it buffers the pH by attracting KOH for a further dissolution during ageing. According to *Palomo et al., (1999)*, metakaolin is one of the best materials for producing high strength cements. Due to high reactivity and small size of particles, metakaolin improves the mechanical strength, reduces the transport of water and salts through the sample, as well as it prevents the alkali aggregate reaction from occurring.

Heterogeneity of amorphous materials and their ability to dissolve in alkaline solution are some of the essential factors, that affect the hardening process. The mechanical properties of alkali activated cements are greatly dependent on the concentration of alkali hydroxide in the solution. The flexural strength and density of geopolymer increase, along with the increase of alkali concentration, what is attributed to the enhanced dissolution of aluminosilicate solid (*Granizo et al., (2007))*. The fraction of non-reacted solid, at the cost of binder phase, reduces the maximal flexural force. However, the deficit of alkali hydroxide results in lower decomposition of condensed silicate chains, what

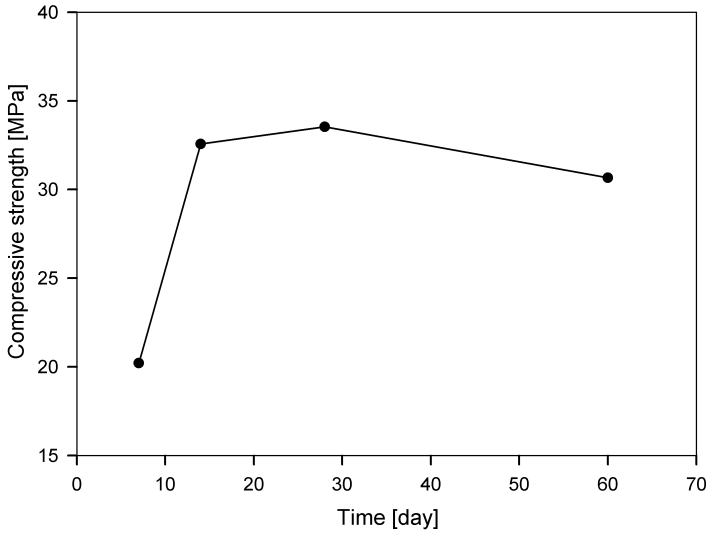

Fig. 4.4. The compressive strength development of metakaolin based mortar with residues of undissolved metakaolin after *Rüscher et al., (2010b)*.

consequently leads to lower drop in strength. Fig. 4.4 shows the example of mechanical strength of metakaolin based mortar, containing a large portion of non-reacted metakaolin similar to Cem.6 (*Rüscher et al., (2010b)*).

Geopolymers synthesised with different alkali cations exhibit differences in thermal stability and setting temperatures (*Duxson et al., (2005b)*). *Rahier et al., (2006)* found, that metakaolin inorganic polymer derived from sodium silicate sets at a faster rate than those derived from potassium silicate. Moreover, the sodium inorganic polymer was found to be stronger than its potassium based equivalent (*Steveson et al., (2005)*). It has been reported, that the excess of alkali ions leads to lower degree of condensation of silicate species, what results in longer strengthening process and lower ultimate strength (*De Silva et al., (2008)*). Alkali activation of metakaolin with water glass produces higher strength than activation with alkali hydroxide alone (*Luz et al., (2007)*). This can be explained by the absence of condensed silicate fraction, which maximizes the strengthening and is in line with hardening theory of Cem.1. According to *Lutz et al., (1999)*, the addition of KOH into the alkaline solution must finally lead to lower degree of condensation of silicate species, what is reflected with slower hardening of weakening process and lower ultimate strength.

It has been found, that the physical properties of metakaolin-based geopolymer improves significantly, if more silicate is added (Fig. 7.1) (*Palomo (1999); Barsoum et al., (2006)*). The same effect has also been found for fly ash-based geopolymers (*Qing-Hua et al., (1992); Criado et al.,*

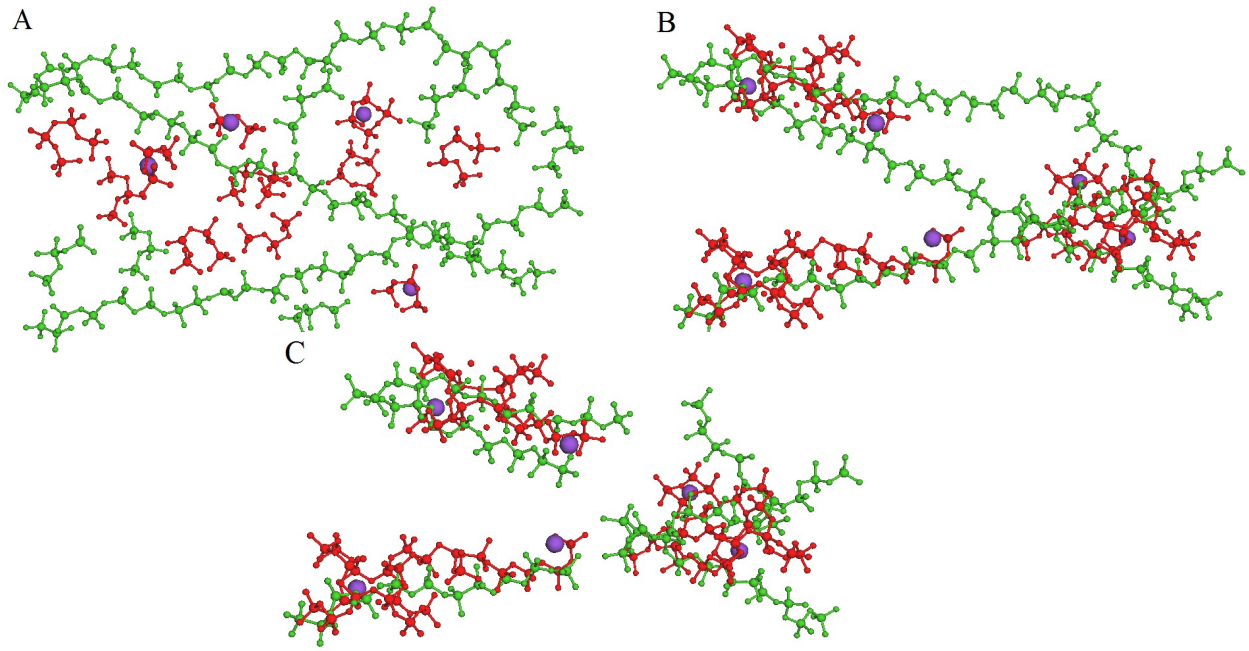

Fig. 4.5. The structural development of aluminosilicate gel; green units- polycondensed silicate species, red units- dissolved aluminate and silicate from metakaolin, violet points-potassium ions, A) dissolution of metakaolin and condensation of silicate units, B) formation of aluminosilicate network, C) decomposition of polycondensed silicate species and formation of aluminosilicate network.

(2005)). The addition of soluble silicates into the alkaline solution has been described as one of most important conditions for preparing strong inorganic binder (*Lee et al., (2003)*). It has been found, that the gradual increase of slag amount at the cost of metakaolin contributes to the increase of compressive strength (*Wang et al., (1995a); (1995b)*). Slag contains high amount of CaO, so increasing its content, increases both the concentration of silica and calcium, what evidently leads to better strength. In case of metakaolin-slag based geopolymer, the presence of CaO provokes the formation of CSH gel type, besides the formation of aluminosilicate phase (*Alonso et al., (2001a, 2001b); Lecomte et al., (2006)*.

Summary of geopolymerization process of Cem.1 and a simple view of the basic structural developments

Concluding the analysis based on FTIR investigations, Molybdate measurement and strength development of Cem.1, in hardening process, following reactions may be distinguished:

a)dissolution of metakaolin to potassium aluminate and potassium silicate units during the first 13 h of ageing,

b)condensation of silica species, due to dissolution of metakaolin particles during the first day of curing,

c)shortening of polycondensed chains, due to the release of OH groups, which takes place as the consequence of aluminosilicate growing and network cross-linking,

d)including decomposed silicate units into the three dimensional aluminosilicate network between 25^{th} and 525^{th} of ageing.

Three steps of Cem.1 geopolymerization process are schematically presented in Fig. 4.4. Stage A shows the dissolution of silicate and aluminate species in metakaolin (red units) and polycondensation of silicate species (green units). Further development (stage B) demonstrates the condensation process of dissolved aluminate and silicate to aluminosilicate network and still present polycondensed fraction of silicate chains. The next step of ageing (stage C) indicates further formation of aluminosilicate network and silicate chains decomposition, whereas some portion of shortened silicate chains are included into aluminosilicate framework. It may be concluded, that all oligomeric units become part of aluminosilicate network during 525 h of ageing.

4.2.2. Ageing process of Cem.2-7

The influence of alkali ions on DOSPM of asymmetrical stretching

According to the literature, the concentration of alkali is one of most important factors determining the geopolymerization process (*Antonić et al., (1994))*. Referring to *Osswald et al., (2006)*, the presence of alkali ions determines the condensation process of silica in silicate solution and shifts the maximum of asymmetrical stretching to lower frequencies. This effect was also seen in the potassium silicate glasses and silica solution system. Therefore, it might be expected, that the significant increase of alkali content in silicate solution will tend to depolymerization of aluminosilicate network and silicate chains shortening in geopolymer system. This process is favoured in geopolymer composition with molar ratio K/Al>1. Potassium water glass with the same concentration of alkali ions was used to prepare Cem.1-7. According to Fig. 4.6, for lower K/Al ratios, DOSPM shifts towards lower wavenumbers with the increase of potassium content. Above K/Al=1.2 the behaviour of DOSPM is opposite and shifts towards higher wave numbers. The variation in the alkali ions concentration goes together with changes in the amount of OH groups, which are used to dissolve metakaolin powder. The higher the amount of KOH in water glass, the higher the amount of aluminosilicate is dissolved. Higher degree of this reaction results in further shift towards lower frequencies. In case of Cem.2, due to the excess of silicate solution the

geopolymer contains silica-rich aluminosilicate framework and condensed alkali-silicate fraction, what is reflected with the DOSPM shift to higher frequencies.

FTIR study of ageing process of Cem.3-7

As it has been pointed above, DOSPM of asymmetrical stretching of Cem.1 indicates the dissolution process and polycondensation of silicate units during first 24 h of ageing. After 1 day of curing, a systematic displacement in the range of asymmetrical stretching shows the decomposition of condensed silicate species and formation of aluminosilicate network. The other six compositions of alkali activated cement have been investigated to extend the knowledge about DOSPM displacement in relation to metakaolin/water glass ratio. According to the literature (*Steveson et al., (2005))*, geopolymerization reaction is determined mainly with Si/Al and K/Al molar ratios of alkali activated binder. Therefore, the changes in composition should result in different peak position and kinetics of DOSPM shift over ageing time. The alkali activated cements were prepared by mixing different amounts of metakaolin and potassium water glass to check the influence of non-reacted solid on the DOSPM stretching. It has been found that after 1st day of ageing the infrared spectra of alkali activated cement Cem.3-7 indicate DOSPM displacement towards lower wave numbers. The detailed FTIR study of Cem.3 and Cem.4 ageing process proves, that DOSPM systematically shifts towards lower frequencies after initial 24 h of curing (Fig. 4.6). Moreover, the distance of DOSPM displacement increases with the amount of water glass in geopolymer composition. This suggests higher dissolution of metakaolin leading to lower fraction of non-reacted solid (*Luz et al., (2007))*. Referring to the literature, the DOSPM of asymmetrical stretching can be expected at higher frequencies in the earlier ageing stages of geopolymer containing residues of non-reacted metakaolin (*Jirasit et al., (2006))*.

FTIR study of ageing process of Cem.2

In distinction to Cem.3-7, which contains partially non-reacted metakaolin, Cem.2 contains excess of water glass. Significant changes in the structure of Cem.2 during ageing process are reflected with DOSPM shift from 1014 cm^{-1} to 1018 cm^{-1}. The final DOSPM position is related to condense silica and silica-rich aluminosilicate framework. In contrary to Cem.3-7, the DOSPM shift of Cem.2 is related to the partial decomposition of condensed silicate and three dimensional network's formation. DOSPM displacement to higher frequencies indicates the increase of Si/Al ratio as given by the nominal composition and with ageing time. According to the linear relation for glasses, the

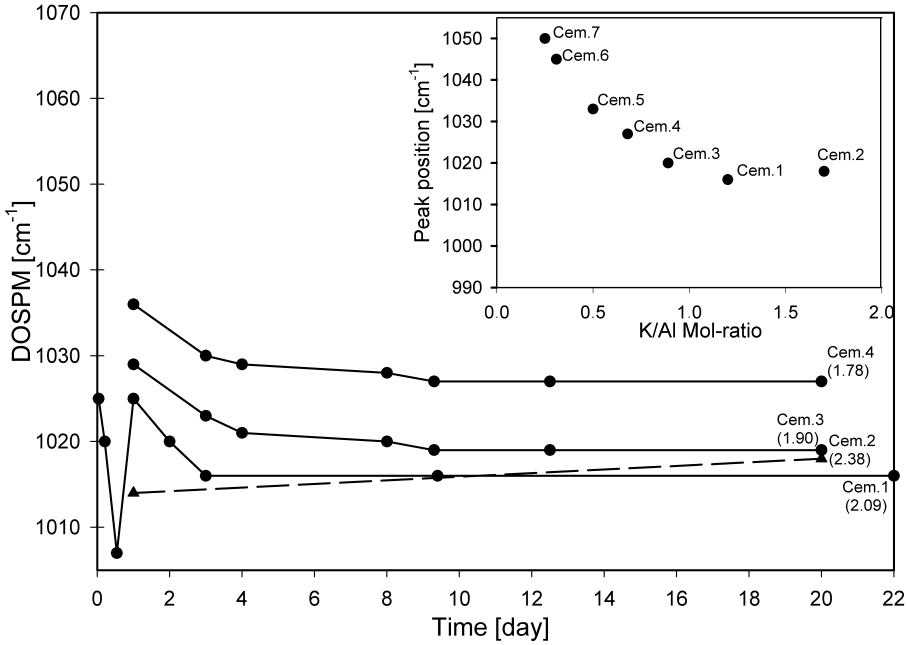

Fig. 4.6. The DOSPM of asymmetrical stretching of geopolymers with residues of unreacted metakaolin (Cem.2-Cem.6), with excess of potassium water glass (Cem.2) and fully reacted geopolymer (Cem.1). The relation between molar ratio K/Al and DOSPM of asymmetrical stretching for metakaolin based geopolymer (Cem.1-Cem.7).

increase of Si-O bond concentration in aluminosilicate framework should be accompanied with the peak shift towards higher frequencies, as observed. According to *Rüscher et al. (2010b)*, silica-rich cements prepared from rice husk bark ash (RHBA) indicate different tendency in DOSPM shift than samples with high Al content (Fig. 7.2). The composition with molar ratio Si/Al>1000, after 3 h of ageing indicated the DOSPM shift from 1016 cm^{-1} to 1045 cm^{-1}. This DOSPM displacement has been assigned to the condensation process of silica-rich framework. The tendency in DOSPM displacement was similar for all tested silica-rich cements. The furthest shift was noted for geopolymer with the highest silica content, what is in good agreement with the relation between DOSPM and Si/Al ratio for glasses.

Dissolution process of metakaolin during ageing of Cem.3-7

It has been assumed, that the final DOSPM at 1016 cm^{-1} of Cem.1 is related to fully reacted composition. Afterwards, from each spectra of Cem.3-7 recorded after 20 days of ageing, the definite spectrum of non-reacted metakaolin has been numerically subtracted (Fig. 3.19). The subtracted spectrum has been scaled according to the distance between the final DOSPM of

geopolymer and position 1016 cm^{-1}. For example, from spectrum of fully reacted composition, the peak position is already at 1016 cm^{-1}, so multiplication factor is 0, what indicates 0 % of non-reacted metakaolin. If for example the subtracted raw solid spectrum needs to be scaled with the value of 0.75, one concludes that 25% of metakaolin has been reacted. It has been observed, that the increase of undissolved metakaolin mass leads to smaller shift towards lower frequencies. Moreover, both the spectra of Cem3-7 with subtracted absorption fraction of non-reacted metakaolin and spectra of Cem.1, exhibit the final DOSPM at 1016 cm^{-1} and both overlap in the range of symmetrical and asymmetrical stretching. According to that, the spectra of Cem.3-7 recorded after 20 days of ageing consist of two components: the absorption part of binder phase and non-reacted metakaolin. As it is showed in Fig. 4.7, the straight line was drawn between peak position at 1070 cm^{-1}, which is indicated by raw metakaolin powder and 1016 cm^{-1} related to complete dissolution of metakaolin. This correlation satisfies equation y=-1.85x-1981.5. Fig. 4.7 shows, that the evaluated mass of reacted metakaolin (black spheres) is in good agreement with this formula for every cement. This confirms, that the higher fraction of dissolved metakaolin in geopolymer composition, the further shift to lower frequencies. The molar ratio Si/Al of geopolymer binder phase of each cement has been calculated from subtracted part of metakaolin. It has been found that the final binder phase of all cement indicates similar molar ratio Si/Al within the range of 1.8-1.9 irrespective of starting composition. According to that, the final peak position in range of asymmetrical stretching is mainly determined with the concentration of non-reacted metakaolin, which covers the absorption spectra of aluminosilicate binder. These results confirm, that the amount of reacted metakaolin in every composition is limited with the concentration of OH groups, so the amount of reacted metakaolin should increase with higher content of silicate solution.

Table 12 The theoretical and evaluated fraction of reacted metakaolin in Cem.3-7.

Cement	Theoretical mass of dissolved metakaolin [g]	Theoretical mass of dissolved metakaolin [%]	Molar ratio Si/Al	Calculated from DOSPM shift mass of dissolved metakaolin [g]	Calculated from DOSPM shift mass of dissolved metakaolin [%]	Molar ratio Si/Al
Cem.7	15	20	2.09	24	32	1.83
Cem.6	18	25.7	2.09	31.5	45	1.8
Cem.5	24	40	2.09	39	65	1.82
Cem.4	28.8	55	2.09	43.16	83	1.86
Cem.3	33	73.3	2.09	37.8	84	1.89

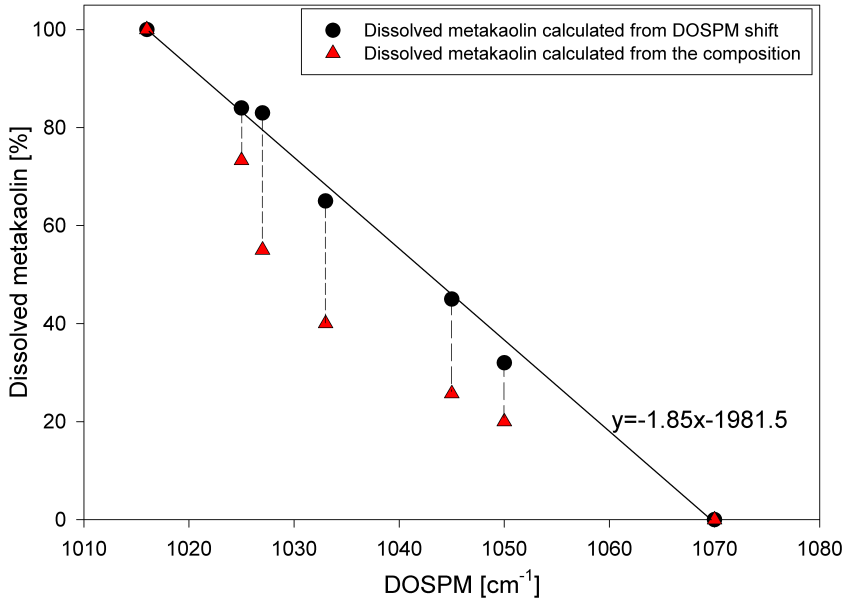

Fig. 4.7. The dependence between dissolved portion of metakaolin and final DOSPM of asymmetrical stretching, a) red triangles: theoretical amount of dissolved metakaolin, b) black spheres: calculated amount of dissolved metakaolin from FTIR spectra.

The theoretical Si/Al ratio of Cem.1 was calculated from the initial composition and equals 2.09 as given by the mixture with 62.5 g water glass in order to dissolve 32.7 g metakaolin. A theoretical Si/Al ratio of 2.09 has been calculated for Cem.3-7 for the maximal solubility of metakaolin (Table 12). Referring to linear dependence for glasses, the final peak position at 1016 cm^{-1} implies the molar ratio Si/Al=1.9. However, as mentioned before, theoretical Si/Al ratio for geopolymer with completely reacted metakaolin should equal the value of 2.09. It seems, that small discrepancies between theoretical and experimentally obtained molar ratio of Si/Al could result from too small intensity of subtracted raw metakaolin spectrum. Following this idea, the DOSPM at 1016 cm^{-1} also indicates some residues of non-reacted solid, which have not been considered in spectra subtraction and in consequence have contributed to the discrepancy between the obtained and expected Si/Al ratios of the geopolymer binder phase. According to linear dependence for glasses (Fig. 4.2), it might be suggested, that fully reacted composition, without excess of water glass and characterized by theoretical Si/Al=2.09, will indicate DOSPM at higher frequencies, namely at 1021 cm^{-1}.

In order to estimate the DOSPM of binder phase after one day of ageing (spectra E*), a definite fraction of undissolved metakaolin spectrum was subtracted. The subtracted spectrum was the sum of the undissolved metakaolin spectrum, present in the final spectra of Cem.3-7, and the difference

between the non-reacted metakaolin spectrum between 1st and 20th day of ageing. The DOSPM of asymmetrical stretching of spectrum E* is related to binder phase and minor amount of non-reacted metakaolin because the kinetic of ageing process of every composition is different and the DOSPM at 1016 cm^{-1} indicates some residues of non-reacted metakaolin. The DOSPM in the spectrum E* occurs below the characteristic position at 1016 cm^{-1}. Therefore, according to the linear dependence for glasses, the binder phase in geopolymer body after one day of ageing indicates lower Si/Al ratio, than after 20 days of curing. Hence, the DOSPM shift after 1 day of ageing in the system of Cem.3-7 is related to the dissolution of metakaolin in geopolymer followed with the formation of aluminosilicate network. Conclusion from this, the dissolution process leads to the increase of Si/Al ratio of binder phase between 1st and 20th day of ageing.

4.3. The relation between Raman spectroscopy of glasses and geopolymers

4.3.1. Raman spectroscopy of glasses

Raman scattering as a complementary technique to infrared absorption spectroscopy has been used in order to extend knowledge about the structure of glasses and to study the structural changes during ageing time of geopolymers. However, Raman investigations of metakaolin based binders has not been published so far, probably because of fluorescence problem and a low signal to noise ratio.

It was shown that the Raman spectra of Glass.1-4 confirms the behaviour of appearing bands in relation to silica content discussed by *McMillan et al., (1982)*. The Raman study of geopolymers was extended with investigation of potassium silicate glasses in order to study in detail the Si-O bonding and alkali cations in the system of silicate, (Fig. 3.21). It is generally known, that silica glass consists of a three dimensional framework of SiO_4 tetrahedra and alkali oxides breaks the Si-O-Si bridging oxygen, what leads to the formation of NBOs (non-bridging oxygen). The absence of aluminium, which balance the charge in glass network, contributes to the formation of $Si\text{-}O^-$ units and de-polymerization of silicate framework (*Hanna et al., (1964))*. The bands in the range of 430-500 cm^{-1} are related to Si-O-Si linkages of silicate network. The decrease of that peak's intensity peak is assigned to de-polymerization process of silicate framework, due to the higher concentration of alkali ions and lowering the amount of Q^4 groups with Q^3, Q^2, Q^1. *Furukawa et al., (1981)*, observed the same effect of peak narrowing at about 520 cm^{-1} and shift to higher frequencies with increase of Na_2O fraction. Similarly, *McMillan et al., (1986)* pointed, that in the system of dry sodium silicate glasses the displacement of 550 cm^{-1} band should be interpreted in terms of decrease in average Si-O-Si angle, what is often accompanied with a decrease in average polymerization of the silicate units. Referring to the literature (*Hanna et al., (1964))*, the high frequency range of sodium silicate glasses is related to $Si\text{-}O^-$ vibrations of non-bridging oxygen. According to that fact, the changes in 1000-1200 cm^{-1} regime resulted from different concentration of potassium ions in the structure of silica glass, what was attributed to $Si\text{-}O^-$ units, ie. non bridging oxygens (NBO).

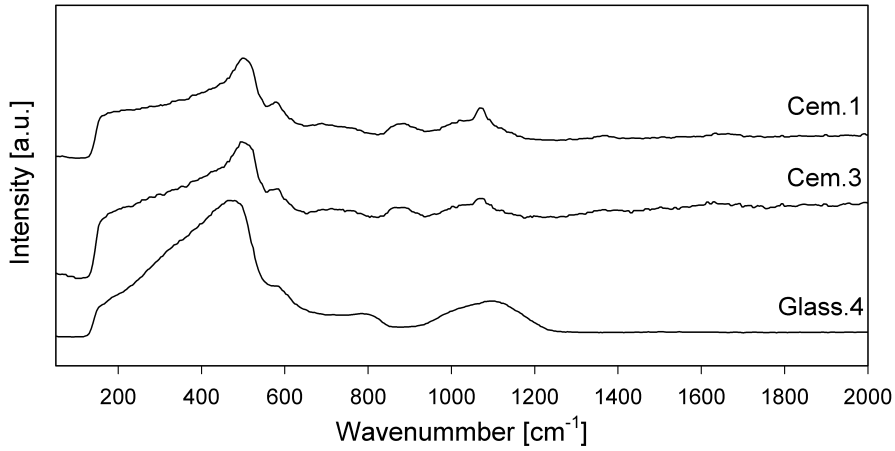

Fig. 4.8. Raman spectra of geopolymers (Cem.1, Cem.3) and sodium aluminosilicate glass (Glass.4).

4.3.2. Raman spectroscopy of geopolymers

Raman spectra of geopolymers resemble the spectra of glasses (compare Fig. 4.8). Unlike this amorphous aluminosilicate, the spectra of inorganic binders indicates high intensity of background. This effect results from residues of non-reacted metakaolin, which exhibits high fluorescence signal. The most intense Raman vibrations of inorganic binders occur within 400-500 cm^{-1}, 580-650 cm^{-1}, 700-880 cm^{-1} and 1000-1200 cm^{-1} regions (Fig. 4.8). It has been found, that the vibrations in the first regime are sensitive for changes of Si/Al ratio of initial composition. Similarly to the peak behaviour in the glass systems, the maximum of intensity at about 520 cm^{-1} shifts with the increase of silica towards lower frequencies in geopolymers. Therefore, the first regime has been assigned to T-O-T vibrations of aluminosilicate network, where T is Si or Al. Unlike Raman measurement with the infrared laser line (1064 nm), the green laser line (532 nm) excites two additional vibrations in geopolymer spectra. These vibrations indicate strong relation to the amount of water glass used in mixture, ie. the intensity increase with the rise of silica content (Fig. 3.22). According to that, these bands have been assigned to the motion of silicon against tetrahedral cage.

An important question concerns the 1064 cm^{-1} peak in the spectrum (Fig. 3.23). It has been noted, that this peak remains at the same position irrespective of starting composition Si/Al ratio and using NaOH or KOH. Moreover, its height increases with the rise of silica from water glass and fades with the increase of non-reacted amount of metakaolin. This dependence suggests, that the 1064 cm^{-1} peak is related to Si-O. As the ageing process of cements is also accompanied with carbonation process, the geopolymeric samples have also been tested in this regard. before measurement the samples were cured in closed containers and were investigated in nitrogen atmosphere to avoid this

undesirable process. The characteristic band at 1064 cm^{-1} occurs at the same position both in the spectra of potassium and sodium geopolymer, what suggests, that the type of alkali ions doesn't play any role here. Moreover, the distribution of peak intensity in high frequency region doesn't overlap with the most intense bands exhibited by K_2CO_3 or Na_2CO_3 at 1060 cm^{-1} and 1078 cm^{-1}, respectively (Fig. 3.23). Therefore the 1064 cm^{-1} band doesn't indicate any relation to carbonation process in geopolymer body.

The acid leaching experiment of Cem.1 was carried out to verify the relation between the vibrations in high frequency region and condensation process of silicate species in geopolymer body, It has been found, that acid treated geopolymer indicates a new band at 987 cm^{-1}, whereas 1064 cm^{-1} peak remains at the same position and only slightly increases in intensity. New vibrations have been assigned to the formation of K_2SO_4. According to the literature (*Osswald et al., (2006)*), a peak shift towards higher wave numbers in 1000-1200 cm^{-1} region occurs as a result of higher molecular weight of condensed silicate species. This effect was not observed in the study of acid treated geopolymer, so the dependence between condensation process of SiO_4 tetrahedra and Raman vibrations at 1064 cm^{-1} was ruled out. The experiment of condensed silicate solution was in contrary to previous observations, in which the changes in Raman pattern of water glass were accompanied with the exhibition of new band at 1060 cm^{-1}.

Raman study of ageing process of Cem.1 and Cem.8

According to the ageing study of potassium (Cem.1) and sodium geopolymer (Cem.8), the changes in Raman pattern have been observed in the range of T-O-T vibrations and at 1064 cm^{-1}. It has been found, that the increase of peak height at 1064 cm^{-1} is accompanied with the sharpening of broad peak in the lower frequency region, which is assigned to the slowly growing aluminosilicate network and probably cross-linking of silicate chains. Although the intense condensation of geopolymer framework starts after first 24 h of ageing, the 1064 cm^{-1} band becomes strongest in intensity after three days of curing. This effect correlates in time with development of Cem.1 maximum flexural force. The changes in intensity of 1064 cm^{-1} peak (PeakII) in relation to the maximum at 490 cm^{-1} (Peak I) over time for many series of Cem.1 were measured with help of green laser line (Fig. 4.8). The low frequency peak doesn't indicate any considerable changes in intensity during ageing time, but it serves as a normalization basis for Peak II, which indicates characteristic changes. It has been found that the maximal intensity of 1064 cm^{-1} band is seen

between 100 h and 300 h after preparation. Above 500 h of ageing the Peak II/Peak I ratio is lower than at earlier stage of geopolymerization and remains stable over further curing time. It might be stated that the changes in intensity at 1064 cm^{-1} correlate with the changes in geopolymeric structure. According to Molybdate activity of silicate units, the maximal intensity of 1064 cm^{-1} peak should by assigned to the intense condensation of geopolymeric framework, whereas stable behaviour of peak intensity above 500 h of curing indicates low variation in aluminosilicate structure.

As it has been mentioned before, early strength of the Cem.1 results from coexistence of two structural units: aluminosilicate network and silicate chains. Therefore, it might be stated, that the reason of 1064 cm^{-1} vibrations results from the interaction of both structural phases. Moreover, crucial role is played here by the concentration of alkali ions, because the vibrations in high frequency region of metakaolin based geopolymer are not seen in composition with lower alkali content (K(Na)/Al<1). According to the literature (*Hanna et al., (1964))*, higher alkali fraction, than required to balance the charge of Al, results in higher concentration of $Si\text{-}O^-$ non-bridging oxygen bonds. So, the increase of alkalis in geopolymer composition correlates with lower condensation of silicate chains and higher concentration of non-bridging oxygen. $Si\text{-}O^-$ bonds, in decomposed chains, require additional metallic donors. That is why, it interacts with alkali cations, which are strongly attached to the sialate molecules. Concluding, 1064 cm^{-1} peak is related to $Si\text{-}O^-$ non-bridging oxygen bonds interacting with alkali ion in cross-linked aluminosilicate network.

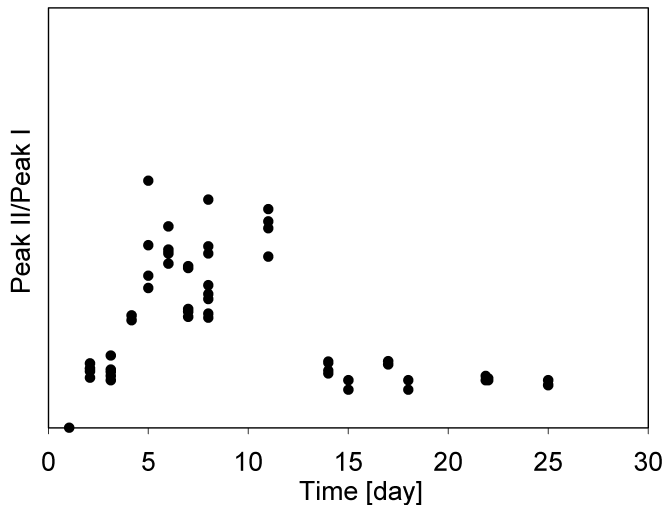

Fig. 4.9. The dependence between intensity ratio Peak II/Peak I and ageing time for Cem.1. The intensities were estimated from experiments carried out with CRM 200 equipment.

4.4. Thermal analysis of geopolymer

Water is one of the reactants and also one of the products in geoplymerization process. The dissolution of alumina and silicate consumes water, but on the other hand, the polymerization reaction between alumina and silicate produces water. According to FTIR study, during first 24 h of ageing, the hydroxide groups dissolve the alumina and silicate in metakaolin powder. After dissolution, OH^- are released, leading to the formation of aluminosilicate network and decomposition of the silicate chains. The samples were closed during curing to avoid the loss of water, so the evaporation of water, as the reason of fast weakening of Cem.1, can be excluded (*Perera et al., (2007b))*. This is in line with the observed mass losses in TG experiments.

The FTIR spectra of samples that have been heated up to 1000 ^oC confirms the existence of two processes running during heating: de-hydroxylation and de-carbonation (*Rahier et al., (2006); Subaer et al., (2006))*, as well as it indicates high stability of alkali activated cement at elevated temperatures (*Barbosa et al., (2003a, 2003b))*. No significant change is observed in the density of peak distribution below 950 ^oC. Above 950 ^oC the changes in infrared pattern are more visible, mostly with the shift to another frequency and broadening of T-O-T peaks. These changes may indicate the modifications of bond length and angles resulted from partial crystallization process to leucite and kalsilite. Similar to FTIR spectra, the X-Ray diffraction pattern of thermal treated geopolymer doesn't show no significant transformation below 950 ^oC. Above that temperature, the existence of many sharp peaks and decrease in intensity of amorphous broad hump is noted, which proves the formation of crystalline fraction in alkali activated cement.

Thermal treatment up to 600 ^oC was carried out to find the relation between the variation in geopolymeric structure and curing time with elevated temperature (Fig. 3.30, Fig. 3.31). It has been expected, that if the geopolymer is cured in sealed container, the mass loss during thermal treatment should be similar for all geopolymers characterized with the same composition and irrespective of tested samples ageing time. According to the literature (*Xu et al., (2003))*, the polymerization between Al-O and Si-O units produces water and higher extend of water loss in the further stage of geopolymerization indicate higher degree of polymerization. Besides, the extend of a water loss in the geopolymerization process indicates the extend of the added water in inorganic binder encapsulation. It has been stated, that the discrepancies between the final mass loss of heated Cem.1 samples (the first thermal treatment) results from fast evaporation of water, which occurs after

opening the pores and powdering the sample. This effect has been observed during the first hour of curing at ambient temperature in protective atmosphere. The variation in the rate of water release results from different strength of water bonding in geopolymeric structure and should undergo significant change during curing time of alkali activated cement. Following this argument, weaker bounding of water in geopolymeric body leads to faster removing molecular water from geopolymeric framework and vice versa. The highest release of water at ambient temperature recorded during the first thermal treatment was noted for 800 h and 24 h cured sample. According to the Molybdate analysis during first 24 h of ageing, the dissolution of metakaolin powder and polycondensation of silicate chains occur, whereas after 525 h of curing a disproportionate ion of aluminosilicate network takes place. This structural development over time in geopolymer body explains different nature of water bonding. It has been found, that the samples with curing time longer than 24 h and shorter than 432 h indicate lower evaporation of water. This effect explains a higher degree of aluminosilicate network's polymerization.

One of most important features of zeolites is a reversible water absorption after thermal treatment. While water moves in and out of these pores, the zeolites framework still remains rigid. During heating up to 400 °C water is removed, without decomposition of the crystal structure. This process is reversible. The pores should be bigger than water molecule, at least of diameter 0.5-0.7 nm, to absorb water. After the first thermal treatment up to 600 ^{o}C, geopolymers were put in humid conditions for 24 h and again heated. According to the mass loss of water, which was much lower and faster during second experiment, it might be stated, that the first heating enforces to significant changes in geopolymer structure, while second heating influenced the structure much less. The range of DOSPM indicates a broadening of the thermal treated sample and a slightly increased peak width of twofold heated geopolymer. From this investigation it may be concluded, that during the first heating the pore size and distribution undergoes modifications whereas structural modification are less significant in further heating cycles. Smaller pores size explains low ability to absorb water from humid environment and faster rate of water release. Hence, it might be stated, that some modifications of aluminosilicate framework and lowering the capacity of geopolymeric structure of keeping water absorbed, is generated with thermal heating up to 600 ^{o}C.

In this study, the location of endothermic peak has been used as the indicator of the water release rate from aluminosilicate structure. It has been found, that the endothermic peak appears at lower temperatures during the second thermal treatment. Referring to the literature, the change of

endothermic peak to lower temperatures means weaker binding between water and the network in the geopolymer gel phase. Furthermore, it also reflects a change from physically adsorbed water to chemically bonded water (*Xu et al., (2003))*. Moreover, 800 h and 24 h cured samples indicate endothermic peak at lower temperatures than the rest of the tested samples. This observations confirms the relation between the condensation of aluminosilicate network and the rate of water loss.

Concluding, the rate of the physically or chemically bounded water loss in gel phase is related to the formation process of network and increases the disordering of the gel phase. Each stage of geopolymerization process is characterized with different ability to keep water in the structure. Fast rate of H_2O release has been assigned to low condensation and partial decomposition of the aluminosilicate framework.

5. SUMMARY

Most of studies concern either the optimisation of the chemical composition-mechanical strength relationship or focus on the spectroscopy of rather complex compositions and much less on the question, which nano-structural units are responsible for obtaining high strength or what underlying mechanisms are responsible for often observed weakening of certain geopolymer compositions during ageing (*Rüscher et al., (2009))*. Thus the primary focus of this work was to answer the question, what determines the properties of an aluminosilicate gel during hardening rather than to optimise directly its properties in order to make it suitable for building materials. For this reason the alkali activation of metakaolin was investigated, which could be seen as a model system for the processes, involved during geopolymerization. For better understanding of the geopolymerization process this study has been extended with the investigations of silicate and aluminosilicate glasses.

It has been shown, that the DOSPM of asymmetrical stretching for aluminosilicate glasses follows a linear relationship on the Al molar ratio (x=1/(1+Si/Al)) and satisfies an equation: y=-257x+1105. This relation comes remarkable close to that obtained by *Fichtner-Schmittler et al., (1990)* for faujasite type zeolites. On the basis of FTIR measurement of silica solution there has been claimed a close equivalence in DOSPM between $Q^4(4Al)$, $Q^4(3Al)$, $Q^4(2Al)$ and Q^0, Q^1, Q^3 for the aluminosilicates and silicates, respectively. The linear relations for glasses implies the final DOSPM at 1016 cm^{-1} for Si/Al=1.9, what is in good agreement with the theoretical ratio for Cem.1 (Si/Al=2.09).

Alkali activation of metakaolin leads to the formation of an aluminosilicate network in a continuous reaction during ageing between 25 h and 525 h. The condensation of aluminosilicate network includes monomeric ($Q^4(4Al)$) and dimeric ($Q^4(3Al)$) units, which are formed during 25 h of curing and which comprise about 20 % of the total silicate units. The 20 % of polycondensed silicate units are formed during ageing between 13 h and 25 h. These units originate from the water glass and according to Molybdate measurement, all of them become a part of the aluminosilicate network during ageing up to about 525 h. The driving force for the further reaction has been assigned to the fact, that the aluminosilicate should tend to a Si/Al ratio of 1 thus leading to a disproportionation.

Infrared study of ageing process at 25 °C supported with Molybdate measurement gave new insight into the strengthening and weakening of alkali activated metakaolin. It has been stated, that the coexistence of two structural units (silicate chains, aluminosilicate network) determines the

hardening effect of geopolymer. The right proportion and spatial distribution of both structural phases maximize mechanical strength. The increase in strength coincides with the shift in the DOSPM from 1025 cm^{-1} to 1016 cm^{-1} which is dominated with the slowly growing aluminosilicate network and cross-linking the polysilicate chains. However, weakening over 200 h of ageing results from the decrease of polycondensed silicate fraction. Fast condensation of silicate chains occurs as the consequence of dissolution of metakaolin to potassium aluminate and potassium silicate units. This process is seen with the rapid shift of the DOSPM from 1007 cm^{-1} to 1025 cm^{-1} for ageing between 13 h and 25 h. The subsequent destruction of silicate chains results from the condensation of aluminosilicate framework, which leads to the release of OH^- groups and is reflected with the DOSPM displacement to lower frequencies.

Different trends could be resolved in the DOSPM and in the molybdate activity are seen in the series of samples aged at 25 °C within 96 h. The Molybdate and FTIR investigation for the series of samples cured at 50 °C, 70 °C and 130 °C were not carried out in so far. Probably a further separation of the structural development could be more complicated because of the fast processes being relevant here. Above 100 h DOSPM of asymmetrical stretching remains at 1016 cm^{-1} and covers further development of aluminosilicate network. It has been found, that the second derivative of infrared geopolymer spectra cured above 100 h indicates some changes in the range of asymmetrical stretching. This fact confirms further variation in geopolymer structure. Moreover, the systematic changes of intensity in the range of Si-OH stretching and H_2O bending mode result from condensation of aluminosilicate network and decomposition of silicate chains running simultaneously. Further support for structural changes in the later stage of ageing was also given with acid leaching experiments. The acid effect as observed in the IR absorption spectra and by the Molybdate method has been discussed in detail. A minimum shift in the DOSPM for acid treated samples indicates the highest stability against acid, which could be assumed for the most suitable protection of Al-O-Si bonds within an aluminosilicate network. Any meaningful changes in the DOSPM can only be seen in kinetically controlled leaching experiments with low condensed acid. Thus, at longer time of acid treatment the DOSPM always tends to 1080 cm^{-1} irrespective of tested samples ageing time.

The concentration of alkali is one of the most important factors determining the geopolymerization process. It has been claimed, that the potential of dissolution of metakaolin powder depends on the concentration of alkali hydroxide in geopolymer composition. On the basis of X-Ray diffraction

study of metakaolin-based cements (Cem.3-7), the relation between the width of characteristic broad hump and alkali activation of metakaolin was found. The increase of water glass fraction at the cost of metakaolin in geopolymer composition leads to the peak sharpening.

Further FTIR study focus on geopolymers containing high portion of non-reacted metakaolin. It has been proposed, that with help of spectral subtraction method, it is possible to separate the fraction of undissolved solid and geopolymer binder phase. For this reason, the peak at 1016 cm^{-1} has been assumed as the final DOSPM of asymmetrical stretching of fully reacted composition (Cem.1). Infrared spectra of metakaolin was subtracted from the spectra of Cem.3-7, The DOSPM shift from peak position related to alkali activated cement after 20 days of ageing was estimated. After subtraction of a definite contribution of the metakaolin spectrum, a close similarity with the spectrum of Cem.1 was observed. According to that, it has been stated, that with help of spectral subtraction method, it is possible to separate the absorption part of spectrum of non-reacted and reacted phase. The content of dissolved solid and molar Si/Al ratio of binder phase after 20 days of ageing for each geopolymer was calculated from the part of removed raw metakaolin infrared spectra. It has been stated, that the final DOSPM of metakaolin based cement results from two components: the infrared absorption part related to undissolved metakaolin and the geopolymer binder phase and the calculated molar Si/Al ratio (within range 1.8-1.9) of binder phase is similar for all tested compositions.

The theoretical molar Si/Al=2.09 ratio calculated from starting composition for each alkali activated cement (Cem.3-7) is higher than Si/Al ratio estimated from spectral subtraction method for geopolymer cured 20 days at room temperature. From that, it has been concluded, that DOSPM at 1016 cm^{-1} also indicates some residues of non-reacted metakaolin. Thus the DOSPM of fully reacted composition should be exhibited at higher wave numbers (around 1020 cm^{-1}) and the final real and theoretical molar ratio Si/Al of binder phase should be the same.

The Raman spectra of glasses confirm the similar behaviour of all bands in relation to the silica content discussed by *McMillan et al. (1982)*. On the basis of Raman study of glasses, silicate solution and alkali activated cements with different portion of metakaolin, the characteristic Raman vibrations in lower frequency range has been related to T-O-T vibrations of the aluminosilicate network. The characteristic peak at 1064 cm^{-1} has been assigned to $Si\text{-}O^{-}$ non-bridging oxygen bonds in decomposed silica chains, which interact with alkali ions in aluminosilicate cross-linked

network. It has been found, that the position of that band doesn't depend on the type of alkali ions, but on their concentration. The excess of alkali leads to the shortening of silicate chains and to the increase of $Si\text{-}O^-$ bonding, what explains the absence of that band in the Raman spectra of geopolymer characterized with K/Al<1.

Thermal analysis consisted of heating up the sample to 600 ^oC, then holding it in the humid conditions to absorb water, followed by second heating step. It has been found that the first thermal treatment of Cem.1 indicates about 25 % of mass loss, whereas the second heating shows about 10 % of mass release. This difference has been related to the changes in geopolymeric structure caused by the first heating. However, lower mass loss in the second run has been assigned to lower ability to re-absorption of molecular water, due to smaller size of pores. It might be expected, that repeated thermal treatment of twofold heated samples will not contribute to any further structural changes and should indicate similar mass loss (about 10 %). During the primal heating, the difference in mass loss between samples with different ageing time showed that each stage of geopolymerization process is characterized with different ability to keep the water in geopolymeric structure. Fast rate of H_2O release has been assigned to low condensation and partial decomposition of aluminosilicate framework, what has been seen on example of alkali activated cement cured during 24 h and 800 h at room temperature.

6. REFERENCES

1. Alonso, S. and Palomo, A., Alkaline activation of metakaolin and calcium hydroxide mixtures: Influence of temperature, activator concentration and solids ratio, *Materials Letters*, 47, 55-62, (2001a).
2. Alonso, S. and Palomo, A., Colorimetric study of alkaline activation of calcium hydroxide-metakaolin solid mixtures, *Cement and Concrete Research,* 31, 1, 25-30, (2001b).
3. Antonić, T., Čižmek, A., and Subotić, B., Dissolution of amorphous aluminosilicate zeolite precursors in alkaline solutions. 2. Mechanism of the dissolution, *Journal of the Chemical Society—Faraday Transactions*, 90, 1973–1977, (1994).
4. Bakharev, T., Sanjayan, J. G. and Cheng, Y. B., Effect of elevated temperature curing on properties of alkali-activated slag concrete, *Cement and Concrete Research*, 29, 10, 1619-1625, (1999).
5. Bakharev, T., Resistance of geopolymer materials to acid attack, *Cement and Concrete Research*, 35, 658-670, (2005a).
6. Bakharev, T., Geopolymeric materials prepared using class F fly ash and elevated curing temperature, *Cement and Concrete Research*, 35, 6, 1224-1232, (2005b).
7. Barbosa, V. F. F., Mackenzie, K. J. D. and Thaumaturgo, C., Synthesis and characterization of materials based on inorganic polymers of alumina and silica: sodium polysialate polymers, *International Journal of Inorganic Materials*, 2, 309-317, (2000).
8. Barbosa, V. F. F. and Mackenzie, K. J. D., Thermal behaviour of inorganic geopolymers and composites derived from sodium polysialate, *Materials Research Bulletin*, 38,2, 319-331, (2003a).
9. Barbosa, V. F. F. and Mackenzie, K. J. D., Synthesis and thermal behaviour of potassium silicate geopolymers, *Materials Letters*, 57, 1477-1482, (2003b).
10. Barrer, R., M., Hydrothermal Chemistry of Zeolites, Academic Press, London, (1982).
11. Beard, W., C., Infrared studies of Aqueous Silicate Solutions, *Molecular sieves,* 3, 162-168, (1972).
12. Bell, J., L., Nanoporosity in Aluminosilicate, geopolymeric Cements, *Microsc. Microanal*., 10, (2004).
13. Bell, J., L., Driemeyer, P., E., Kriven, W., M., Formation of Ceramics from metakaolin Based Geopolymers: Part I-Cs-Based Geopolymer, *J. Am. Ceram. Soc.*, 92, 1, 1-8, (2009).
14. Breck, D., W., Zeolite Molecular Sieves, Wiley, New York, (1974).

15. Brough, A., R., Dobson, C., M., Richardson, I., G., Groves, G., W., Alkali activation of reactive silicas in cements: in situ ^{29}Si MAS NMR studies of the kinetics of silicate polymerization, *Journal of Materials Science*, 31, 3365-3373, (1996).

16. Brough, A., R., Atkinson, A., Sodium silicate based, alkali-activated slag mortars. Part I Strength, hydration and microstructure, *Cement and Concrete Research*, 32, 865-879, (2002).

17. Clark, D., E., Ethridge, E., C., Dilmore, M., F., & Hench, L., L.,Quantitative analysis of corroded glass using infrared frequency shifts, *Glass Technology*, 18, 4, 121-124, (1977).

18. Criado, M., Palomo, A. and Fernandez-Jimenez, A., Alkali activation of fly ashes. Part 1: Effect of curing conditions on the carbonation of the reaction products, *Fuel*, 84, 2048-2054, (2005).

19. Comrie, D., C., Peterson, J., H., Ritcey, D., J., Application of Geopolymer technology to waste stabilization, Geopolymer '88 Proceedings , 161-165, (1988).

20. Davidovits, J., Geopolymers: inorganic polymeric new materials, *Journal of Thermal Analysis*, 37, 1633-1656, (1991).

21. Davidovits, J., Chemistry of geopolymeric systems, terminology, in: The Proceedings of Geopolymere '99, St. Quentin, France, 9-39, (1999).

22. Davidovits, J., Geopolymer Chemistry and Application, (2008).

23. De Silva, P., Sagoe-Crenstil, K., Sirivivatnanon, V., Kinetics of geopolymerization: Role of Al_2O_3 and SiO_2, *Cement and Concrete Research*, 37, 512-518, (2007).

24. De Silva, P., Sagoe-Crenstil, K., The Effect of Al_2O_3 and SiO_2 On Setting and Hardening of Na_2O-Al_2O_3-SiO_2-H_2O Geopolymer Systems, *J. Aust. Ceram. Soc*., 44, 1, 39-46, (2008).

25. Duxon, P., Lukey, G., C., van Deventer, J., S., J. The effect of alkali metal type and silicate concentration on the thermal stability of geopolymers, Geopolymer Green Chemistry and Sustainable Development Solutions, edited by Joseph Davidovits, (2005a).

26. Duxson, P., Lukey, G., Van Deventer, J. S. J., Mallicoat, S. W. and Kriven, W. M., Microstructural characterisation of metakaolin-based geopolymers, *Ceramic Transactions*, 165 (Advances in Ceramic Matrix Composites X), 71-85, (2005b).

27. Duxson, P., Lukey, G. C., Separovic, F. and Van Deventer, J. S. J., Effect of alkali cations on aluminium incorporation in geopolymeric gels, *Industrial and Engineering Chemistry Research*, 44, 832-839, (2005c).

28. Duxson, P., Provis, J. L., Lukey, G. C., Mallicoat, S. W., Kriven, W. M. and Van Deventer, J. S.

J., Understanding the relationship between geopolymer composition, microstructure and mechanical properties, *Colloid and Surfaces A: Physicochemical Engineering Aspects*, 269, 1-3, 47-58, (2005d).

29. Duxson, P., Lukey, G., Van Deventer, J. S. J., Evolution of Gel structure during Thermal Processing of Na-Geopolymer Gels, *Langmuir*, 22, 8750-8757, (2006).
30. Duxson, P., Lukey, G., Van Deventer, J. S. J.,The thermal evolution of metakaolin geopolymers: Part 2-Phase stability and structural development, *Journal of Non-Crystalline solids*, 353, 2186-2200, (2007a).
31. Duxon, P., Mallicoat, S., W. Lukey, G., C., Kriven, W., M., van Deventer, J., S., J., The effect of alkali and Si/Al ratio on the development of mechanical properties of metakaolin-based geopolymers, *Colloids and surfaces. A, Physicochemical and engineering aspects*, 292, 8-20 (2007b).
32. Engelhardt, G., Hoebbel, D., Tarmak, M., Samoson, A.,and Lippmaa, E., ^{29}Si-NMR Untersuchung zur Aninostruktur von kristallinenTetramethylammonium-alumosilicaten und alumosilicatlösungen, *Z. für Anorg. und Allg. Chem*., 484,22-32, (1982).
33. Fichtner-Schmittler, H., Lohse, U., Miessner, H., Manek, H., E., Correlation between unit cell parameter, skeletal stretching vibrations and molecular fraction of aluminium of faujasite type zeolites for Si/Al=1.1-1000, *Zeitschrift für physikalische Chemie*, Leipzig, 271, 69-79, (1990).
34. Fletcher, R., A., MacKenzie, K., J., D., Nicholson, c., L., and Shimada, S., The composition range of alumosilicate geopolymers, *J. Europ. Ceramic Soc.*, 25, 1471-1477, (2005).
35. Furukawa, T., Fox, K., E., White, W., B., Raman spectroscopic investigation of the structure of silicate glasses. III. Raman intensities and structural units in sodium silicate glasses, *J. Chem. Phys.*, 75, 7, (1981).
36. Glukhovsky, V. D., A new building material. *Bulletin of Technical Information*, Glavkievgorstroy, (1957).
37. Granizo, M., L., Blanco-Varela, E., M., T., Martinez-Ramirez, T., Alkali activation of metakaolins: parameters affecting mechanical, structural and microstructural properties, *J. Mater. Sci.,* 42, 2934–2943, (2007).
38. Handke, M., Mozgwa, W.,Vibrational spectroscopy of amorphous silicates, *Vibrational Spectroscopy*, 5, 75-84, (1993).
39. Hanna, R., Su, G-J., Infrared absorption spectra of sodium silicate glasses from 4 to 30 μm,

Journal of the American Ceramic Society, 47, 12, 597-601, (1964).

40. Herr, R., Lutz, W., Ritzmann, A., Hillemeier, B., Schubert, K., Neue Erkentnisse über die Struktur von Geopolymerbinder mit Hilfe von Molybdatmethode, Tagung Bauchemie, Erlangen, (2004).
41. Hos, J., P., McCormick P., G., Byrne, L.,T., Investigation of synthetic aluminosilicate inorganic polymer, *J. of Materials Science*, 37, 2311-2316, (2002).
42. Iler, R., K., The Chemistry of Silica : Solubility, Polymerization, *Colloid and Surface Properties, and Biochemistry*, New York, Wiley, (1979).
43. Jirasit, F., Rüscher, C., H., Lohaus, L., A study the substantial improvement of fly ash-based geopolymeric cement with the addition of metakaolin, *Int. Conference on pozzolan, concrete and geopolymer*, Thailand, 1-15 , (2006).
44. Kim, D., Lai, H.-T., Chilinger, G., V., Yen, T., F., Geopolymer formation and its unique properties, *Environ. Geol.*, 51, 103-111, (2006).
45. Komnitsas, K., & Zaharaki, D., Geopolymerisation: A review and prospects for the minerals industry, *Minerals Engineering*, 20,1261 –1277, (2007).
46. Kriven, W. M., Bell, J. L., Effect of alkali Choice on Geopolymer Properties, *Cer. Eng. And Sci. Proc.*, 25, (3-4), 99-104, (2003a).
47. Kriven, W., M., Bell, J. L. and Gordon, M., Microstructure and microchemistry of fully reacted geopolymers and geopolymer matrix composites, *Ceramic Transactions*, 153, 227-250, (2003b).
48. Kriven, W., M., Bell, J. L. and Gordon, M., Geopolymer Refractories for the Glass Manufacturing Industry, *Cer. Eng. And Sci. Proc.*, 25, [1], 57-79, (2004).
49. Kriven, W., M., Bell, J. L., Gordon, M., and Wen, G., Geopolymers: more Than Just Cements, Geopolymer, Green Chemistry and Sustainable Development Solutions, edited by Joseph Davidovits. Proc. World congress Geopolymer, 2005, St. Quentin, France. Published by the Geopolymer Institute, St. Quentin, France (2005).
50.. Lee, W., K., W., and van Deventer, J., S., J., Use of infrared spectroscopy to study geopolymerization of heterogeneous amorphous aluminosilicates, *Langmuir*, 19, 8726-8734, (2003).
51. Lecomte, I., Henrist, C., Liegeous, M., Maseri, F., Rulmont, A., Cloote, R., (Micro)-structural comparison between geopolymers, alkali-activated slag, cement, and Portland cement, *J. Europ. Ceramic Soc.*, 26, 3789-3797, (2006).

52. Luz G., M., Blanco-Varela, M., T., Martinez-Ramirez, S., Alkali activation of metakaolins: parameters affecting mechanical, structural and microstructural properties, *J. Mater. Sci.*,42, 2934-2943, (2007).

53. Lutz, W., Chemie und Eigenschaften von Geozement, DFG-Projekt Wi 1069/10-1, (1999).

54. Lutz, W., Heidemann, D., Hübert, C., Wieker, W., Contribution of silica Gels to Superimposed ^{29}Si MAS NMR Spectra of Y Zeolites Dealuminated by Steaming, *Z. Anorg. Allg. Chem.*, 627, 2559-2564, (2001).

55. Lutz, W., Rüscher, C., H., Heidemann, D., Determination of the framework and non-framework [SiO_2] and [AlO_2] species of steamed and leached faujasite type zeolites:calibration of IR, NMR, and XRD data by chemical method, *Microporous and Mesoporous Materials*, 55, 193-202, (2002).

56. MacKenzie, K., J., D., What are these things called geopolymer? A Physico -Chemical perspective, *Ceramic Transaction- Advances in Ceramic Matrix Composites IX*, 153, 175-186, (2003).

57. McMillan, P., Piriou, B. and Navrotsky ,A., A Raman spectroscopic study of glasses along the joins silica-calcium aluminate, silica-sodium aluminate, and silica-potassium aluminate, *Geochimica et Cosmochimica Acta*, 46, 2021-2037, (1982).

58. McMillan, P., F., Richard, L., Remmele, Jr., Hydroxyl sites in SiO_2 glass: A note on infrared and Raman spectra, *American mineralogist*, 71, 772-778, (1986).

59. Nicholson, C., Fletcher, R., Miller, N., Stirling, C., Morris, J., Hodges, S., MacKenzie, K., and Schmücker, M., *Building Innovation through Geopolymer Technology*, Chemistry in New Zealand, 10-12, September, (2005).

60. Osswald, J., Fehr, K.,T., FTIR spectroscopic study on liquid silica solutions and nanoscale particle size determination, *J. Mater. Sci.*, 41, 1335-1339, (2006).

61. Pacheco-Torgal, F., Castro-Gomes, J., Jalali, S., Alkali activated binders: A review Part 1. Historical background, terminology, reaction mechanisms and hydration products, *Construction and Building Materials*, 22, 1305-1314, (2008).

62. Palomo A., Macías A., Blanco M.T. & Puertas F., Physical chemical and mechanical characterization of geopolymers, in: Proceedings of the 9th International Congress on the Chemistry of Cement, 505–511, (1992).

63. Palomo, A., Blanco-Varela, M., T., Granizo, M., L., Puertas, F., Vazquez, T., Grutzeck, M., W., Chemical stability of cementitious materials based on metakaolin, *Cement and Concrete*

Research, 29, 997-1004, (1999).

64. Perera, D., S., Cashion, J., D., Blackford, M., G., Zhang, Z., Vance, E., R., Fe speciation on in geopolymer with Si/Al molar ratio of ~2, *J. of the Eur. Ceram. Soc.*, 27, 7, 2697-2703, (2007a).
65. Perera, D., S., Uchida, O., Vance, E., R., Finnie, K., S., Influence of curing schedule on the integrity of geopolymers, *J. Mater. Sci.*, 42, 3099-3106, (2007b).
66. Provis, J. L., Duxson, P., Lukey, G. C. and Van Deventer, J. S. J., Statistical thermodynamic model for Si/Al ordering in amorphous aluminosilicates, *Chemistry of Materials,* 17, 11, 2976-2986, (2005a).
67. Provis, J. L., Duxson, P., Van Deventer, J. S. J. and Lukey, G. C., The role of mathematical modeling and gel chemistry in advancing geopolymer technology, *Transactions of the Institution of Chemical Engineers Research and Design,* 83(A7), 853-860, (2005b).
68. Qing-Hua, C., Tagnit-Hamou, A., Sarkar, S., L., Strength and microstructural properties of water glass activated slag, in: F.P. Glasser, G.J. Young, J.F. Young, T.O. Mason, P.L. Pratt (Eds.), Advanced Cementitious Systems: Mechanisms and Properties, *Materials Research Society*, Pittsburgh, Pennsylvania, Mater. Res. Soc. Symp. Proc., 245, 49-54, (1992).
69. Rahier, H., Simons, W., van Mele, B., Low-temperature synthesized aluminosilicate glasses, *Journal of Materials Science*, 32, 2237-2247, (1997).
70. Rahier, H., Wastiels, J., Biesemans, M., Willlem, R., Van Assche, G., Van Mele, B., Formation, molecular structure and thermal properties of geopolymers, Workshop Geopolymer Binder, Weimar, Germany, (2006).
71. Rahier, H., Wastiels, J., Biesemans, M., Willlem, R., Van Assche, G., Van Mele, B., Reaction mechanism, kinetics and high temperature transformations of geopolymers, *J. Mater. Sci.*, 42, 2982-2996, (2007).
72. Rowles, M., O'Connor, B., Chemical optimization of the compressive strength of aluminosilicate geopolymers synthesized by sodium silicate activation of metakaolinite, *J. of Materials Chemistry*, 13, 1161-1165, (2003).
73. Roy, D., M., Alkali activated cements Opportunities and challenges, *Cement and Concrete Research*, 29, 249-254, (1999).
74. Rüscher, C. H., Buhl, J.-Ch. and W. Lutz: Determination of the Si/Al ratio of Faujasite-type zeolites. In: A. Galarneau, F. Di Renzo, F. Fajula and J. Vedrine (Eds.): Studies in Surface Science and Catalysis 135, *Zeolites and Mesoporous Materials at the Dawn of the 21st*

Century Elsevier, 1-9, 13-P15, (2001).

75. Rüscher, C., H., Salman, N., Buhl, J-Chr., Lutz, W., Relation between growth-size and chemical cmposition of X and Y type zeolites, Letter to the editor, *Microp. Mesop. Mat.*, 92, 309-319, (2006).

76. Rüscher C. H., Mielcarek E., Lutz W., Ritzmann A., Kriven W. M., The Ageing Process of Alkali Activated Metakaolin., *8th Pacific Rim Conference on Ceramic and Glass Technology*, Vancouver, Canada, 2009, Ceramic Transactions 2010, Vol. 215, 1-10, in press.

77.Rüscher, C., H., Mielcarek, E., Lutz, W., Ritzmann, A., Kriven, W., M., Weakening of Alkali Activated Metakaolin During Aging Investigated by the Molybdate Method and Infrared Absorption Spectroscopy, *Journal of American Ceramic Society*, (2010a), in press.

78. Rüscher, C., H., Mielcarek, E., Wongpa, J., Jirasit, F., Lutz, W., New insights on Geopolymerisation using Molybdate, Raman, and Infrared Spectroscopy, *34th International Conference and Exposition on Advanced Ceramics and Composites (ICACC)*, Vol.31, Q12, Daytona Beach, FL, U.S.A., January 24-29, (2010b), submitted.

79. Skvara, F., Kopecka, M., Properties of a cement based on alkali activated slag, *Ceramics-Silikáty* , 41, 29– 34, (1997).

80. Skvara, F., Alkali activated materials or geopolymers?, *Ceramics−Silikáty*, 51, 3, 173-177, (2007).

81. Steveson, M., Sagoe-Crentsil, K., Relationships between composition, structure and strength of inorganic polymers, Part I metakaolin-derived inorganic polymers, *Journal of Materials Science*, 40, 2023-2036, (2005).

82. Subaer and van Riessen, A., Thermo-mechanical and microstructural characterization of sodium -poly(sialate-siloxo) (Na-PPS) geopolymers, *J. Mater. Sci.*, (2006).

83. Thilo, E., Wieker, W., Stade, H., Über die Beziehung zwischen dem polymerisationsgrad silicatischer Anionen und ihrem Reaktionsvermögen mit Molybdänsäure, *Z. anorg. Allg. Chem.*, 340, 261, (1965).

84. Wang, S., D., Pu, X.-C., Scrivener, K., L., Pratt, P., L., Alkali activated slag cement and concrete: A review of properties and problems, Adv. Cem. Res., 7, 93-102, (1995a).

85. Wang, S., D., Scrivener, K., L., Hydration products of alkali activated slag cement, *Cem. Concr. Res.*, 25, 561– 571, (1995b).

86. Wang, H., Li, H., Yan., F., Synthesis and mechanical properties of metakaolinite-based

geopolymer, *Colloids and Surface A: Physicochem. Eng. Aspects*, 268, 1-6, (2005).

87. Wieker, W., Fahlke, B., On the mechanism of the formation of of Molecular sieves and related compounds, *Stud. Surf. Sci. Catal.*, 24, 161-181, (1987).
88. Wieker, W., Hübert, C., Heidemann, D., Recent Results of Solid State NMR Investigations and their Possibilities of Use in Cement Chemistry, Int. Conference Cement Chemistry, Göteborg, Sweden, (1997).
89. Van Jaarsveld J., G., S., Van Deventer J., S., J.,& Lorenzen L., The potential use of geopolymeric materials to immobilize toxic metals: Part I. Theory and applications, *Minerals Engineering*, 10, 659 –669, (1997).
90. Van Jaarsveld, J., G., S., Van Deventer J., S., J., & Lukey, G., C., The effect of composition and temperature on the properties of fly ash- and kaolinite-based geopolymers, *Chemical Engineering Journal*, 89,63 –73. (2002).
91. Xu, H. and Van Deventer, J. S. J., The geopolymerisation of alumino-silicate minerals, *International Journal of Mineral Processing*, 59, 247-266, (2000).
92. Xu, H., Van Deventer J., S., .J., Lukey, G., C., Effect of Alkali Metals on the Preferential Geopolymerization of Stilbite/Kaolinite Mixtures, *Ind. Eng. Chem. Res.*, 40, 3749-3756, (2001).
93. Xu, H., & Van Deventer J., S., J., Geopolymerisation of multiple minerals, *Minerals Engineering*, 15, 1131 –1139, (2002).
94. Xu, H., Deventer, S., J., The effect of alkali metals on the formation of geopolymeric gels from alkali-feldpars, *Colloids and surfaces A: physicochem. Eng. Aspects* , 216, 27-44, (2003).
95. Yip, C., K., Lukey, G., C., & Van Deventer J., S., J., The coexistence of geopolymeric gel and calcium silicate hydrate at the early stage of alkaline activation, *Cement and Concrete Research*, 35, 1688–1697, (2005).
96. Yu, P., Kirkpatric, R., J., Poe, R., McMillan, P., F., Cong, X., Structure of Calcium Silicate Hydrate (C-S-H): Near-, Mid-, and Far- Infrared Spectroscopy, *Journal of the American Ceramic Society*, 82, [3], 12-48, (1999).
97. Yunsheng, Z., Wei, S., Zongjin, L., Preparation and microstructure of K-PSDS geopolymeric binder, *Colloids and surfaces A: Physicochem Eng. Aspects*, 302, 473-482, (2007).
98. Yunsheng, Z., Wei, S., Zongjin, L., Infrared Spectroscopy study of Structural Nature of of Geopolymeric Products, Journal of Wuhan University of Technology. *Mater. Sci. Ed.*, 23, 4, 622-627, (2008).

99. Wikipedia: The Free Encyclopedia. Wikimedia Foundation Inc. http://wikipedia.org/
100. ArgusLab, Mark A. Thompson, Planaria Software LLC, Seattle, WA, http://arguslab.com/

7. APPENDIX

Table 13: The chemical composition of raw materials (by weight %): FA- fly ash from Mae Moh power plant, RHBA-rice husk-bark ash, WG_2-sodium water glass after Rüscher et al., (2010b).

Raw material	**SiO_2**	**Al_2O_3**	**Fe_2O_3**	**CaO**	**SO_3**	**Na_2O**
RHBA	84.75	0.16	-	2.78	0.6	-
FA	36.02	20.58	15.91	18.75	2.24	-
WG_2	33.28	-	-	-	-	15.36

Table 14: The chemical composition (by weight %) of 4 silica reach geopolymeric cements: Cem.8; Cem.9, Cem.10, Cem.11, Cem.12, (FA- fly ash from Mae Moh power plant, RHBA-rice husk-bark ash, WG_2-sodium water glass) Rüscher et al., (2010b).

Mixture	**FA**	**RHBA**	**WG_2**	**NaOH**	**Si/Al Molar Ratio**
Cem.9	59.26	14.81	18.52	1.07	2.09
Cem.10	57.14	14.29	20.41	1.08	3
Cem.11	55.17	13.79	22.17	8.87	3.01
Cem.12	-	50	35.72	14.28	>1000

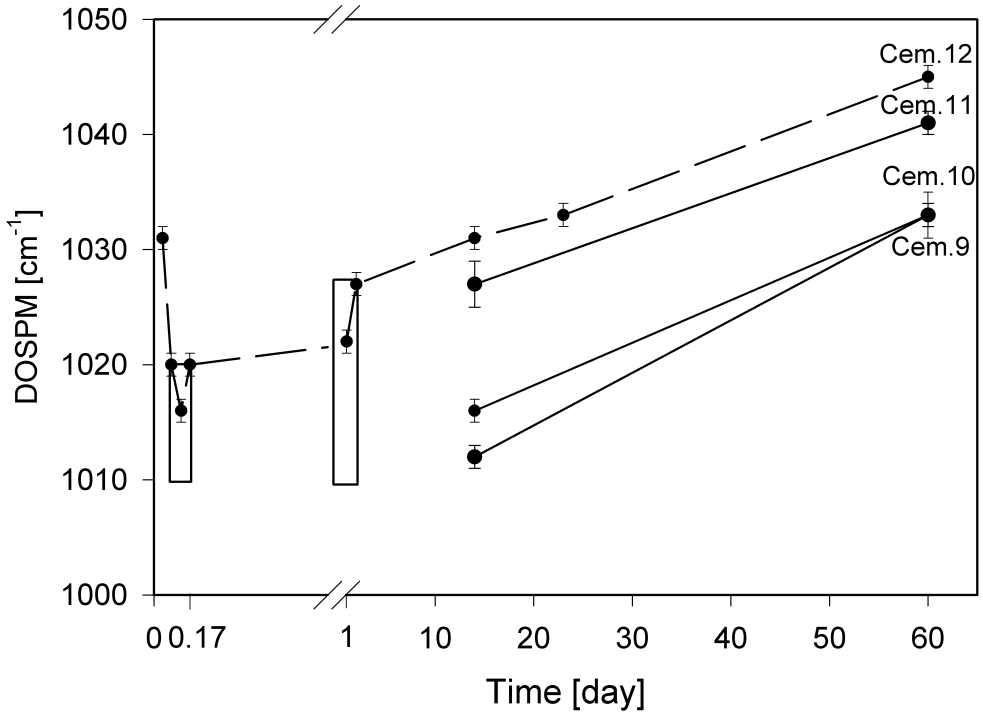

Fig. 7.1. The relation of DOSPM of asymmetrical stretching and ageing time for silica reach geopolymers (Cem.9-12) after *Rüscher et al., (2010b)*.

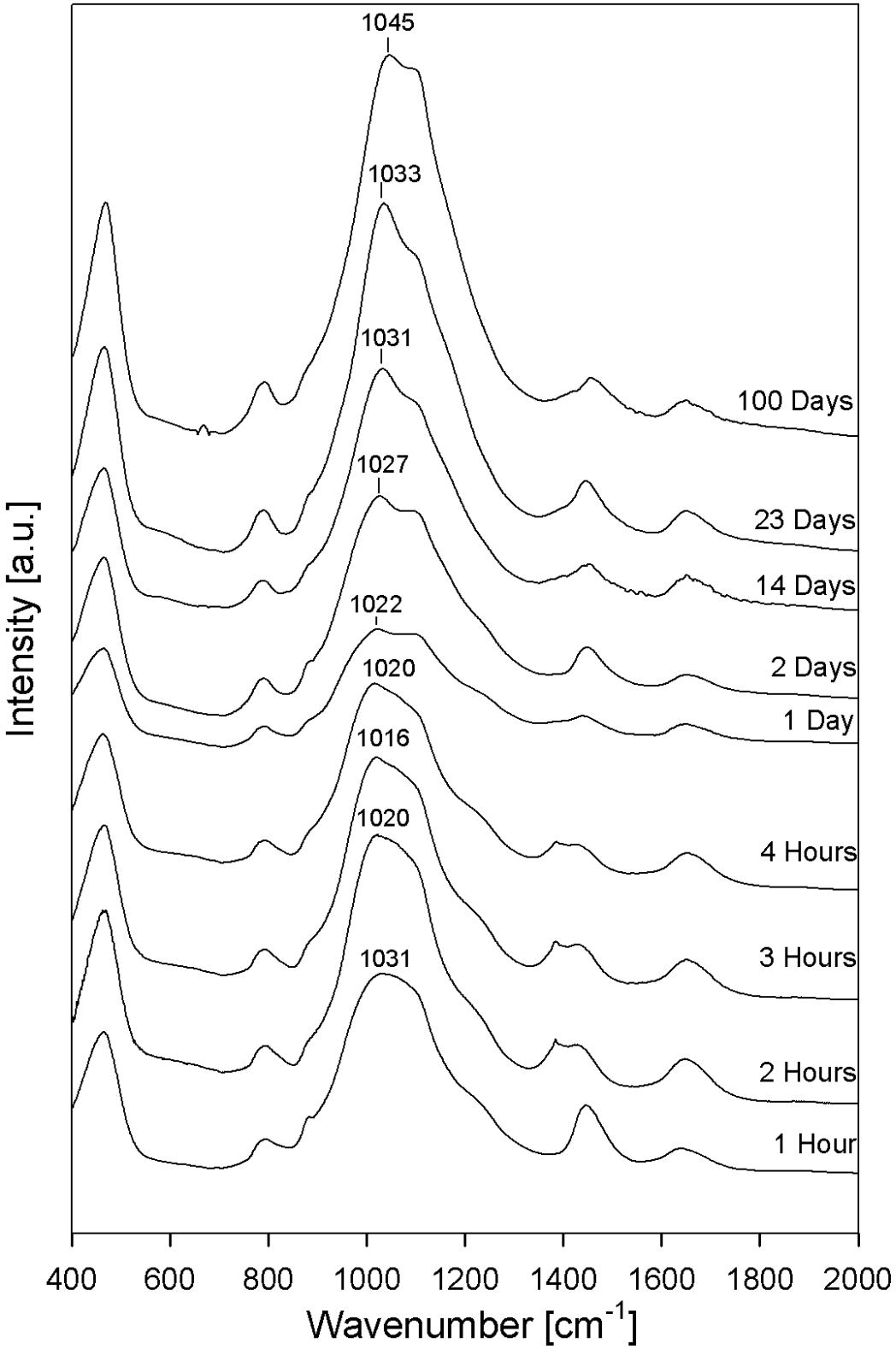

Fig. 1 The FTIR study of ageing effect of silica reach geopolymer Cam.11 characterized by molar ratio Si/Al>1000 after *Rüscher et al., (2010b)*.

LIST OF PUBLICATIONS

Full papers

Pätzold, R., Keuntje, M., Theophile, K., Müller, J., **Mielcarek, E.**, Ngezahayo, A., Anders von Ahlften, A., In situ microbial mapping of nitrificants and anammox bacteria in biofilms by means of confocal resonance Raman microscopy, *J. of Microbiol. Methods*, 72, (3), 241-248, (2008).

Rüscher C. H., **Mielcarek E.**, Lutz W., Ritzmann A., Kriven W. M., The Ageing Process of Alkali Activated Metakaolin., *8th Pacific Rim Conference on Ceramic and Glass Technology*, Vancouver, Canada, 2009, Ceramic Transactions 2010, Vol. 215, 1-10, in press.

Rüscher, C., H., **Mielcarek, E.**, Lutz, W., Ritzmann, A., Kriven, W., M., Weakening of Alkali Activated Metakaolin During Aging Investigated by the Molybdate Method and Infrared Absorption Spectroscopy, *Journal of American Ceramic Society*, (2010), in press.

Rüscher, C., H., **Mielcarek, E.**, Wongpa, J., Jirasit, F., Lutz, W., New insights on Geopolymerisation using Molybdate, Raman, and Infrared Spectroscopy, *34th International Conference and Exposition on Advanced Ceramics and Composites (ICACC)*, Vol.31, Q12, Daytona Beach, FL, U.S.A., January 24-29, (2010), submitted.

Rüscher, C., H., **Mielcarek, E.**, Wongpa, J., Jaturapitakkul, C., Jirasit, F., Lohaus., L., Silicate-, aluminosilicate and calciumsilicate gels for building constructions: chemical and mechanical properties during ageing*, Europ. J. Min.*, (2010), submitted.

Conference contributions

Rüscher, C., H., **Mielcarek, E.**, Jirasit, F., Lutz, W., Lohaus, L., Anders von Ahlften, A., struktur und eigenschaften von Geopolymer Binder: Direkter Nachweis der Oberflächenreaktivität in Säuren, DGK conference, Bremen, Germany, (2007). (poster)

Mielcarek, E., Rüscher, C., H., Raman and IR spectroscopyic investigations of alumosilicate glasses and alumosilicate binders, DGK conference, Erlangen, Germany, (2008). (poster)

Mielcarek, E., Rüscher, C., H., Anders von Ahlften, A., Lohaus, L., structural transformations in

alumosilicate gels during hardening, DGK conference, Hannover, Germany, (2009). (poster)

CURRICULUM VITAE

Personal details:

Name: Elżbieta Marta Mielcarek

***Address*:** Callinstrasse 25/04, Hannover 30167, Germany

Date of birth: 01.02.1981

Place of birth: Sulechów, Poland

Nationality: Polish

Gender:Female

Education:

Primary school: Janusza Kusocińskiego Primary school, Sulechów, Poland
Year:1987-1996

Secondary school: High (secondary) school, Sulechów**,** Poland
Year:1996-2000 (with certificate)

Bachelor of science: Department of Physics, Adam Mickiewicz University in Poznań, Poland
Year:2000-2003 (with certificate)

Master of science: Department of Physics, Leibniz University Hannover, Germany
Year: 2003-2006 (with certificate)

Doctoral study: since September 2006: PhD student in Institute of Mineralogy in Hannover, Leibniz University of Hannover
Scholarship program: "Georg-Christop-Lichtenberg-Stipendium" provided by Ministry of Science and Culture, Land Niedersachsen, Germany